LA-14206
Approved for public release;
distribution is unlimited.

Gamma-Ray Measurements of Holdup Plant-Wide: Application Guide for Portable, Generalized Approach

Los Alamos
NATIONAL LABORATORY
EST. 1943

The World's Greatest Science Protecting America

This work was supported by the U.S. Department of Energy, Office of Security Policy, Policy Integration and Technical Support.

Los Alamos National Laboratory, an affirmative action/ equal opportunity employer, is operated by the University of California for the United States Department of Energy under contract W-7405-ENG-36.

National Nuclear Security Administration

This report was prepared as an account of work sponsored by an agency of the United States Government. Neither the Regents of the University of California, the United States Government nor any agency thereof, nor any of their employees make any warranty, express or implied, or assume any legal liability or responsibility for the accuracy, completeness, or usefulness of any information, apparatus, product, or process disclosed, or represent that its use would not infringe privately owned rights. Reference herein to any specific commercial product, process, or service by trade name, trademark, manufacturer, or otherwise does not necessarily constitute or imply its endorsement, recommendation, or favoring by the Regents of the University of California, the United States Government, or any agency thereof. The views and opinions of authors expressed herein do not necessarily state or reflect those of the Regents of the University of California, the United States Government, or any agency thereof. Los Alamos National Laboratory strongly supports academic freedom and a researcher's right to publish; as an institution, however, the Laboratory does not endorse the viewpoint of a publication or guarantee its technical correctness.

LA-14206
Issued: June 2005

Gamma-Ray Measurements of Holdup Plant-Wide: Application Guide for Portable, Generalized Approach

Phyllis A. Russo

Los Alamos
NATIONAL LABORATORY
EST. 1943

The World's Greatest Science Protecting America

GAMMA-RAY MEASUREMENTS OF HOLDUP PLANT-WIDE: APPLICATION GUIDE FOR PORTABLE, GENERALIZED APPROACH

Phyllis A. Russo
Los Alamos National Laboratory

May 2005

This work was supported by the US Department of Energy, Office of Security and Safety Performance Assurance, Office of Materials Inventory and Technology Development

List of Tables

Page

Table VI.1. The Encapsulated HEU (93.2 % ^{235}U) Holdup Standards…….……32
Table VI.2. The Low-Burnup (93.5% ^{239}Pu) Plutonium Metal Spheres……...33
Table VI.3. The Low-Burnup (93.9% ^{239}Pu) Plutonium Metal Foils……...……34
Table VI.4. The Low-Burnup (94.0% ^{239}Pu) Plutonium Oxide Standards……...……36
Table VII.1. Common Gamma Rays for Holdup Analysis……41
Table VII.2. Compton-Edge Data for NaI and CZT Detectors……..44
Table VII.3. Gamma-Ray Peak Data for NaI and CZT…….…45
Table VII.4. Gamma-Ray Peak Data for BGO and $LaCl_3$…….…….53
Table VII.5. Portable Gamma-Ray Detectors for Holdup Measurements…….56
Table VIII.1. Gamma-Ray Mass Attenuation Coefficients……..…..…….81
Table IX.1. Usual Components of Calibration and Measurement Distances, r_0 and r…...…..102
Table IX.2. Mean Gamma-Ray Interaction Depth in NaI Crystals …….....……..102
Table IX.3. Statistical Criterion for Practical Deposit Thickness with 10% 1σ Statistics..…111
Table IX.4. Statistical Criterion for Practical Deposit Thickness with 20% 1σ Statistics…..112
Table IX.5. Numerical Evaluation of Systematic Error in Total U Mass for 1001-keV Measurements of LEU…….…114
Table IX.6. Monte Carlo Simulation of Complex Systematic Effects of Deposit Distribution on Gamma and Neutron Response for Converters……..……....116

List of Figures and Captions

Page

Figure VI.1. Encapsulated HEU holdup standards cover a range of thickness from 0.003 to 0.048 g U/cm^2 for the five oxides and 1.28-1.31 g U/cm^2 for the two metals. The ^{235}U enrichment is 93.2%. ……31

Figure VI.2. Five low-burnup (93.5% ^{239}Pu) plutonium metal spheres (0.2, 0.5, 1.0, 2.0 and 5.0 g Pu) are pictured before encapsulation. The capsules are shown below. ……...…33

Figure VI.3. One of the five sets of encapsulated plutonium metal foil standards includes three thicknesses (0.6, 1.3 and 2.5 g Pu/cm^2). Each low-burnup (93.9% ^{239}Pu) foil has a 2-cm diameter……34

Figure VI.4. One of the five sets of encapsulated plutonium oxide standards includes three thicknesses (0.4, 0.9 and 1.8 g Pu/cm^2). The oxide in each low-burnup (94.0% ^{239}Pu) standard is confined to a cylinder that is 2.7 cm in diameter. …...36

Figure VI.5. Neutron counter (IPAN) results for each drum (solid points) and the corresponding sum of package results obtained using the gamma-ray holdup measurement methodology (open points). Packages added to the first eight drums were measured by near positioning of the gamma detector ("area" geometry). Packages added to the remaining forty drums were measured by distant positioning of the gamma detector ("point" geometry). The fully loaded drum held 3-5 packages typically, but sometimes many more (up to ~35)……38

Figure VI.6. Field verification data for specific mass of uranium (in g ^{238}U/cm) in a line deposit of LEU *vs*. measurement position on a 75-m-long static duct measured by two teams using the 1001-keV gamma ray and NaI detectors. Count times were 45-60 s. A horizontal dashed line indicates the average result for each team. The solid line is a plot of the results measured on a previous date by two different teams. ……..39

Figure VII.1. Gamma-ray spectra of low-burnup (93% ^{239}Pu) plutonium measured with four different gamma-ray detectors: NaI, CZT, CdTe and Ge (top to bottom). ……...43

Figure VII.2. Spectra of LEU (~3% ^{235}U) duct-holdup deposits were measured with short count times using a 5-cm-thick NaI detector and a tungsten plug inserted into the collimator to count room background ("Plug In"). Deposits exceed the maximum thickness for 186-keV gammas in a and c. The random uncertainty in the net 1001-keV rate is 20% in both a and c despite higher room-background continuum in c. Note evidence of the 238-keV gamma ray in a, indicating reactor-return material. The deposit measured in b is too thin to analyze at 1001 keV, and the random uncertainty in the net 186-keV rate is 90% because of the high continuum from room background. 47

Figure VII.3. Gamma-ray spectra of deposits in the exhaust ductwork in one wing of a multimission research facility measured with Ge and CZT. The asterisk marks the expected position of the 186-keV gamma ray of ^{235}U. ……..…...48

Figure VII.4 Gamma-ray spectra of deposits at a second location (see Fig. VII.3) in the exhaust ductwork in one wing of a multimission research facility measured with Ge and CZT. An asterisk is positioned at 186 keV. ……..……...48

Figure VII.5. NaI and CZT spectra of ^{235}U in HEU deposits that include recycled material. The 186-keV analysis peak has a potential interference at 238 keV for the 61% enrichment. Dashed vertical lines mark both energies. ……....49

Figure VII.6. This spectrum of uranium in LEU deposits that include recycled material was measured with the 2.5-cm-diameter by 5-cm-thick NaI detector in a 300-s count. The 186 keV peak has a potential interference at 238 keV. Dashed vertical lines mark peak and high-energy continuum ROIs at both 186 and 1001 keV. …….…….……....……...50

Figure VII.7. Top: Portable measurements of ^{235}U deposits in a process filter system are performed with a portable Ge detector weighing ~10 kg with its tungsten collimator-shield. Bottom: CZT and NaI also in use for measurements of process filters weigh ~1 kg each with their respective tungsten and lead shields. ……...…...51

Figure VII.8. The compact NaI detector (see Fig. VII.6) is shown during measurements of plutonium deposits in overhead ducts. The detector is mounted on a telescoping pole. The bottom-frame exploded view from the middle frame shows a wooden meter stick used as a positioning standoff from the duct. ..……...52

Figure VII.9. Gamma-ray spectra of ^{137}Cs measured with a 5-cm^2 by 2.54-cm-thick $LaCl_3$ scintillator and with the same-size NaI scintillator. The energy resolution (FW.5M) at 662 keV is 4.0 and 6.9%, respectively. …….....54

Figure VII.10. The gamma-ray spectra, top to bottom, are those of low-, medium- and high-burnup plutonium (6%, 18% and 24% ^{240}Pu, respectively), measured with a 5-cm^2 by 2.54-cm thick $LaCl_3$ scintillator and with the same-size NaI scintillator. The improved energy resolution at 414 keV is illustrated by the distinct peak in the $LaCl_3$ spectrum at this energy in the full range of isotopics. ……...…...55

Figure VII.11. The Peltier-cooled portable CdTe detector is shown in use for portable isotopics measurements of plutonium in a process glove box. ……..…...57

Figure VIII.1. A point source is positioned on the axis of the cylindrically collimated detector at distance ***r*** from the crystal. The field of view (dashed circle) is in the source plane perpendicular to the detector axis. ……..……...63

Figure VIII.2. Nine, equally spaced off-axis positions of the point source used to measure the two-dimensional radial response of the gamma-ray detector at a fixed distance $\boldsymbol{r_0}$ are illustrated. The axial position (center) is the source position illustrated in Figure VIII.1. The detector response is constant for a source at any point along each concentric circle. Because of this radial symmetry, the two-dimensional response can be determined with a small number of measurements. …….……..…...64

Figure VIII.3. Normalized net, room-background-subtracted rate of the ^{239}Pu 414-keV peak *vs*. displacement of the point source from the detector axis. A smooth curve

connects the data points. This one-dimensional radial response was measured at a distance r_0 of 40 cm with a collimated NaI detector (2.54-cm diameter by 5-cm long crystal). Collimator depth and diameter were both 2.54 cm. Data obtained on both (positive and negative) sides of the detector axis) confirm the radial symmetry. ……..…..65

Figure VIII.4. a) A collimated NaI detector (radial response described by Figure VIII.3) measures the gamma-ray spectrum of holdup in the pipe at the location marked by the white bar-coded label. This vertical pipe appears as a narrow line in the detector's relatively wide field of view at this measurement distance. The finite-source effect on the specific mass for the line deposit is small in this case. b) The same detector is positioned at the same measurement distance from a second bar-coded measurement location on a horizontal duct whose diameter is four times that of the vertical pipe in a). Proximity of the neighboring overhead equipment may prevent use of a larger measurement distance without including additional deposits in the field of view. The horizontal duct appears as a broad line in the detector's somewhat wider field of view at this measurement distance. The finite-source effect on the specific mass for the line source is much larger in this case. ...……...70

Figure VIII.5. A very large overhead duct is measured from below with a portable collimated Ge detector. The largest measurement distance for any detector positioned beneath this duct is comparable to the duct diameter because of the proximity of the equipment to the floor. The duct width is always a significant fraction of the width of the field of view of the collimated gamma-ray detector for common ventilation ducts such as this. The duct surface completely fills the field of view of this collimated detector, a geometry that is most likely (depending on the dimensions of the deposit) best-suited to analysis of the holdup as an area deposit. ……..…...71

Figure VIII.6. The diagonally shaded area represents a finite area deposit superimposed on the field of view of the cylindrically collimated detector. Concentric circles indicate equally spaced loci of constant response. The radial positions defined by these circles mark the axial source displacements used to obtain the radial response plotted in one dimension in Figure VIII.3. The finite area deposit fills the field of view in two dimensions, as prescribed by the two-dimensional model for the area deposit. ……..…..…...72

Figure VIII.7. The diagonally shaded area represents a finite line deposit superimposed on the field of view of the cylindrically collimated detector. Concentric circles indicate equally spaced loci of constant response. The radial positions defined by these circles mark the axial source displacements used to obtain the radial response plotted in one dimension in Figure VIII.3. The finite line deposit is centered in the field of view with a length that exceeds the width of the field of view in one dimension, as prescribed by the two-dimensional line model. The finite width w exceeds that prescribed by the one-dimensional constraint for the line deposit (narrow, solid line). ……...…..…...73

Figure VIII.8. The diagonally shaded area represents a finite point deposit superimposed on the field of view of the cylindrically collimated detector. The concentric circles indicate equally spaced loci of constant response. The intersections of the circles with a diameter mark the axial source displacements in the one-dimensional radial response plotted in Figure VIII. 3. The finite point deposit is centered in the field of view, as prescribed by the two-dimensional model for the point source. Its finite width ***w*** (which gives its area ***a***) exceeds that prescribed by the two-dimensional constraint for the point deposit (small, solid point). ……..…..…...74

Figure VIII.9. The data from Figure VIII.3 (normalized net, room-background-subtracted count rate of the ^{239}Pu 414-keV gamma-ray peak *vs*. displacement of the point source from the detector axis) are shown in blue. The measurements were performed at a distance r_0 of 40 cm with a collimated NaI detector. The red curve is the fit of Equation 18 (normalized Gaussian) to these data. The FW.5M of the fit is 22 cm. ...……..…..……....76

Figure VIII.10. The mass attenuation coefficients for uranium and oxygen are plotted *vs*. gamma-ray energy up to 1200 keV. The ratio of the mass attenuation coefficient of oxygen to that of uranium increases by an order of magnitude between 186 and 1001 keV so that the values are nearly comparable at 1001 keV. ……..……..……...82

Figure VIII.11. True *vs*. measured thickness (areal density of plutonium, g/cm^2) is plotted for 414-keV gamma rays from plutonium metal, PuO_2 and PuO_3 as determined by Equation 25a. The measured thickness corresponds to that determined experimentally from the specific holdup mass corrected for the effects of room background, equipment attenuation, and the finite source dimension. The straight line has a slope of 1. Therefore, the correction factor for self-attenuation is the ratio of the curved line to the straight line. …...……..83

Figure VIII.12. True *vs*. measured thickness (areal density of uranium, g/cm^2) is plotted for 186-keV gamma rays from uranium metal, UO_2,U_3O_8 , and $UO_2(NO_3)_2{\cdot}6H_2O$ as determined by Equation 25a. The measured thickness corresponds to that determined experimentally from the specific holdup mass corrected for the effects of room background, equipment attenuation, and the finite source dimension. The straight line has a slope of 1. Therefore, the correction factor for self-attenuation is the ratio of the curved line to the straight line.……...84

Figure VIII.13. True *vs*. measured thickness (areal density of uranium, g/cm^2) is plotted for 1001-keV gamma rays from uranium metal, UO_2, U_3O_8, and $UO_2(NO_3)_2{\cdot}6H_2O$ as determined by Equation 25a. The measured thickness is that determined experimentally from the specific holdup mass corrected for the effects of room background, equipment attenuation, and the finite source dimension. The straight line has a slope of 1. Therefore, the correction factor for self-attenuation is the ratio of the curved line to the straight line. ……...84

Figure VIII.14. Calculated results for point deposit of ^{235}U in U_3O_8 measured at 186 keV and ***r*** = 40 cm using a 2.5-cm by 2.5-cm cylindrical collimator: a) Corrected specific mass *vs*. measured, Equation (11), is plotted for the finite point

source. The true deposit width ***w*** of 10 cm corresponds to an area ***a*** of 79 cm^2 for the point source. The dashed line drawn for reference passes through the origin with a slope of 1. The middle (solid) line is the specific mass of the finite point source corrected by Equations (14) and (22) for the finite-source effect only. The top (heavy solid) line is the specific mass also corrected for self-attenuation, Equations (38), (47), and (50). b) Percent difference between corrected and measured specific mass *vs*. measured value is plotted for the point deposit. The relative finite-source correction (dashed line) is constant, and the relative total correction including self-attenuation (solid line)increases nonlinearly with areal density. Note: Point areal density is m_P/a. …..…..……...93

Figure VIII.15. Calculated results for point deposit of ^{235}U in U_3O_8 measured at 186 keV and ***r*** = 40 cm using a 2.5-cm by 2.5 cm cylindrical collimator: a) Fully corrected (Equations (38), (47), and (50)) *vs*. measured (Equation (11)) specific mass is plotted for three values of the point-deposit width parameter w. The true deposit width of 10 cm (gray, middle curve) corresponds to a point-source area of 79 cm^2. The true width parameter ***w*** is lower and higher by one third than a width of 7.5 cm (pink, upper curve) and 15 cm (blue, lower curve), respectively. The dashed line through the origin with slope of 1 is for reference. b) Percent difference between the corrected and true specific mass of the point deposit with ***w*** = 10 cm *vs*. the measured value is plotted in a practical mass range (up to a true deposit thickness of 0.35 g U/cm^2 in this case; see Section IX.6) for holdup measured at 186 keV. Corrected results are the solid gray line at 0% obtained using the true (***w*** = 10 cm) width, triangles (pink) for the underestimate (***w*** = 7.5 cm) of true width, and dashes (pink) for the overestimate (***w*** = 15 cm) of true width. Crosses (gray, lowest curve) mark the uncorrected result. Note: Point areal density is m_P/a. ……..……...94

Figure VIII.16. Calculated results for line deposit of ^{235}U in U_3O_8 measured at 186 keV and ***r*** = 40 cm using a 2.5-cm by 2.5-cm cylindrical collimator: a) Corrected specific mass *vs*. measured, Equation (12), is plotted for the finite line source. The true deposit width ***w*** is 10 cm. The dashed line drawn for reference passes through the origin with a slope of 1. The middle (solid) line is the specific mass of the finite line source corrected by Equations (15) and (21) for the finite-source effect only. The top (heavy solid) line is the specific mass also corrected for self-attenuation, Equations (39), (48), and (51). b) Percent difference between the corrected and measured specific mass *vs*. the measured value is plotted for the line deposit. The relative finite-source correction (bottom dashed line) is constant, and the relative total correction including self-attenuation (top solid line) increases nonlinearly with areal density. Note: Line areal density is m_L/w. ……..……...97

Figure VIII.17. Calculated results for line deposit of ^{235}U in U_3O_8 measured at 186 keV and *r* = 40 cm using a 2.5-cm by 2.5 cm cylindrical collimator: a) Fully corrected (Equations (39), (48) and (51)) *vs*. measured (Equation (11)) specific mass is plotted for three values of the line-deposit width parameter ***w***. The true deposit width is 10 cm (gray, middle curve). The true width parameter is lower and higher by one third than a width of 7.5 cm (pink, upper curve) and

15 cm (blue, lower curve), respectively. The dashed line through the origin with slope of 1 is for reference. b) Percent difference between corrected and true specific mass of the line deposit with ***w*** = 10 cm *vs*. the measured value is plotted in a practical mass range (up to a true deposit thickness of 0.7 g U/cm^2 in this case; see Section IX.6) for holdup measured at 186 keV. Corrected results are the solid gray line at 0% obtained using the true (***w*** = 10 cm) width, triangles (pink) for the underestimate (***w*** = 7.5 cm) of true width, and dashes (pink) for the overestimate (***w*** = 15 cm). Crosses (gray, lowest curve) mark the uncorrected result. Note: Point areal density is $\boldsymbol{m_L/w}$. ……..…….....98

Figure VIII.18. Calculated results for area deposit of ^{235}U in U_3O_8 measured at 186 keV and ***r*** = 40 cm using a 2.5-cm by 2.5-cm cylindrical collimator: a) Corrected specific mass *vs*. measured, Equation (13), is plotted for the area source. The dashed line drawn for reference passes through the origin with a slope of 1. The solid line is the specific mass of the area source corrected by Equations (40), (49), and (52) for self-attenuation. b) Percent difference between the corrected and measured specific mass *vs*. the measured value is plotted for the area deposit. The finite-source correction does not apply to this model of the generalized area deposit. (That is, areal density for the area deposit is $\boldsymbol{m_A}$.) The relative correction for self-attenuation increases nonlinearly with areal density. ……..……...99

Figure IX.1. Figure IX.1. A mechanical positioning device is shown in use for calibrating the 2.5-cm by 5.0-cm compact NaI detector to measure LEU. The calibration standard is mounted on the detector axis at r_0 = 40 cm. An additional device shown at the right (nearly fully collapsed for storage) illustrates the variable position of the calibration standard, detector distance, and relative angle between source and detector axes allowed by this simple device……... ……...103

Figure IX.2. The radial response (normalized gamma-ray count rate *vs*. displacement of the source from the on-axis position) of the 2.5-cm diameter by 5-cm-thick NaI detector with 2.5-cm by 2.5-cm collimator is plotted for 186-, 414- and 1001-keV gamma rays. The FW.5M of each radial response curve is 23 cm, 22 cm and 19 cm, respectively. ……..…….....104

Figure IX.3. Three sketches of the transverse cross section of a converter show the a) "axial", b) "volume", and c) "shell" models for radial distribution of uranium within the converter. Red shading indicates the uranium deposit. The gamma and neutron detectors and their positions are indicated by small and large rectangles, respectively, at the top of each sketch. ……..…....116

Figure X.1. a) Dimensioned sketch, not to scale, of subbasement (downstream) portion of exhaust ductwork in one wing of a large multimission nuclear-materials research facility. Blue numerals/letters indicate measurements performed with NaI at these positions. The associated solids filter (SF-5) is sketched separately. ……..…….....120

Figure X.1. b) Dimensioned sketch, not to scale, of basement (upstream) portion of exhaust ductwork from Figure X.1.a). Blue numerals/letters mark measurements performed by NaI at these positions, and black indicates that

both NaI and Ge measurements were performed. The red-shaded areas were not accessible for measurements. ...……..…….....121

Figure X.2. Eleven normalized Gaussians displaced successively by 70% of one FW.5M sum to a uniform distribution (dark curve) between the first and last Gaussian. ...……...……...126

Figure X1.1. Measured specific mass of uranium is plotted vs. linear position along part of the ventilation system of an LEU facility. Two arms (Lower Section and Drop Line) with exhaust from various process locations feed the Main Line of the system. Holdup measured in the arms and the Main Line is shown in separate plots with a common position axis. The linear position on each arm at its juncture with the Main Line is the position on the Main Line at this juncture. Because the width of ventilation ductwork varies with location, the thickness of measured deposits with the same specific mass can differ. Therefore, the width (diameter, in this case) of the equipment cavity is also plotted vs. linear position on each map for visual assessment of deposit thickness (areal density or mass per unit area). Distance increases in the direction of process flow. 131

Table of Contents

Page

ABSTRACT……...……...13

I. INTRODUCTION AND SCOPE……...14

II. SUMMARY…… 16

III. IMPACTS OF PROCESS HISTORY AND FACILITY DESIGN……18

III.1. Process History……18

III.2. Facility Design……..20

III.3. Excluded Nuclear Material Forms……..……..21

IV. IMPACTS OF CUSTOMERS AND STATUS OF FACILITY OPERATIONS…...22

IV.1. Operations Status……..22

IV.2. Safeguards Customers……..23

IV.3. Criticality-Safety Customers……24

IV.4. Waste-Management Customers……25

IV.5. Other Health and Safety Customers/Concerns……25

V. PERSONNEL FOR HOLDUP MEASUREMENTS……...……27

V.1. Scientific Staff……27

V.2. Measurements Staff……27

V.3. Personnel for Planning, Implementation, and Analysis……28

VI. STANDARDS FOR CALIBRATION, VALIDATION, AND FIELD VERIFICATION……..……...31

VI.1. Calibration Standards for Measurements of Uranium and Plutonium……..31

VI.2. Calibration Standards for Measurements of LEU……34

VI.3. Standards for Validation of Holdup Measurements……35

VI.4. Field Verification……..38

VII. EQUIPMENT AND SETTINGS…….……...40

VII.1. Room-Temperature Detectors, Spectrometer Tools, and Spectra……...40

VII.2. Peltier-Cooled CdTe Detectors for Isotopics and Mass……..57

VII.3. Ancillary Detection Equipment and Sources……..58

VIII. MODELS, METHODOLOGIES, AND ALGORITHMS……...……62

VIII.1. Generalized Geometry Holdup (GGH) Method……62

VIII.1.1. Assumptions and constraints……...62

VIII.1.2. Calibration……...63

VIII.1.3. Obtaining and analyzing specific mass: overview……..67

VIII.2. Correcting Specific Mass for Effect of Equipment Attenuation……68

VIII.3. Correcting Specific Mass for Effect of Finite Source Dimension ***w***……..69

VIII.3.1. Concept of the finite source in holdup measurements……69

VIII.3.2. Models of finite sources……..72

VIII.3.3. Correct measured specific mass finite source dimension ***w***……74

VIII.4. Correcting Specific Mass for Effect of Self-Attenuation……...78

VIII.4.1. Self-attenuation in holdup measurements……...78

VIII.4.2. Determine self-attenuation from the measured areal density……..79

VIII.4.3. Correct measured specific mass for self-attenuation……..85

VIII.5. Computing Total Isotope Mass in the Extended Equipment……89

VIII.6. Sensitivity of Specific Mass and Total Mass to Uncertainty in ***w***……91

VIII.6.1. Introduction……91

VIII.6.2. Point deposits……...…….....92

VIII.6.3. Line deposits……...95

VIII.6.4. Area deposits…….....100

IX. PROCEDURES FOR MEASUREMENTS AND ANALYSIS……..101

IX.1. Calibration Measurements……..101

IX.2. Measurements of the Radial Response……...103

IX.3. Room Background Measurements……..105

IX.4. Holdup Measurements……..……..107

IX.5. Measurement Control……108

IX.6. Thick Deposits and Defining the Limiting Thickness……110
IX.7. Thin Deposits and Measuring Zero……112
IX.8. Numerical Evaluation of Systematic Effects……..113
IX.9. Monte Carlo Evaluation of Complex Systematic Effects……...……115
IX.10. Automation of Measurements and Analysis……116

X. PLANNING MEASUREMENTS, AND DETERMINING MEASUREMENT PARAMETERS……..……...……119
X.1. Dimensioned Sketches for Planning and Performing Measurements……..119
X.2. Equipment Walk-down, Radiation Survey, Determining Deposit Width ***w***……122
X.3. Use Width and Spacing of Equipment to Bound Measurement Distance ***r***.....124
X.4. Determine Measurement Spacing ***l*** and Count Time ***t***……125
X.5. Mark/Tag Measurement Locations, Define Coordinates……127

XI. IMPLEMENTING HOLDUP MEASUREMENTS……...……129
XI.1. Three "M"s of Implementation: Measurement, Mapping, Monitoring ……..129
XI.2. Archiving to Support Future Measurements……...130
XI.3. Reporting for Communication within the Measurements Program……132
XI.4. Reporting for Accountability, Safeguards Closeout, Waste Compliance……...133
XI.5. Reporting for Criticality Safety Screening……134

XII. DOCUMENTING HOLDUP METHODS AND METHODOLOGIES…..…….136
XII.1. Documentation for Training, Assessment, and New Operations……..136
XII.2. Documentation for Reporting Results……...137

XIII. ACRONYMS AND ABBREVIATIONS ..……...……138

XIV. ACKNOWLEDGEMENTS ……..……140

XV. REFERENCES……...……141

ABSTRACT

This document is a guide for planning and performing measurements of nuclear material holdup using portable gamma-ray spectroscopy. Its focus on nuclear materials standards, measurement equipment and detectors, calibration models, measurement protocols, analysis algorithms, and error determination for holdup measurements is of particular interest to specialists in quantitative nondestructive gamma-ray measurements. Aspects of this focus are also of interest to the organizations that use the measurement results: safeguards, criticality safety, and waste management in particular. Those sections that describe the relationship between the required holdup measurements and (i) process history and design and (ii) facility status and (iii) "customers" of holdup measurements and those that deal with the (iv) planning, (v) implementing, and (vi) documenting holdup measurements will also serve interests of the operations groups responsible for setting up holdup measurement programs and organizations. The sections on verification and validation of holdup measurements and those that discuss the treatment of systematic effects on the measurement results address the additional interests of regulators of nuclear safeguards, criticality safety, and nuclear waste management.

I. INTRODUCTION AND SCOPE

Gamma-ray spectroscopy is an important technique for the measurement of quantities of nuclear material holdup in processing equipment. Gamma-ray spectroscopy is isotope specific in measurements that quantify mass or determine isotopic distributions. Spectroscopy allows independent measurements of single or multiple isotopes. Gamma-ray detectors can be collimated and shielded against background. The detectors with shielding, along with associated spectrometer electronics, can be highly portable for measurements throughout the plant including areas of limited access.

Because the equipment in large facilities such as those dedicated to uranium isotopic enrichment, uranium or plutonium scrap recovery, or various stages of fuel fabrication is extensive, the total holdup may be large by its distribution alone, even if the average deposit thickness is small. Good safeguards practices include unbiased measurements with the smallest uncertainties possible. Even a small relative bias in the overall result for holdup in a large facility can translate to a significant quantity. Unbiased measurements of holdup also contribute to reduced operations costs for safeguards, criticality safety, and management of waste. Quantitative measurements of the deposits in low-enriched uranium processes (enrichment or fuel fabrication) can also mitigate safety risks from mechanical instability caused by very large accumulations that fill and block flow in large-diameter piping and ductwork.

Processing equipment can be massive as well as extensive. Equipment for high-throughput operations may also contain localized multikilogram deposits during operations and when shut down. Measuring the in-process inventory in such cases challenges the capabilities and compromises the accuracy of gamma techniques because of very large attenuation effects by equipment and deposits. Neutrons are highly penetrating and, therefore, applicable to measuring large deposits contained in massive equipment. Although neutrons are difficult to shield, counting coincident neutrons from plutonium spontaneous fission is effective at reducing background. Large polyethylene-moderated ^{3}He slab detectors used to quantify in-process plutonium in glove boxes are most successful as safeguards tools for internal material control and accountability (MC&A), inspector verification of operator declarations, and support of mixed-oxide fuel fabrication.[1-3] Although the spontaneous-fission neutron yield from uranium is relatively low for coincidence counting, the high α,n neutron yield from fluorine enables measurements of uranium deposits using total neutrons from holdup of uranium as UF_6 and UO_2F_2 in enrichment plants.[4, 5] These and other important measurement techniques are the subject of a future application guide on neutron measurements of plutonium and uranium in-process inventory and holdup.

Quantitative measurements of holdup benefit from simple, generalized procedures that enable performing and analyzing thousands of measurements. This guide presents a useful approach to portable gamma-ray measurements that invokes simple geometric models (point, line and area) to describe the deposits.[6-14] It describes the corresponding methodology for self-consistent application to calibration procedures, measurements, and the analysis algorithms that address most deposits, despite the essentially unique geometry of each. It details generalized corrections that account for most departures of realistic holdup deposits from the original simple models. These corrections, which address both the geometric and attenuation models of holdup deposit, rely on a single parameter in an approach that compensates self-consistently for the uncertain knowledge of its magnitude. Because of the simplicity and generality of the generalized-geometry holdup (GGH) approach, portable measurements of deposits can be performed rapidly

plant-wide. Simple algorithmic guidance to formalize the process of optimally choosing hundreds of measurement distances, spacings and count times is described in this guide. Finally, formal but simple and available procedures for evaluating and combining random and systematic errors are illustrated.

The holdup algorithms presented in this application guide apply to deposits that are less than a maximum thickness for the gamma rays used to perform the measurements. The algorithms also apply to deposits for which gamma attenuation is dominated by the actinide material.

Automation of the measurement process, reduction and analysis of spectral data, and computation of plant-wide holdup[11-13] are readily achieved with this generalized approach. The need for ready user access to all of the (measurement and analysis) parameters in the automated analysis phase distinguishes the automation needs for measurements and analysis.

This report does not address quantitative approaches to portable gamma-ray measurements of holdup that *require* cryogenically cooled high-resolution (germanium) gamma-ray detectors. While such approaches – which have been developed both commercially and by facilities for internal implementation – are practical for holdup measurements of some equipment, they are not feasible for plant-wide measurements at hundreds or thousands of locations with access limitations. Large process modules located near the ground level (converters and compressors in a gaseous diffusion plant are examples) may be well suited for measurements with germanium detectors and may benefit particularly from the advantages of high resolution because of the complexity of this equipment.

This report is a guide for users in the application of generalized methods and methodologies of portable quantitative gamma-ray holdup measurements. The guide applies to implementation in domestic and international nuclear facilities and addresses the needs for holdup measurements by customers in safeguards, criticality safety, and waste management. The report compiles useful information and data. It documents technologies, methodologies, algorithms, and procedures that apply to portable holdup measurements based on gamma spectroscopy. Information and data in this guide are derived from the cumulative measurement experience in many different facilities. No single unified guidance, representative data set, or generic procedure applies to every facility. The unique design, history and operational culture (including safeguards, safety, *etc*.) of each facility dictate many requirements for these measurements. The information in this report is, in large part, a reminder of the considerations that dictate requirements for measurements. The specific models and methodologies do apply to all facilities, but their implementation will necessarily vary from one facility to the next. Specifying an institutional program for holdup measurements requires all four of the following:

- Understanding of the models, methodologies and technologies for measurements.
- Detailed knowledge of the facility.
- Knowledge of needs of (possibly multiple) customers for holdup measurement results.
- The experience of having performed the measurements plant wide.

II. SUMMARY

Routine portable nondestructive-analysis (NDA) measurements of in-process deposits of special nuclear material (SNM) use low- and medium-resolution gamma-ray spectroscopy and methodologies that are implemented with generalized models of SNM holdup deposits. The unique operation history and design of each facility along with the needs of its internal customers for the NDA results determine how these portable NDA techniques are implemented. This application guide focuses on the methodologies and models of holdup measurements. It provides detailed guidance on implementation of the NDA methods to potential users. It considers the impacts of operation history, process design, and the variety of customer needs for holdup measurement results on the design and implementation of the holdup measurement program. It recommends specific formal approaches for implementation.

Quantitative measurements of holdup are an essential part of nuclear safeguards and safety functions of an operating facility engaged in the processing of special nuclear materials. Portable nondestructive analysis of in-process SNM also falls on the critical path for the decontamination and decommissioning (D&D) of facilities that no longer process special nuclear materials. Prominent D&D interests – including safeguards, criticality safety, and waste management – rely on the portable NDA results to plan, schedule and carry out such functions of the D&D as 1) inventory-difference reconciliation and accountability closeout, 2) process cleanout, and 3) compliance with loading limits of waste containers for shipment and storage. The D&D project maximizes the emphasis on holdup measurements, brings unique demands to the needs for these measurements, and emphasizes the importance of implementation in operating facilities with a view toward future needs for D&D.

Implementing the routine portable NDA measurements of holdup is impacted not only by circumstances of the process history and equipment but also by staffing, standards resources, and the design of the equipment for portable NDA measurements. Customer expectations influence the design of the portable NDA measurements. The planning process for portable NDA measurements is of utmost importance in obtaining and using the most relevant information in designing each measurement activity. Sections III-V discuss these details.

Generalized geometric models and associated methodologies for portable NDA measurements of holdup have evolved in response to the variety of materials, deposit geometries, equipment descriptions, measurement environments, and access limitations associated with holdup measurements and in response to the very large number of portable measurements that must be performed to quantify holdup. The required standards and other reference materials are described in Section VI. The detection equipment, which constrains the models and dictates spectrometer setup requirements, is discussed in Section VII with guidance and numerous examples that apply to holdup materials of greatest interest. Section VIII provides the detailed analysis algorithms, including analytical forms for propagated random uncertainty, to aid users in developing analysis tools. Details and examples of recommended procedures for measurements and analysis are given in Section IX. This includes approaches to quantifying systematic and total measurement uncertainty. Section X provides specific formal guidance for planning and performing measurements. The guidance emphasizes procedures that conform to the analysis models and adhere to established measurement control practices, both crucial to minimizing and quantifying systematic measurement uncertainties.

Section XI specifies requirements for implementing a holdup measurement program, starting with a description of the three functional deliverables of the measurement program. Maintaining up-to-date documentation of methods and methodologies meets the needs of providers and users of portable NDA results, satisfies formal requirements, contributes to the overall quality of the portable NDA, and reinforces optimal outcomes for ongoing operations or effective closure. Archiving 1) holdup measurement data, 2) detailed measurement results, and 3) the measurement plan for each process location sustains: ongoing operations, the practicality of future measurements, and the long-term integrity of holdup measurement results for inactive facilities that may apply to a D&D scheduled in the distant future. Section XII describes the multiple demands, immediate and long-term, for relevant documentation of the holdup methodology, emphasizing the importance of documentation.

III. IMPACTS OF PROCESS HISTORY AND FACILITY DESIGN

III.1. Process History

Holdup measurements are performed in domestic facilities operated for the US Department of Energy (DOE). Many facilities originally processed only low-burnup plutonium or high-enriched uranium. Others in the US and abroad perform measurements of plutonium, uranium, and mixed plutonium-uranium oxide in support of nuclear fuel cycles. As the DOE complex matured in several decades, the missions at some DOE facilities expanded to include high-burnup fuel-cycle material. Needs for R&D on nuclear materials, materials processing, and fuel-cycle concepts have further expanded DOE missions and consequently extended the range of material types in the processes. Downsizing trends also consolidate wider ranges of material types in common processing areas.

Measurements of holdup at most facilities in both the US and abroad must typically cover a substantial range of materials at each facility. Process history determines which materials may be deposited as holdup. The range of deposit thickness, presence of different material types (isotopic mixtures), and chemistry of the process in some cases influence or complicate the approaches required to perform holdup measurements.

The range of ^{235}U enrichment in some facilities includes depleted (0.3%) up to 97%, and that of ^{240}Pu at other facilities includes 3% to 45%. A special project such as the satellite radiological heat source program with processes dedicated to materials highly enriched in ^{238}Pu represents one of the many unique isotopic mixtures that require measurements by portable gamma NDA to determine holdup quantities.

Nuclear measurement techniques based on gamma rays or neutrons determine the mass of one or some – but not all – isotopes and must be weighted by the isotopic composition to obtain the total plutonium or uranium mass. Uncertainty in the isotopic composition results in uncertainty in the measured plutonium or uranium mass of holdup deposits. Therefore, process history that includes a range of nuclear material types can have an important impact on needs for portable holdup measurements. The combination of process knowledge, such as that described in the following paragraph, and direct measurements of the isotopic compositions of holdup deposits (Section VII.2) offers solutions to obtaining the required knowledge on isotopic composition of holdup deposits.

A recent study[15] uses the documented history in each process line of a particular facility undergoing D&D to estimate the average plutonium and uranium isotopic composition in each line from the component compositions weighted by throughput. The historic data, as well as data on the last materials processed in each line, produce two distinct “isotopic mappings” of plutonium materials deposited throughout the process. Agreement between the “theoretical average” and “last” isotopic distributions in some process locations contrasts with differences as large as a factor of two for ^{240}Pu and approximately 1.1 for ^{239}Pu at other locations.

The accuracy of direct gamma-ray measurement of the usually dominant ^{239}Pu isotope suffers the least from uncertainty in the plutonium isotopic composition. Such direct measurements use gamma spectroscopy and rely on the 400-keV energy region in which gamma rays of ^{239}Pu dominate. However, gamma rays from other isotopes such as ^{241}Am, ^{237}Np, and ^{22}Na can interfere with the measurements of ^{239}Pu in this energy region. The presence of each of these

isotopes increases with increasing burnup of the reactor fuel. Particular chemical processes contribute to the presence of ^{22}Na as well. Therefore, process history also influences the interferences encountered in gamma-ray holdup measurements.

Americium-241 grows in from the beta decay of ^{241}Pu to equilibrium in approximately 40 years. Near-depletion of ^{241}Pu from several decades of aging of high-burnup (high-^{241}Pu) material results in an ^{241}Am content near 10 weight percent. Alternatively, scrap recovery concentrates americium by aqueous or pyrochemical extraction. Corresponding process areas may contain holdup residues with americium fractions comparable to those of plutonium. Both the Compton continuum from the 662-keV gamma ray produced in ^{241}Am decay and the discrete gamma rays near 376 keV from ^{241}Am decay can contribute to a positive bias in low-resolution gamma-ray measurements of plutonium. A further complication with americium is that the α,n neutron yield from high-americium oxides or other americium compounds increases with ^{241}Am content, reducing the precision of neutron coincidence measurements of plutonium in large deposits that might also be difficult to measure with gammas. Attention to the choice of gamma-ray detector and spectral analysis regions is necessary to avoid the interfering effects of ^{241}Am, as described in Section VII.1.

The ^{241}Am alpha-decay daughter is ^{237}Np, which may also follow plutonium in aqueous chemical separations. In-growth of ^{237}Np does not reach equilibrium and, therefore, the ^{237}Np content increases with time. A direct interference from its decay gamma-ray at 416-keV eliminates the use of certain gamma-ray detectors in measurements of plutonium when the neptunium content exceeds several hundred ppm by weight relative to plutonium, as described in Section VII.1.

Sodium-22, a positron emitter, comes from fluorine presence, an outcome of PuF_4 production or contamination from aqueous processing, *etc*., in high-burnup process materials. It builds up to equilibrium in seven to eight years as the ^{19}F(α,n) reaction product. Compton continuum from the 511-keV gamma ray produced in ^{22}Na decay can also contribute to a potential positive bias in measurements of plutonium deposits with low-resolution gamma-ray detectors. The very high α,n neutron yield from ^{19}F generally eliminates the use of neutron coincidence measurements of plutonium in large deposits with significant fluorine contamination. Attention to the choice of gamma-ray detector and spectral analysis regions is necessary to avoid the interfering effects of ^{22}Na, as described in Section VII.1.

Process history influences the range of uranium enrichment, which in turn influences the manner in which holdup measurements may be performed. The accuracy of direct gamma-ray measurement of the ^{235}U isotope is most affected by uncertainty in the uranium isotopic composition for low-enriched (<20% ^{235}U) material but is also significant in high-enriched uranium if the isotopics cover the full range of enrichment up to 97% ^{235}U. The 186-keV gamma ray is commonly used in holdup measurements of uranium for its high specific yield. An additional need for knowledge of the gamma isotopics comes from the relatively high attenuation of gamma rays at this lower energy. Correcting for self-attenuation effects, which are influenced by the total uranium content of the deposit and may be substantial at 186 keV, requires knowledge of the isotopic composition.

The 1001-keV gamma ray from the ^{238}U/^{234m}Pa equilibrium (achieved in ~3-4 months, or 4-5 ^{234}Th half lives) decay produced in ~1% of ^{238}U decays might be measured instead of the 186-keV gamma ray produced in ~50% of ^{235}U decays when the uranium enrichment is low and deposits are large. The higher-energy gamma ray, whose net yield despite a low branching ratio

is comparable to that at 186-keV for low-enriched materials, is less attenuated by large deposits and processing equipment. This is helpful when deposits are large and shielded by thick equipment, but measurements of the higher-energy gamma ray also require larger detectors and particular attention to measurements of background, as discussed in Section VII.1.

Process history may include the use of recycled uranium as feed. Some domestic operations and most throughout the world use recycled uranium from the reprocessing of reactor returns. The equilibrium gamma ray at 238-keV produced (after ^{212}Pb beta emission) near the bottom of the ^{232}U/^{232}Th decay chain interferes with the low-resolution analysis of the 186-keV peak of ^{235}U in recycle material. Attention to the choice of gamma-ray detector and spectral analysis regions is necessary to avoid the interfering effects of this ^{232}U decay-product gamma ray, as described in Section VII.1.

III.2. Facility Design

The design of a nuclear processing facility, like the process material, influences and often complicates the approaches required to perform holdup measurements. Facilities in need of holdup measurements cover the extremes: from high-throughput plutonium chemical separations processes in shielded and remote canyons to small (hood-size) test processes for uranium. Facility requirements for uranium enrichment represent a special case in which equipment is massive and extensive beyond requirements for other types of processing. However, the equipment in a reprocessing plant is composed of repeating mechanical units. The process material tends to be chemically uniform, without radiological impurities and is isotopically defined within a specified range. Except for enrichment facilities, aqueous separations processing (spent-fuel reprocessing or scrap recovery) is most demanding of process equipment and space, and pyroprocessing (also for reprocessing spent fuel or recovery of scrap) is least demanding of space. High-throughput solids processing (oxide production and fuel fabrication) is often carried out in continuous automated processing with massive equipment. Impacts of facility design are treated in documentation by the Nuclear Regulatory Commission on design considerations for minimizing holdup in wet,[16] dry,[17] and drying[18] processes.

The process equipment within a plutonium facility is assembled within the secondary containment of a glove box, restricting direct access to the surfaces of the process equipment. This limitation adds to reliance on engineering drawings for equipment dimensions and measurement distances and increases the shielding of gamma rays used to quantify holdup. The higher-energy gamma-ray spectrum of ^{239}Pu compared to that of ^{235}U compensates in part for this additional shielding. Direct physical and visual access to the uranium processing equipment is a benefit in determining the best information on mechanical parameters and in accurate positioning of detectors for measurements. Additional benefits apply to measurements of in-process solutions, which are best performed at contact with equipment.[19, 20]

Measurements in high-contamination or high-radiation areas are performed manually in supplied air or remotely. Because of the great difficulties associated with such measurements, the detection equipment may be overdesigned. The use of unusually heavy detector shielding to minimize background[21] and high-resolution detectors to eliminate interferences are both extra assurances that repeat measurements will not be required in the most difficult measurement environments.

Equipment for robotics-automated processing may fill – horizontally and vertically – the interiors of extensive glove boxes that are also unusually tall because the operator does not require access except for maintenance. Access to such equipment for measurements can be difficult.

Although the equipment in a uranium enrichment facility is extensive and massive, mechanical repetition contributes to simplification of the holdup measurement process, compensating in part for the large number of measurements that are required.

The exhaust ductwork of a nuclear processing facility should (but may not always) contain thin deposits. The total holdup may be large because of the extent of the ductwork. Measurement problems with ductwork may include high signal-to- background ratios for ducts in close proximity to bulk process material and access difficulties for ducts that are greatly elevated or belowground.

Glove boxes and other process equipment may incorporate shielding that is removable for certain operations or maintenance needs. It is a great benefit to portable gamma measurements of holdup to perform measurements with the shielding removed in order to improve physical access, visual access, and gamma-ray signals. Back-to-back positioning of glove boxes is a floor-space saving measure that limits measurement access from one side of the glove box and often concentrates sources of high background in the field of view of the detector. Extending glove boxes down to nearly floor level also makes better use of space in process areas but challenges the ability to perform measurements of deposits on the glove-box floor.

III.3. Excluded Nuclear Material Forms

The term holdup usually applies to nuclear material that adheres to the surfaces of process equipment, but can also include residual material that accumulates as “heels” in tanks or other vessels. Heels can be thin layers of solids, or possibly solutions or sludge. Furthermore, holdup can accumulate on the surface of certain particulate filter media rather than on the surface of process equipment. Solutions, sludge, or surface deposits on powdered filter media are forms of nuclear material that cannot be treated by the methodologies described in this application guide.

The holdup algorithms presented in this application guide apply to deposits for which gamma attenuation is dominated by the actinide material. This includes most solid deposits, and does not include solutions, oily sludge, and certain filter media such as Al_2O_3 (alumina) for which gamma attenuation by other than the actinide material equals or exceeds the attenuation by the actinide. Generalized procedures for measurements of residual nuclear materials of this description, which also apply to quantifying nuclear material inventory in bulk solutions, are documented elsewhere.[19, 20]

IV. IMPACTS OF CUSTOMERS AND STATUS OF FACILITY OPERATIONS

IV.1. Operations Status

The status of facility operations defines the customer base for portable NDA of holdup. The discussions below reduce operations status in the lifetime of a facility to two categories: operational and D&D.

Holdup measurement data obtained in an operational facility contributes to knowledge useful to the operator for process control. When the operations organization manages the cleanout of process materials for D&D, the holdup measurement data also contribute to improved understanding of the status of the cleanout efforts. These obvious benefits to the operations organization are not discussed further in the discussions below, which focus on the interests of the safeguards, safety, and waste management in the quantities and distributions of holdup.

Safeguards and criticality safety are prominent in the customer base for portable NDA of holdup at any period in the lifetime of a facility. Measurements of in-process inventory and holdup in international safeguards are performed in operating facilities for internal material control and for verification by safeguards inspectors of operator-declared of SNM inventory.[1, 2] These measurements serve domestic safeguards functions of accountability for SNM or verification of in-process inventory in operating facilities.[19-25] Nonetheless, driving forces for portable NDA programs developed to measure holdup at some operating domestic sites also include environmental management concerns for criticality safety and controls on emissions.[24-29] A facility whose operations are shut down temporarily with a plan for restart will sometimes need to extend portable NDA measurements performed with holdup measurement equipment to materials other than holdup (using methodologies different than those used for holdup) in order to satisfy safeguards requirements.[20] When a facility enters D&D the prominent interests of waste management in holdup measurements combine with those of safeguards and criticality safety.

The transition to D&D has other impacts on portable holdup measurements besides the addition of a major customer. The importance of validating holdup methodologies and verifying the measured quantities is magnified during D&D. The D&D causes order-of-magnitude increases in measurement needs because sampling approaches that might be used during inventory periods no longer apply, the customer base is expanded, and demands of the shutdown schedule on the critical-path tasks are great. Measurements under D&D must address the full breadth of isotopic, radiological, chemical, and mechanical variation in the deposit materials. Methodologies that are the most versatile mechanically, spectroscopically, and analytically become most useful in this circumstance. The D&D requires valid and defensible but realistic approaches to estimating and propagating measurement uncertainty for the variety of equipment measured. The need to determine the isotopic composition of deposits on line becomes important under D&D. The need to staff up for portable measurements of holdup under D&D results in an initial burst of inexperienced measurements personnel. Once fully trained and experienced the complement of qualified measurements personnel must be retained through the period of critical tasks.

The direct customers of portable NDA for holdup measurements are the internal organizations (supported by operations funding or by the D&D project) for safeguards, safety and waste management. Counterpart organizations in the DOE for safeguards, safety, and waste

management are ultimate recipients of several variations of the (measured) holdup declaration for domestic DOE facilities.

A prevailing customer need for the best measurements places demands on portable gamma-ray NDA to optimize holdup results for operating facilities as well as D&D. Safeguards customers of portable holdup measurements are familiar, possibly from years of interaction, with benefits and limitations of models used to quantify nuclear materials in the deposits of an operating process. Additional demands of D&D require further understanding on the part of safeguards customers plus new familiarization for criticality safety engineers and waste management personnel in the use, capabilities and limitations of portable gamma-ray NDA for holdup measurements.

IV.2. Safeguards Customers

The safeguards function includes adjustment of the inventory difference (ID) based on portable NDA measurements of material in the process. The objective is a balance between material input and output, or a net ID of zero. This objective impacts the portable NDA measurements with the requirement of optimized measurement methods and procedures to give accurate results for holdup and a thorough understanding of measurement uncertainties. Impacts on costs are discussed in the following paragraphs. While these discussions are generic, the DOE Order[30] and Manual[31] for control and accountability of nuclear material specify inventory requirements and safeguards categories. Unmeasured holdup is defaulted to the safeguards category of the facility.

The material balance in an operating facility with changing input and output is dynamic. High throughput in specific processes can dictate the need for holdup measurements in these particular process lines during inventory periods. The uncertainty in the measured holdup contributes to the limit of error in the ID (LEID). One example of impact on cost of reduced uncertainty in holdup measurements is that a smaller LEID can reduce the required frequency of inventory.

The material balance during D&D is static in that both input and output quantities go to zero. As process material is removed, the D&D site (or facility within the site) approaches limits for increasingly diminished safeguards categories. The cost of safeguards and security decreases accordingly if confidence in the knowledge of quantities of material remaining in the process is sufficient to downgrade security for a diminished safeguards category. Other reports discuss some of the many impacts of the D&D project on approaches to MC&A[32, 33] and the corresponding role of holdup measurements.[34]

Holdup measurement results reported for safeguards purposes generally require the quantity of isotope and element – and their uncertainties – for a given area in which a material balance is drawn. Therefore requirements to map the distribution of deposits within what may be a large area do not exist specifically for safeguards. This can simplify the measurements of holdup, in some cases, because groupings of equipment can, within the limits of the methodology, be measured as a single unit of equipment. Nonetheless, large accumulations of process deposits can cause uncertainty in the measured holdup, raising the LEID to limits that dictate process cleanout. Knowledge of the distribution of deposits in an operating facility reduces the cost of such cleanouts dictated by safeguards requirements. Knowledge of the distribution of deposits in a facility under D&D primarily supports the interests of customers other than safeguards.

IV.3. Criticality-Safety Customers

The criticality safety function includes ensuring that accumulations of nuclear materials in process equipment do not exceed safe limits. This requires estimating at a high level of confidence the largest deposit quantities that could be present, consistent with the best knowledge of these deposits and their expected rates of increase. Such knowledge is provided by the individual portable NDA measurements of holdup deposits.[35]

The safety engineer requires this conservative knowledge of both the quantity of the deposit at each location and the distribution of the deposits within process equipment. The information must be updated regularly for safety in an operating process. It must be maintained throughout any cleanout process, whether the facility is operating or under D&D, until materials are packaged within safe limits in containers.

Regarding the packaging of materials removed during cleanout, safety interests are served by ensuring that contents of waste containers comply with safe limits. The cost of underpacking containers is container excess. This increases requirements for measurements, storage, and transfer. Therefore, despite needs to estimate quantities conservatively for safety, the requirements of optimized measurement methods and procedures and a thorough understanding of measurement uncertainties prevail for the sake of safe but cost-effective operation.

Deposits of nuclear materials on surfaces of most glove boxes and on surfaces of a major fraction of process equipment, especially exhaust equipment, may be small enough (less than 0.001 g SNM per cm^2 or less than 540 g on all interior surfaces of a 6-m by 3-m by 1-m glove box, for example) to neglect corrections (of less than 0.1%, in this case) for self-attenuation. This will not be the case for accumulations in bulk-processing equipment, nor does it apply to material spilled on floors (likely to be analyzed as part of a surface) or in troughs and on ledges of a glove box.

Correcting for gamma-ray self-attenuation is an integral part of current holdup methodology. A common general procedure applies to self-attenuation corrections for “area” holdup deposit geometries (applicable to many surfaces) as well as “line” and “point” geometries. Inherent in performing these corrections is defining for each measurement location the measured areal density (mass per unit area) of the deposit. This measured quantity combined with the uncertainty in the quantity determines if a deposit exceeds a maximum thickness for the measurement gamma ray. Unless the material emits a much higher-energy gamma ray with sufficient intensity, a deposit that exceeds this thickness cannot be quantified by the passive gamma technique. Lacking other methods to measure the deposit, it is potentially unsafe. The use and limitations of this approach as a screening technique for unsafe deposits are described in Sections VIII.4.3 and IX.6.

Optimized portable gamma-ray NDA for holdup measurements requires implementing the fully developed and validated methodology. Implementing the fully developed methodology offers the benefit of screening, within limits, for unsafe deposit thickness. (Refer to Section XI.3) Applying numerical approaches to determine the realistic total uncertainty in the portable holdup measurement result (refer to Section XI.3) provides an upper limit for each measured deposit to be compared to the limit for unsafe deposit thickness. Quantitative gamma-ray holdup measurements can contribute significantly to assurances of the “incredibility” of deposits that are critically unsafe.

IV.4. Waste-Management Customers

The waste management function during a D&D is aligned with that of criticality safety in the need for estimates at a high level of confidence of the largest deposit quantities that are possible, consistent with the best knowledge of the deposits. The interests of waste management regarding the packaging of waste containers include ensuring that the nuclear material content of the waste containers does not exceed shipping limits.

Loading limits on waste containers vary greatly with the type of waste and the waste-storage site. Refer to published criteria for low-level or mixed waste shipped to the Nevada Test Site (NTS)[36] or for transuranic waste shipped to the Waste Isolation Pilot Plant (WIPP)[37] for examples.

The costs of repacking a single waste crate are very high. Nonetheless and analogous to the safety issue on packaging, the costs of underpacking large crates come from the substantial costs to pack, measure, ship and store excess crate. Therefore, despite needs to estimate quantities conservatively for waste shipments, the requirements of optimized measurement methods and procedures and a thorough understanding of measurement uncertainties prevail for the sake of cost-effective waste-management operations.

Like the safety engineer, waste management requires knowledge of both the quantity of the deposit at each location and the distribution of the deposits within process equipment, in principle. Nevertheless, administrative controls that track the measured deposit quantities from the time of the on-line measurements to the loading of contaminated process equipment parts and contents into waste crates are most often unrealistic in practice because of the circumstances of equipment breakdown. Waste crates placed alongside the equipment breakdown operations are loaded as the operations proceed in environments with airborne contamination requiring multi-layer anti-contamination clothing with respirator protection in most cases.

It has been more effective for portable-measurements personnel to measure the individual parts and other contents of process equipment as each piece is broken off from the bulk and "packaged", before loading each item into the crate, than to relate each part to a previous measurement of holdup. Such measurements of the broken-out parts and contents of the process may proceed using the same equipment and measurement methodology that was employed when these components were measured within the process. While these holdup measurements of the packaged equipment may be adequately bounding, an additional set of quantitative measurements is required in support of waste management alone. Optimized results rely on implementing the fully developed methodology to minimize the waste-management costs incurred by underpacking.

The portable measurement capability utilized to quantify deposits in packages of process equipment prior to loading in waste containers may be useful in some circumstances for identification of other isotopes whose presence is unexpected. However, this type of screening is far more effective with commercial tools, equipped with large high-resolution detectors and not necessarily portable, designed optimally for isotope identification.

IV.5. Other Health and Safety Customers/Concerns

The accumulation of holdup deposits incurs safety risks beyond those of criticality safety. Interests of radiation safety are served by the information obtained in measurements of holdup. Knowledge of deposit quantities and the expected rates of accumulation of deposits that is

provided by the results of portable NDA measurements of holdup contributes to a capability to assess expected radiation dose rates in process areas over time. The circular aspect in this case is that radiation dose is incurred by personnel who perform the portable gamma-ray measurements of holdup deposits.

The case of low-enriched uranium (LEU) holdup deposits can also involve additional safety risks from mechanical instability caused by very large accumulations that fill and block flow in large-diameter piping and ductwork. The phenomenon of larger deposits is an outcome of the significantly higher accountability and criticality-safety limits – often corresponding to larger dimensions of process equipment – for LEU compared to limits for similarly processed high-enriched uranium (HEU) in the same chemical forms.

An undetected blockage of process flow can lead to subsequent rapid accumulation of material upstream of the blockage. Air leaking into process equipment in older enrichment facilities has caused buildup of solid oxide forms (principally UO_2F_2) from chemical reactions with UF_6 gas, which eventually manifest in high measured differential pressures as near-blockages develop. Equivalent concerns arise in vacuum and ventilation equipment in LEU-fuel fabrication facilities. Routine measurements of deposits within the process lines can mitigate this type of safety issue.

A serious safety issue is the buildup of solid deposits in large ventilation ducts to masses that exceed the mechanical tolerance of the ductwork. Such issues arise when criticality-safety risk limits are less restrictive, as for LEU, and allowed dimensions of equipment are very large. Mitigating the risk of the collapse of such equipment should include a combination of filtration of process-exhaust feed streams to these ducts and measurements of the deposits.

The nuclear material safety category is a significant influence on costs for a facility that handles or has handled special nuclear materials. The cost of demolition of such facilities is also significantly influenced by the nuclear material safety category. However, the cost benefit of reducing the holdup in a plutonium facility that is under D&D to below safety Category 4 (8.4 g Pu), for example, cannot be realized unless the holdup can be measured by validated NDA techniques for quantitative holdup measurements established and documented. Therefore, the benefit of maintaining the quantitative holdup measurement capability persists both throughout the operational lifetime of a facility and throughout its D&D.

V. PERSONNEL FOR HOLDUP MEASUREMENTS

Personnel who respond directly to the portable NDA functions for holdup measurements include scientific staff and measurements staff. The scientific staff must be fully capable of fulfilling the responsibilities of the measurements staff as well as a wide range of unique assignments. Other essential personnel groups interact with scientists and measurements staff in planning and performing measurements and analyzing the data.

V.1. Scientific Staff

The range of assignments unique to the scientific staff normally includes the following.

- Design and specify measurement equipment, detectors and sources
- Develop, formally document, and maintain methodologies (including software) for measurements, analysis, and error propagation
- Specify and oversee the calibration of measurement systems, validation of calibrations, and archiving calibration results and data
- Specify, implement, monitor and archive measurement control for each system
- Verify the needs of the direct customers for each set of measurements
- Plan measurements including documenting of measurement plans, ensuring involvement of measurements personnel with the appropriate training and instruction for each set of measurements, and scheduling
- Oversee holdup measurements (implementation of measurement plan), which often require hands-on participation
- Oversee and (usually) perform the analysis of holdup data and uncertainty
- Formally document the measurements, report the results, and archive results and data

The breadth of this range of assignments requires individuals who are trained and experienced as scientists; are knowledgeable and experienced in portable NDA measurements; are experienced with facility operations, organization, and procedures; and understand the reporting requirements. The scientist must be thoroughly familiar with the models used to interpret holdup measurement data in order to specify methods and procedures for implementing the models (acquiring the data as well as analyzing it) that are consistent with the models. Because measurement campaigns emerge regularly with requirements that deviate from those of other campaigns, the scientists must be able and qualified to perform the measurements as well.

V.2. Measurements Staff

The range of assignments for the measurements staff normally includes the following.

- Set up, operate and adjust/trouble-shoot portable NDA measurement equipment, nuclear (usually gamma) detectors, and sources.
- Implement documented procedures for operating portable measurement systems, acquiring holdup measurement data, and maintaining measurement control.
- Implement documented procedures for calibrating portable measurement systems and validating calibrations while maintaining measurement control.

- Implement documented measurement plans by performing holdup measurements consistent with the plan, maintaining measurement control
- Supplement documented procedures for equipment operation, calibration, and holdup measurements with additional measurements and observations when the scheduled measurements alone appear insufficient to obtain the information required

The measurements staff must be familiar with operation of the measurement equipment, expectations of spectral data, measurement control procedures, and principles of gamma spectroscopy in order to respond to the first four requirements in which documented procedures govern the activities. It is also most important for measurement staff to be familiar with the models used to interpret holdup data in order to satisfy the fifth requirement listed above and, in most cases, to correctly exercise judgment in executing the documented procedures.

Judgment, supplemental measurements, and observations are required routinely for holdup measurements. These demand an understanding of how particular decisions (on distance, angle, position, subsequent position, intervening equipment, *etc*.) made in the course of the portable gamma measurements influence the quantitative measurement result. It is costly to implement separate measurement activities that require additional access to facilities on another day with different personnel and equipment, repeating earlier measurements for reference, perhaps with different radiological backgrounds and possibly under different environmental (temperature, *etc*.) circumstances in order to supplement holdup measurements with additional data to account for the circumstances not included in the original measurement plan.

Measurements personnel either require a scientist's supervision or, ideally, training (preferably hands-on) in understanding of models and methodologies of holdup measurements in order to be able to exercise judgment in execution of a measurement plan or to supplement the prescribed procedure and work plan as necessary. An understanding of NDA principles and the models used to analyze the portable NDA guides the many choices available to personnel performing portable NDA measurements and is an important key to measurement quality.

The combination of training and measurement experience required for measurements staff to perform holdup measurements independently is substantial. Once training and measurement experience are acquired, maintaining the core of trained and experienced measurements personnel is an important key to success of a large scale program of holdup measurements such as that required for D&D.

V.3. Personnel for Planning, Implementation and Analysis

Process engineers are essential contributors in the planning and execution of any holdup measurement campaign. Process engineers provide access to information on operation history, process chemistry, and equipment design.

The engineer's knowledge of history provides insight on possible isotopic mixtures that comprise holdup deposits. Even the rare single-mission facility or process is likely to have treated a range of plutonium or uranium – sometimes both – isotopic compositions. The decision to either assume process knowledge[15] for the isotopics or measure isotopics *in situ* by NDA or sampling is often a trade-off between lower costs and improved accuracy.

The engineer's knowledge of the process and its chemistry also offers insights on the nature of deposits. An obvious example is gaseous enrichment, which may produce deposits on all equipment surfaces, while major deposits from aqueous processing would tend to accumulate at the bottom of the process cavity, etc. Information on the location and distribution of deposits is important for mapping the holdup measurement locations and for later interpretation of the holdup measurement data in the analysis phase.

Knowledge of equipment design is important on several levels. The process engineer can provide mechanical design information at the process level, which gives equipment (material, thickness) needed to correct measured gamma count rates for attenuation. The alternative of measuring the thickness and inferring composition and density of equipment and containment materials can be time-consuming, costly, and subject to error.

Operations personnel are major and essential contributors in the measurements phase. Operations personnel know the locations of large accumulations of materials. They are also aware of modifications to the original design, which may include the addition or removal of shielding materials, and have knowledge of radiological materials other than holdup deposits that are stored in the process or in process areas.

Operations personnel understand where multi-kilogram deposits accumulate: within the cavities of dense high-throughput bulk-processing equipment, or in visually obscured and shielded crevasses in a hood or glove box in which spilled materials collect. Such deposits might be missed by the measurement techniques without such knowledge. Knowledge of large accumulations is also important for planning holdup measurements in that the routine gamma measurement procedures may not apply for such deposits if thicknesses exceed attenuation limits for gamma-ray measurements or if locations are not accessible to gamma measurements.

The removal of shielding materials (temporarily for ongoing operations and possibly permanently for D&D) can be a major contribution of operations personnel to measurements of holdup. Shielding can be responsible for bias in holdup measurements if its presence or dimensions are unknown. Shielding also attenuates the radiation signal, which reduces the precision of the measurement or increases what otherwise may be short count times and minimal presence of measurements personnel in the process areas. Finally, shielding can obscure visual access to the process equipment, which limits the ability of measurements personnel to position detectors optimally and judge measurement distances accurately.

Operations personnel are also aware of the locations of interim storage of bulk materials that can interfere with holdup measurements by their (temporary and possibly unknown) presence in the field of view or in the background. The former leads to measurements that are biased high in that material in interim storage will be permanently relocated and already has an accountability value. As a background contributor, stored material can contribute to substantially degraded precision in the holdup measurement. Operations personnel can often relocate material in interim storage until measurements are complete. If this is not possible, it is most important that measurements be designed with the knowledge of the presence and locations of such materials.

Prior to performing holdup measurements, operations personnel may possess the only existing knowledge of certain deposit quantities and distributions based on historical experience and results of cleanouts, or other means. The participation of such personnel in the planning phases of holdup measurements as well as in the review of measurement results is valuable both for

optimizing the measurement design and ensuring consistency of the result with historical or by-difference data.

Radiation safety personnel are important contributors in the measurements phase, particularly if shielding has been removed in order to improve measurement quality. While individuals are responsible for the safety of their work, the job of the measurement staff is compounded if they must perform nonquantitative radiation surveys for safety in addition to quantitative portable gamma measurements. The radiation survey postings are important safety guidance for measurements personnel but also offer guidance to knowledgeable measurements staff on the distribution of certain isotopes whose emissions dominate the survey readings.

Statisticians may contribute to planning as well as analysis of holdup measurements. Facilities in which holdup is measured regularly on a sampling basis may involve the statistician – along with operations and safeguards personnel – in developing the sampling plan. The complex propagation of holdup measurement uncertainty can also benefit from the contributions of a statistician.

VI. STANDARDS FOR CALIBRATION, VALIDATION, AND FIELD VERIFICATION

VI.1. Calibration Standards for Measurements of Uranium and Plutonium

The geometry of each portable NDA measurement of process deposits is unique. Large variations in isotopic composition and a variety of interference possibilities are also characteristic of process deposits. It is not practical to consider developing standards that are representative of the range of expectations for the deposit materials and their geometries. The solution instead is to develop and adhere to models inclusive of the range. Section VIII describes the models in detail and Section IX.2 discusses alternative sources that may be used in place of the standards described below to measure geometric response. Nonetheless, a standard is required to calibrate the measurements for quantitative analysis of holdup based on these models. Quantifying holdup deposits using portable NDA measurements relies on i) a detector with a radially symmetric response and ii) positioning by an expert user so that the deposit conforms to a simple geometric model: usually point, line or area. Algebraic forms used in the calibration are derived from these simple models. The calibration also uses a well-characterized point standard of the isotope to be measured in a stable form (metal or compressed powder) with simple uniform geometry (sphere or disk), known packaging, and preferably small but calculable self-attenuation. Details on the calibration methodologies and procedures mentioned below are discussed in Sections VIII.3 and IX.1, respectively.

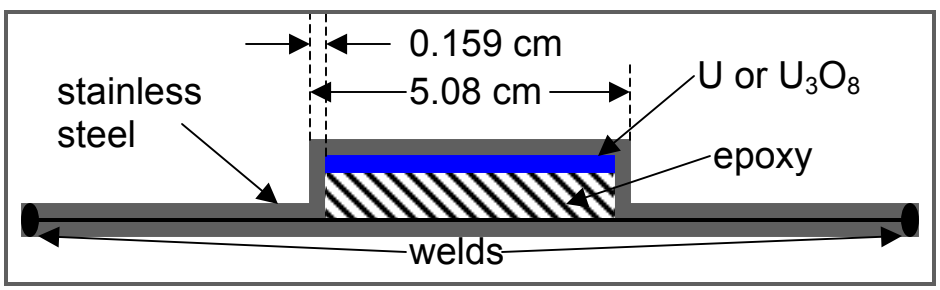

Figure VI.1. Encapsulated HEU holdup standards cover a range of thickness from 0.003 to 0.048 g U/cm^2 for the five oxides and 1.28-1.31 g U/cm^2 for the two metals. The ^{235}U enrichment is 93.2%.

Point standards of high-enriched uranium (HEU) are illustrated in Figure VI.1. These metal and oxide uranium standards were fabricated at Y-12 for use as calibration standards (oxides) measurement-control check sources (metals) and validation standards for uranium holdup measurements.[38] Table VI.1 gives the uranium mass and areal density of each five pressed-powder and two metal-disk standards. The self-attenuation correction factor for each is determined from the far-field form for a slab as indicated in the Table. The oxide is a certified reference material, and the metal is high-purity uranium oralloy. The self-attenuation effects, unlike those for the metals, are small in the range of oxide thickness. These are typical of holdup deposits, which rarely exceed 0.3 g U/cm^2. The calibration measurements with the oxide standards are usually performed at a distance of 40 cm, which is close enough to the nearly 5-cm-diameter standards to require corrections for this finite width.

Point standards of plutonium are illustrated in Figures VI.2 through VI.4. These metal and oxide plutonium working standards were fabricated at Los Alamos for multiple uses in NDA and are employed as calibration standards and validation standards for holdup measurements. The

plutonium mass and isotopics for the three sets of plutonium standards were characterized at Los Alamos by destructive analysis traceable to NIST.

Table VI.1. The Encapsulated HEU (93.2 % ^{235}U) Holdup Standards

ID	Form	g U	g U / cm^2	$CF_{186,\ SELF\ ATTEN}$
1	U_3O_8	0.044	0.0025	1.002
2	U_3O_8	0.086	0.0048	1.003
3	U_3O_8	0.214	0.0120	1.008
4	U_3O_8	0.422	0.0237	1.015
5	U_3O_8	0.845	0.0474	1.030
6	U metal	11.348	1.2756	2.21
7	U metal	11.694	1.3145	2.26

$CF_{186,\ SELF\ ATTEN} = \mu(\rho x) / (1 - e^{-\mu(\rho x)})$ See reference 39.

$\mu_{186,U3O8} = 1.26\ cm^2/g$

$\mu_{186,U} = 1.47\ cm^2/g$

Table VI.2 gives the plutonium mass, sphere diameter and self-attenuation correction factor for the five metal-sphere standards. The self-attenuation correction factor for each is determined from the far-field form for a sphere as indicated in the Table. Point geometry is well represented by the spherical shape, and the effect of the very small widths of these metal spheres is negligible in calibrations performed at a distance of 40 cm. A metal sphere, however, is highly attenuating for even the smallest mass and not typical of holdup deposits.

Table VI.3 gives the plutonium mass and areal density of the three metal-foil standards.[40] The self-attenuation correction factor for each is determined from the far-field form for a slab as indicated in the Table. The thickness of the thinnest foil is above the range of typical holdup deposits (which rarely exceed 0.3 g Pu/cm^2). Calibration measurements with the metal foils are usually performed at a distance of 40 cm, close enough to the 2-cm-diameter standards to require a small correction for the finite width of the foils. The four analogous sets of (three) plutonium metal foils reside at four different DOE sites for use as NDA standards.

Table VI.4 gives the plutonium mass and areal density of three oxide standards.[41] The oxide powder is pressed into a cylindrical cell. The self-attenuation correction factor for each standard is determined from the far-field form for a slab as indicated in the Table. The thickness of the thinnest oxide standard is at the upper end of the range of typical holdup deposits (which rarely exceed 0.3 g Pu/cm^2). Calibration measurements with the oxide standards are usually performed at a distance of 40 cm, close enough to the 2.7-cm-diameter standards to require a small correction for the finite width of the foils. The four analogous sets of plutonium oxide standards are intended for distribution to four different DOE sites for use as NDA standards.

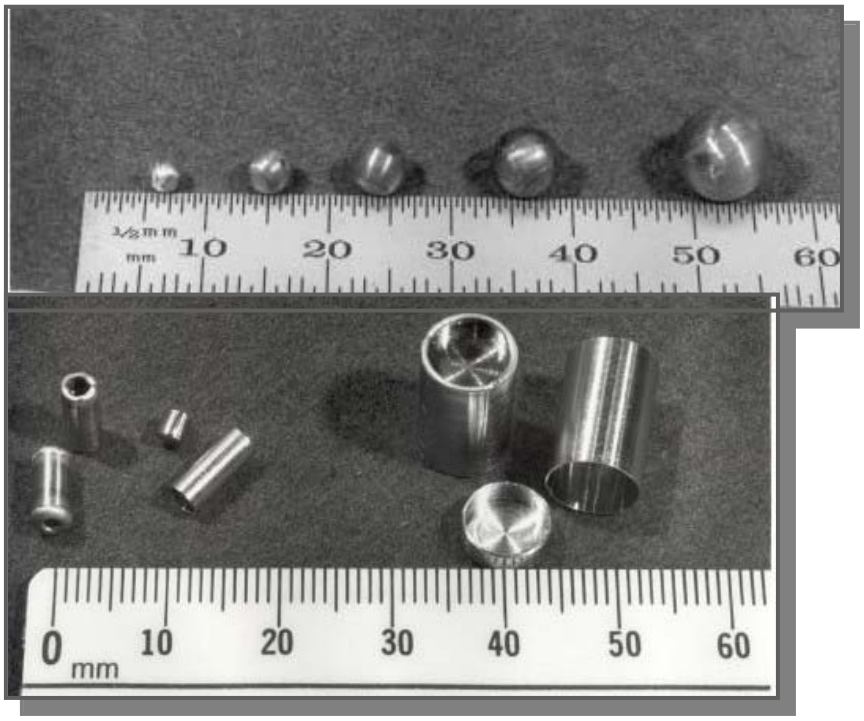

Figure VI.2. The five low-burnup (93.5% ^{239}Pu) plutonium metal spheres (0.2, 0.5, 1.0, 2.0 and 5.0 g Pu) are pictured before encapsulation. The capsules are shown below.

Table VI.2. The Low-Burnup (93.5% ^{239}Pu) Plutonium Metal Spheres

ID	Form	g Pu	D = Diameter (cm)	$CF_{414,\ SELF\ ATTEN}$
1	Pu metal	5.349	0.805	3.14
2	Pu metal	2.118	0.591	2.49
3	Pu metal	1.066	0.471	2.14
4	Pu metal	0.538	0.374	1.88
5	Pu metal	0.215	0.275	1.62

$CF_{414,\ SELF\ ATTEN} = [(3/2Z)[1 - 2/Z^2 + e^{-Z}(2/Z + 2/Z^2)]]^{-1}$ See reference 39.

$Z = \mu\rho D$

$\mu_{414,Pu} = 0.268\ cm^2/g$

$\rho = 19.56\ g/cm^3$

Figure VI.3. One of the five sets of encapsulated plutonium metal foil standards includes three thicknesses (0.6, 1.3 and 2.5 g Pu/cm^2). Each low-burnup (93.9% ^{239}Pu) foil has a 2-cm diameter.

Table VI.3. The Low-Burnup (93.9% ^{239}Pu) Plutonium Metal Foils

ID	Form	g Pu	ρx (g Pu / cm^2)	$CF_{414,\ SELF\ ATTEN}$
1	Pu metal	1.823	0.580	1.080
2	Pu metal	4.029	1.282	1.182
3	Pu metal	7.913	2.519	1.375

$CF_{414,\ SELF\ ATTEN} = \mu(\rho x) / (1 - e^{-\mu(\rho x)})$ See reference 39.

$\mu_{414,Pu} = 0.268$ cm^2/g

Precedents for calibration using mixed-radionuclide point standards are documented.[42, 43] Such approaches use standard interpolation methods to account for differences in detection efficiency between energies of the source gammas and the actual assay energies, and must also be corrected for the corresponding well known differences in specific disintegration rate (gammas per gram isotope per unit time). Safeguards requirements for representative materials may preclude the use of such standards. However, the increasing needs to measure deposits of radionuclides other than SNM, and also the increasing number of radionuclides now called SNM, may justify such approaches as not only practical but even essential, especially as these lists grow.

VI.2. Calibration Standards for Measurements of Low-Enriched Uranium (LEU)

Calibration standards for measurements of LEU differ from those for HEU. Low-enriched uranium is less than 20% (typically less than 6%) ^{235}U, but determining and reporting ^{235}U as well as total uranium are required for accountability. Accountable quantities and criticality safety limits correspond to much larger masses of LEU than those of HEU. Accordingly, process design and operations both allow relatively large deposits of LEU to accumulate in process equipment. Such deposits may exceed the maximum thickness for the relatively intense 186-keV gamma ray of ^{235}U, whose specific activity (43200 s^{-1}· g ^{235}U^{-1}) exceeds that of the 1001-keV gamma ray

from the equilibrium-daughter of ^{238}U decay by a factor of nearly 600. Quantifying LEU holdup requires detectors designed and calibrated for measurements at both 186 and 1001 keV.

It is possible, in principle, to use those HEU standards described above to calibrate for 186-keV gamma-ray measurements of LEU holdup. However, the gamma-ray energy spectrum of ^{235}U from LEU obtained with the relatively small detectors used for portable holdup measurements has a substantial Compton continuum from the scattering of high-energy gamma rays on which the 186-keV gamma-ray peak sits. While careful treatment of the continuum will avoid systematic effects of variations in its slope, such treatment is difficult with low-resolution detectors and is impossible for the relatively short count times – corresponding to poor statistics – associated with each of hundreds or thousands of holdup measurements.

A compromise is recommended for calibrating for 186-keV gamma-ray measurements of LEU holdup in which a shielded source of depleted uranium (DU, 0.3% ^{235}U) is used along with the HEU standard source to produce the Compton continuum without contributing additional counts in the low-energy (186-keV) region. The arrangement would include a mass (disk, ideally) of depleted uranium metal, which is abundantly available, whose ratio to the mass of HEU in the standard source is similar to the ratio of ^{238}U to ^{235}U in the LEU deposits. The geometric arrangement is a stack in which a disk of lead or tungsten, with an approximate thickness of 0.5 cm, whose diameter equals that of the DU, is placed between the DU and HEU standard source. The HEU standard source faces the detector to be calibrated. The same HEU standard source used to calibrate for 186-keV gamma-ray measurements of HEU holdup can be used in this way to calibrate for 186-keV gamma-ray measurements of LEU holdup.

The use of a depleted uranium metal standard is recommended for calibrating for 1001-keV gamma-ray measurements of LEU holdup. A standard of large mass is needed because of the low specific activity of the 1001-keV gamma ray ($73\ s^{-1} \cdot g\text{-}^{238}U^{-1}$). Precise knowledge of the dimensions of the standard is essential in performing corrections for gamma-ray self attenuation, which are substantial even at the high gamma-ray energy, because of the large mass. (A typical standard of depleted uranium, a metal disk of 500g with a diameter of 6 cm, has a self-attenuation correction factor determined from the far-field form for a slab of 1.8 for 1001-keV gamma rays.) The usual distance of 40 cm for the calibration measurements is close enough to the 6-cm-diameter standards to require a correction for this finite width.

VI.3. Standards for Validation of Holdup Measurements

Measurements to validate the holdup calibration are important because geometric models replace representative standards in the calibration process. Validation can be achieved by several approaches. More than one approach is often taken to meet specific needs, as described below. The approaches include

- measurements of working standards or other well characterized materials of the isotope to be measured, fabricated or selected to represent the geometries of point, line and area deposits,
- addition of working standards or other well characterized materials into the process for measurements along with in-process deposits,
- removal and external analysis of process material by other NDA (or DA) methods, and
- independent measurements of deposits by portable NDA methods other than the calibrated gamma-ray method.

The first two approaches rely on physical standards. The last two use other NDA techniques (DA in some cases) for reference.

Figure VI.4. One of the five sets of encapsulated plutonium oxide standards includes three thicknesses (0.4, 0.9 and 1.8 g Pu/cm^2). The oxide in each low-burnup (94.0% ^{239}Pu) standard is confined to a cylinder that is 2.7 cm in diameter.

Table VI.4. The Low-Burnup (94.0% ^{239}Pu) Plutonium Oxide Standards

ID	Form	g Pu	ρx (g PuO_2 / cm^2)	$CF_{414,\ SELF\ ATTEN}$
1	PuO_2	2.004	0.397	1.050
2	PuO_2	4.967	0.984	1.127
3	PuO_2	9.942	1.969	1.264

$CF_{414,\ SELF\ ATTEN} = \mu(\rho x) / (1 - e^{-\mu(\rho x)})$ See reference 39.

$\mu_{414,PuO2} = 0.248$ cm^2/g

Point standards such as those described in Section VI.1 used to calibrate holdup measurements of a given isotope can double as standards to validate the point calibration. Large thin uranium metal foils laminated in plastic have been configured as lines or areas. Uranium oxide powder has been suspended in binder material and, before hardening, poured into tubes for line sources. Uranium oxide powder has also been sprinkled onto surfaces painted with binder, which are laminated after the binder hardens. Paper or cloth saturated in a nitrate solution of uranium or plutonium has been dried flat and subsequently laminated. Contamination risks and the high costs of packaging to meet safety standards put practical limitations on the fabrication of plutonium standards by these methods. Alternatives that represent line deposits of plutonium include end-to-end arrangements of cans of dilute plutonium powder standards, and plutonium fuel pins. Some examples of standards or other well characterized materials fabricated or selected to validate holdup measurements are documented.[14]

The add-a-source approach involves measuring the SNM mass of process deposits using the calibrated holdup instrumentation and technique, introducing standards into the process, and remeasuring the SNM mass of the process deposits along with the standards. The difference between the two measurements is compared with the reference SNM mass of the combined standards. The approach applies well to plutonium process equipment because space is typically available alongside equipment within a glove box. Material introduced as standards can be fabricated as add-a-source standards. This might be required to address needs for specific deposit geometries such as extended lines in rotary or auger driven calciners.[22] On-line working standards that might otherwise serve to calibrate on-line NDA instruments could be distributed within plutonium glove boxes that are measured as areas.[1]

Deposited material measured as holdup can be removed from or introduced into the process and quantified separately by another method to determine its SNM mass. The difference between the holdup mass determined by the original measurements and that determined in a second set of holdup measurements (after introduction or removal) is compared with the SNM mass of the incremental process material.[19, 23, 44-46] Such validation measurements may be performed before and after a routine process cleanout but may require administrative controls to avoid combining removed material with other process residues before such material is quantified.

Alternative measurement techniques can sometimes be used to measure holdup and validate the results measured by the gamma-ray method. Neutron coincidence measurements performed with slab detectors can validate gamma-ray measurements of plutonium holdup. The neutron methods apply when deposits are substantial and may be preferred to gamma techniques for very thick deposits or unusually dense equipment.[1, 2, 44-46] Thermoluminescent dosimeters have also been used to measure holdup deposits.[47] Validation by alternative techniques can also be achieved by administrative controls on and tracking of process equipment that is disassembled and measured separately during the D-&-D process. Because tracking and administrative controls are often impractical during D&D of a facility, holdup measured for the entire facility prior to disassembly can also be compared to the sum of the measured SNM in the waste containers generated in the D-&-D process.[48]

One example of validation of holdup measurements is driven by the economy of the D&D. The facility uses gamma holdup methodology to measure packages (disassembled process equipment wrapped in plastic) as these items are loaded into crates or drums for shipment and storage. The measurements are performed on the packages establish compliance with loading limits prescribed by the Department of Transportation (DOT) or waste acceptance criteria (WAC) . Once filled, the crates or drums move to a neutron counter for measurement before shipment. Removing items from overfilled crate or drum is costly, as is underfilling to avoid that problem because of the consequences of extra shipping and storage. Figure IV.5[48] is a plot of the neutron counter (IPAN) results for each drum and the corresponding sum of package results obtained using the holdup measurement methodology as described in Section VIII. Packages added to the first eight drums were measured by positioning the gamma detector consistent with an “area” model of the deposit geometry. Packages added to the remaining forty drums were measured by positioning the gamma detector consistent with a “point” model of the deposit geometry. The value of comparison from the standpoint of validation of the holdup methodology is that the discrepancy between the neutron and gamma results for the first eight drums and agreement for the remaining forty suggest that “point” geometry is better suited to measurements of deposits in equipment segments. Refer to Section IX.9 for another viewpoint on gamma/neutron validation.

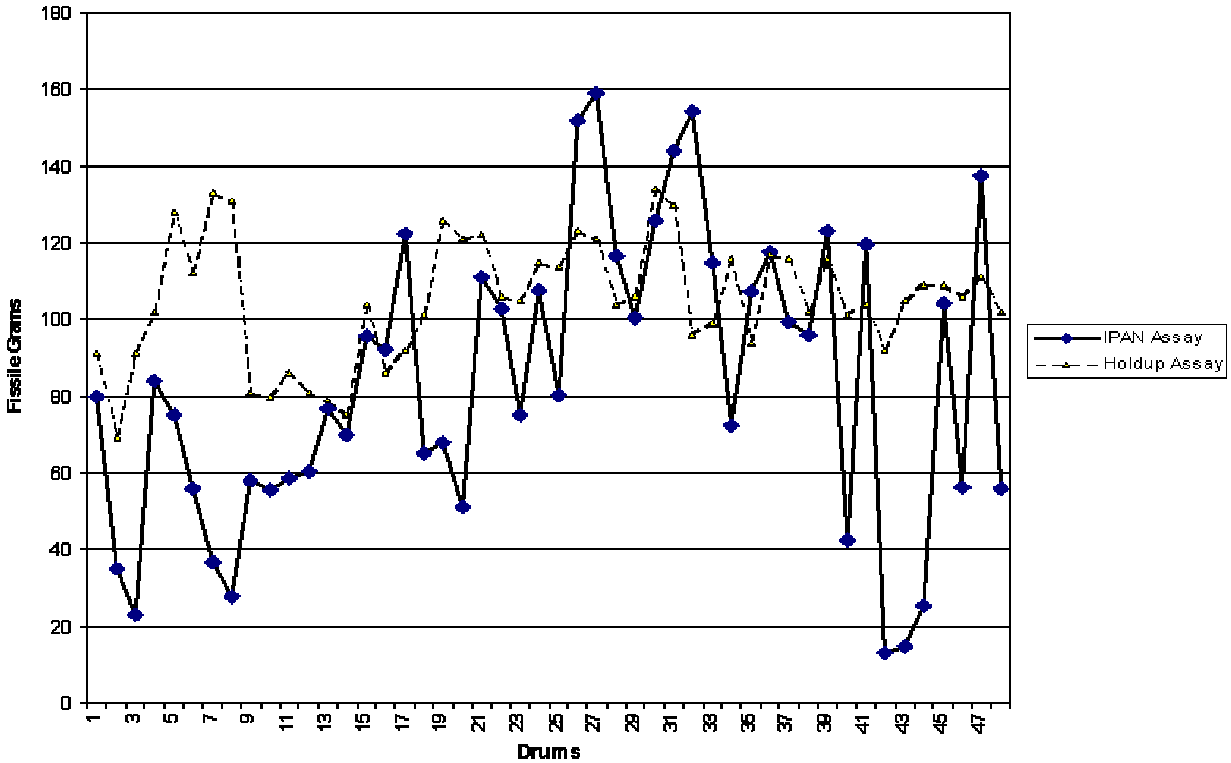

Figure VI.5. Neutron counter (IPAN) results for each drum (solid points) and the corresponding sum of package results obtained using the gamma-ray holdup measurement methodology (open points). Packages added to the first eight drums were measured by near positioning of the gamma detector ("area" geometry). Packages added to the remaining forty drums were measured by distant positioning of the gamma detector ("point" geometry). The fully loaded drum held 3-5 packages typically, but sometimes many more (up to 35).

VI.4. Field Verification

Field verification is a self-referenced multi-team measurement process with benefits that include validation of many aspects of measurement uncertainty. One of these is validation of the variation in results for deposit mass from one measurement team to the next performing measurements of the same process equipment using the same methodology. "Methodology" covers, in this case, the type of measurement equipment, spectral setups, calibration procedures and sources, measurement methods for backgrounds and deposits, and analysis methods. Multiple teams, each equipped with instruments appropriately calibrated for measurements of holdup deposits, may perform field-verification measurements as a half-day-long exercise whose "standard" is the mean measured deposit mass for each multiple-team measurement of the specific process deposit. Examples have been reported in which each team performs measurements at the same locations on designated equipment.[20] Other approaches include alternating ("leapfrogging") the measurement locations for each team on the designated equipment. Figure VI.6 shows the specific mass of ^{238}U in a thick line deposit of LEU (in g ^{238}U/cm) *vs*. deposit position on a 75-m-long duct measured by two teams using the 1001-keV gamma ray and NaI detectors.[49] Short count times and the low branching ratio for the 1001-keV gamma contribute to the large random-error bars on each point from counting statistics. The

random uncertainty in the total mass of uranium measured in the line, however, was 10% for each group, and the results for uranium mass were 143 and 183 kg U. A previous effort (results are also plotted in Fig. VI.6) gave 163 kg U. The "field precision" (standard deviation) in the three measured results in this case is 12.3%.

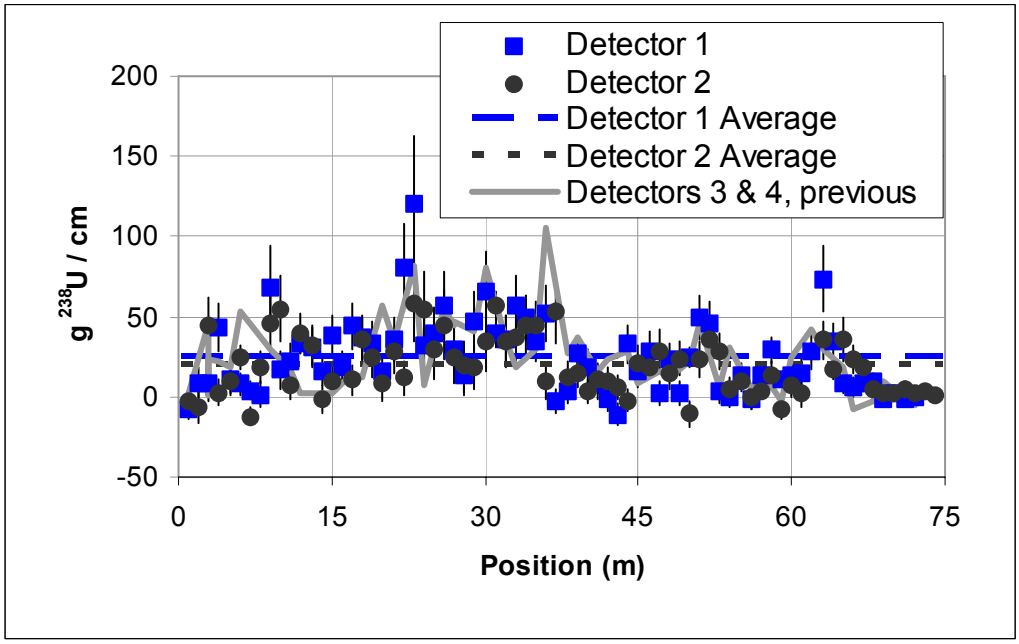

Figure VI.6. Field verification data for specific mass of uranium (in g ^{238}U/cm) in a line deposit of LEU vs. measurement position on a 75-m-long static duct measured by two teams using the 1001-keV gamma ray and NaI detectors. Count times were 45-60 s. A horizontal dashed line indicates the average result for each team. The solid line is a plot of the results measured on a previous date by two different teams.

Field verification results for measurements of plutonium holdup are also documented. Field precision established from these measurements is a component of the overall uncertainty in the results for holdup measurements.[50]

An additional or alternative approach to field verification that may be used in some equipment circumstances is for individual teams to measure a given set of process equipment using two different geometric models, both implemented within the guidelines for applications of the geometric models. One approach is to measure (point, line or area) deposits at different measurement distances to evaluate the impacts of smaller finite-source dimension and larger relative room backgrounds at larger distances and develop intuition on the impacts of the variables that affect portable NDA measurement results. Another approach is to measure the same deposit at different distances sufficient to perform the analysis in different geometries (such as point and area, or line and area).

A primary goal of field verification is to establish an understanding of the magnitudes of many components of the systematic effects associated with the portable measurements of holdup that use models of generalized deposit geometries. A secondary purpose is to explore the additional effects associated with the choice of measurement and/or deposit geometry. Field verification adds to the effectiveness of the measurement program by developing intuition among team members on impacts of geometric variables under the control of measurements personnel.

VII. EQUIPMENT AND SETTINGS

VII.1. Room-Temperature Detectors, Spectrometer Tools, and Spectra

The complex impacts of processing history and process design on portable measurement technology include the need for versatility in the equipment and methodology of portable holdup measurements. Faced with the most common mix of material types for either plutonium or uranium, as described in Section III, the best energy resolution such as that provided by germanium or Peltier-cooled CdTe must necessarily be considered, at least in determining the possibility of measurement bias from spectral interference effects. When process knowledge is unable to specify the isotopics, these high-resolution systems may also be required for preliminary surveys if the range of variation in the isotopic composition is wide. Nonetheless, when isotopics are sufficiently well known and the presence of interferences unlikely, even the lowest resolution scintillators (bismuth germinate, for example) can be implemented for holdup measurements. Any gamma-ray spectrometer detector may be used to implement the models and methodologies for holdup measurements.

An overview of fundamental information on design and performance of different types of detectors in use for gamma spectroscopy is published.[51] Faced simultaneously with problems of limited process access for personnel and equipment and with needs to perform thousands of measurements in some cases, room-temperature detectors are much better suited to the measurements of holdup. The common practical solution has been to use a room-temperature-detector for routine measurements of holdup, with germanium for isotopics measurements as required and as a referee or backup in quantifying holdup deposits in certain interference situations. This section focuses on room-temperature detectors for routine holdup measurements. Noncryogenic high-resolution detectors for measuring the isotopics, which might also serve in some interference situations to back up the holdup measurements performed with lower-resolution detectors, are discussed in Section VII.2.

Software toolkits for gamma spectroscopy are commonly equipped with peak fitting capabilities. More sophisticated software analyzes detector response functions. Both capabilities exist for low- and intermediate-resolution detectors. Both approaches for reduction of spectral data are specific to individual spectra and cannot be derived for one spectrum and applied to others. Peak fitting and response-function analysis require excellent counting statistics, which is most uncharacteristic of gamma-ray spectra obtained in holdup measurements. Reduction of spectral data obtained in holdup measurements is best achieved by analysis of data in energy regions-of-interest (ROIs) for those peaks considered least susceptible to the effects of interference. The minimum requirement to avoid bias from continuum effects, one ROI set on the peak and a second set on the continuum just above the peak, is more easily achieved with the sufficiently intense higher-energy gamma rays of the isotope of interest. Table VII.1 lists the gamma-ray peaks commonly chosen to measure the corresponding isotope listed. Depending on the energy resolution of the room-temperature detector, measurements of multiple isotopes are possible in some cases, as discussed below.

Modern portable multichannel analyzers (MCAs) can store hundreds of gamma-ray spectra. All spectra should be saved and archived for retrieval and reanalysis in the event that reduced data or other evidence indicates issues such as degraded spectrum quality, gain drift or unexpected

spectral interference. The number of channels in the energy spectra for low-to intermediate-resolution gamma detectors should be no less than 1000 for a full energy range of 1000 keV.

Table VII.1. Common Gamma Rays for Holdup Analysis

Isotope	E_γ (keV)
^{238}Pu	153
^{235}U	186
^{241}Pu - ^{237}U	208
^{237}Np	300
^{239}Pu	414
^{241}Am	662
^{238}U - -	1001

Most scintillators exhibit a strong dependence of the effective gain on the temperature of the crystal. Temperature is not always regulated in operating plants, whose operations are frequently the major contributor to temperature gradients of several tens of degrees centigrade at different locations in the plant. Facilities under D&D often stand down without routine utilities, especially heat, for cost savings. Exhaust equipment at many facilities includes outdoor ducts and filter housings. The effective gain of NaI may drop by one to three percent per ten-degree increase in centigrade temperature.[52] Active gain stabilization using a scintillator crystal with an embedded "seed" crystal that contains an alpha emitter is a decades-old commercial option developed for sodium iodide scintillators that relies in the empirical gain. This type of active gain stabilization can also be accomplished with a gamma source mounted on the surface of the crystal. Active stabilization is a commercial option that is usually achieved by automated adjustment of the high voltage to maintain a fixed amplitude for the stabilization pulse. New approaches to stable gain for scintillator spectrometers that rely on intrinsic scintillation characteristics are currently under investigation.[53]

The gain stability of alpha-seeded detectors has not been studied for scintillators with energy resolution worse than that of sodium iodide scintillators. The lower-energy continuum background from the high-energy alpha pulse and other gamma radiation from the seed isotope (^{241}Am is often used) contribute to a reduced measurement sensitivity and affect the precision for very thin deposits. Possible issues with a seed crystal include differences between the seed alpha pulse and the host gamma pulse in the temperature dependence of the apparent gain.

The apparent drift in the gain of a scintillator detector is primarily an effect of changing temperature of the crystal. This change occurs gradually compared to the short count times (usually 10-100 s) that are typical of holdup measurements. A practical and simpler alternative to active stabilization is off-line compensation for gain drift based on the measured centroid of the reference source. The use of a gamma-ray reference source to both compensate for gain drift compensation and achieve the required assurance of spectrum quality and constant response (by

analysis of peak resolution and net rate) is the recommended approach.[54] A source of typically mono-energetic gamma rays is selected for 1) optimum strength consistent with the short measurement times, and 2) peaks that fall below the analysis region for holdup deposits. This source attaches to the detector inside the shield. The use of metal filters reduces gamma- and x-ray background in the vicinity of the reference peak from deposits and the room. The 60-keV gamma ray from long-lived ^{241}Am ($t_{1/2}$ = 460 y) is in common use as a reference peak, as well as the 88-keV gamma ray from ^{109}Cd ($t_{1/2}$ = 450 d). The required source strengths are 0.1-1 μCi.

The gamma-ray reference source fixed to the detector requires analysis of the reference peak for gain-drift compensation and spectrum quality-assurance in every acquired spectrum. It involves maintaining fixed-energy ROIs (by resetting the ROI channel limits) in the event of a change in apparent gain. Refer to Section VII.3 for additional discussion on choosing and implementing the reference source and to Section X.5 for procedures on measurement control.

Although varying the temperature of a solid-state crystal does not affect the gain in moderate temperature ranges, a reference source is essential to ensure the spectrum quality. It is most important to monitor the resolution of an uncooled solid-state detector, which degrades with increasing temperature. Degraded energy resolution invalidates both the calibration and analysis. Compensation for degraded energy resolution is not an option in this case, and stabilization of the temperature is necessary.

Figure VII.1 shows the superimposed gamma-ray spectra of low-burnup (93% ^{239}Pu) plutonium measured with four different gamma-ray detectors.[55-57] These good counting statistics are not representative of spectra measured in count periods of 5-20 s typical of holdup measurements but serve to illustrate the range of spectral performance that impacts the following discussions of room-temperature detectors. Spectra for the thallium-doped sodium-iodide (NaI:Tl or NaI) and coplanar-grid cadmium-zinc-telluride (CPG CZT) detectors, both in routine use for portable holdup measurements, appear in Figure VII.1. Also shown are the high-resolution spectra of germanium (Ge) and Peltier-cooled CdTe (CdTe).

The detectors most commonly used for holdup measurements are NaI. A 1.25- cm-thick NaI crystal absorbs 80% of ^{235}U gamma rays at 186-keV. A thickness of 5 cm absorbs 85% of ^{239}Pu gamma rays at 414-keV. Although much larger crystals are readily available, the weight of a shielded NaI detector with a 2.5-cm diameter crystal can be light enough for use in restricted-access hand-held portable applications typical of holdup measurements.

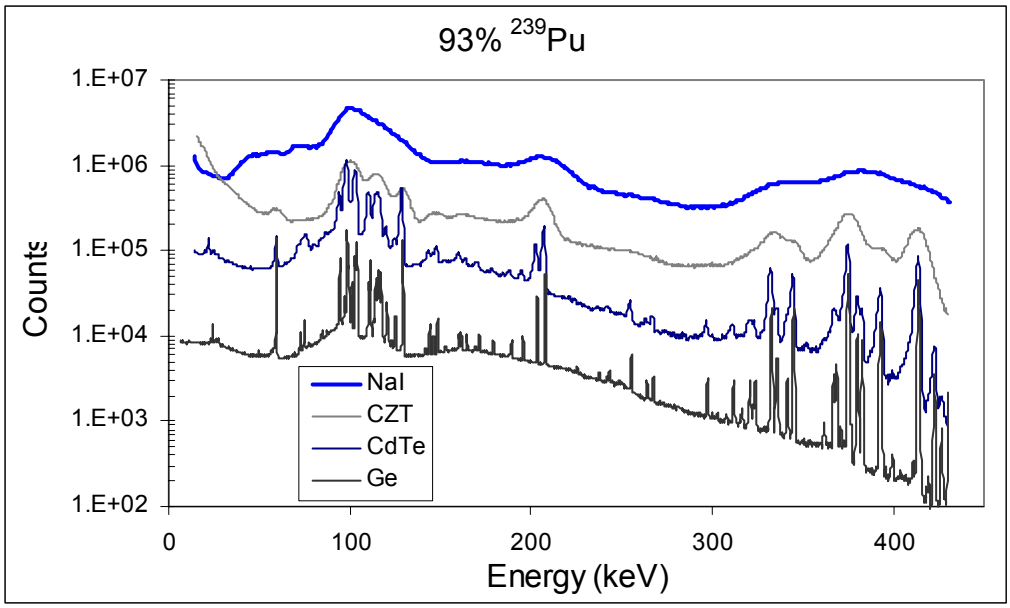

Figure VII.1. Gamma-ray spectra of low-burnup (93% ^{239}Pu) plutonium measured with four different gamma-ray detectors: NaI, CZT, CdTe and Ge (top to bottom).

Though limited in size (cubic crystals as large as 1.5 cm on a side absorb up to 95% and 40% of gamma rays at 186 and 414 keV, respectively), the large intermediate-resolution CZT is equal in sensitivity to the 2.5-cm-diameter NaI detector in many portable measurement applications when contributions from room background are moderate to high because the ratio of peak-to-continuum events for the large CZT exceeds that of the NaI. Resolution advantages of the CZT are also essential in many common interference situations. Regarding common biases caused by the Compton continuum of an interfering peak, both the large CZT detector (3.2% FW.5M at 662 keV) and NaI (7% FW.5M at 662 keV) with proper spectral settings but to a lesser extent

- permit accurate measurements of ^{239}Pu in high-americium material when the 414-keV peak sits on a large Compton continuum, rising at 478 keV, from 662-keV gammas, and
- permit measurements of ^{239}Pu in the complex situation of fluoride contamination and high ^{241}Am when the 414-keV region is i) just above the Compton continuum, rising at 356 keV from 511-keV gammas of ^{22}Na, and ii) just below the 662-keV Compton edge.

Better energy resolution also resolves common discrete interferences. A CZT detector and, in general, not a NaI detector

- resolves the ^{239}Pu 375-keV peak (which includes and is often dominated by activity from ^{241}Am) from the 414-keV peak of ^{239}Pu,
- permits measurements of ^{235}U at 186 keV in the presence of plutonium, and
- resolves 414-keV and other gamma rays (including 345 keV) of ^{239}Pu from dominating lower-energy ^{237}Np gamma rays (especially that at 300 keV) to permit evaluation and extraction of the less intense but interfering ^{237}Np activity at 416 keV.

The data in Tables VII.2 and VII.3 assist in assessing the usefulness of NaI *vs.* that of CZT in common situations of spectral interference. These data can also assist the user in defining energy regions for spectral analysis of holdup deposits when interfering isotopes are present.

Table VII.2 indicates the energy in keV of the Compton (high-energy) “edge”:

$$E_C(180^o) = E_\gamma \left(1 - \left(1 + 2E_\gamma / 0.511 \right)^{-1} \right) \quad ,$$

where E_γ is the initial gamma-ray energy in keV. Table VII.2 also gives the nominal full-width at half maximum (FW.5M) energy resolution for each detector at each Compton-edge energy $E_C(180^o)$, along with the energies corresponding to one FW.5M below and above $E_C(180^o)$. Energy ROIs set up for detectors with low to intermediate energy resolution must heed these limits to avoid bias from continuum effects of significant interfering gamma rays.

Table VII.2. Compton-Edge Data for NaI and CZT Detectors

NaI (FW.5M = 7% at 662 keV)

E_γ	E_C (180°)	% $FW.5M_C$	E_C – $FW.5M_C$	E_C + $FW.5M_C$
238	115	16.8%	95	134
300	162	14.1%	139	185
511	341	9.8%	307	374
583	405	8.9%	369	442
662	478	8.2%	438	517
1274	1061	5.5%	1003	1120

CZT (FW.5M = 3.2% at 662 keV)

E_γ	E_C (180°)	% $FW.5M_C$	E_C – $FW.5M_C$	E_C + $FW.5M_C$
238	115	7.7%	106	124
300	162	6.5%	152	172
511	341	4.5%	325	356
583	405	4.1%	389	422
662	478	3.8%	460	496
1274	1061	2.5%	1034	1088

Table VII.3 lists common actinide peaks, including those from Table VII.1 frequently used to quantify holdup and others that can cause discrete interferences. Table VII.3 also gives the nominal FW.5M for NaI and CZT at each peak energy E_γ along with the energies corresponding to one FW.5M below and above E_γ.

Users may refer to Tables VII.2 and VII.3 to determine settings for energy ROIs representing minimum restrictions – assuming stable or drift-compensated spectrometer operation – necessary for unbiased data in the presence of interferences such as those noted with bullets above. The following five examples give the ROI settings determined for five common interference situations using data in the two tables to illustrate the use of the tables.

Table VII.3. Gamma-Ray Peak Data for NaI and CZT

NaI (FW.5M = 7% at 662 keV)

E_γ	Isotope	% FW.5M$_\gamma$	E_γ - FW.5M$_\gamma$	E_γ + FW.5M$_\gamma$
153	^{238}Pu	14.6%	131	175
186	^{235}U	13.2%	161	211
203	^{239}Pu	12.6%	177	229
208	^{241}Pu - ^{237}U	12.5%	182	234
238	^{232}U decay	11.7%	210	266
300	^{237}Np	10.4%	269	331
345	^{239}Pu	9.7%	312	378
376	^{241}Am	9.3%	341	410
414	^{239}Pu	8.9%	377	451
416	^{237}Np	8.8%	379	453
662	^{241}Am	7.0%	616	708
1001	^{238}U - -	5.7%	944	1058

CZT (FW.5M = 3.2% at 662 keV)

E_γ	Isotope	% FW.5M$_\gamma$	E_γ - FW.5M$_\gamma$	E_γ + FW.5M$_\gamma$
153	^{238}Pu	6.7%	143	163
186	^{235}U	6.0%	175	197
203	^{239}Pu	5.8%	191	215
208	^{241}Pu - ^{237}U	5.7%	196	220
238	^{232}U decay	5.3%	225	251
300	^{237}Np	4.8%	286	314
345	^{239}Pu	4.4%	330	360
376	^{241}Am	4.2%	360	392
414	^{239}Pu	4.0%	397	431
416	^{237}Np	4.0%	399	433
662	^{241}Am	3.2%	641	683
1001	^{238}U - -	2.6%	975	1027

i) Measurements at 414 keV of ^{239}Pu deposits with the potential for high-^{241}Am contamination require minimum and maximum ROI settings of 410 and 438 keV, respectively, with NaI to avoid positive bias from the peak at 376 keV (Table VII.3) and from the 662-keV Compton continuum (Table VII.2).
ii) Measurements at 414 keV of ^{239}Pu deposits with the potential for high-^{241}Am contamination require minimum and maximum ROI settings of 392 (Table VII.3) and 460 keV (Table VII.2) with CZT. Note that the higher resolution retains use of all of the information in the analysis peak without risking bias from the interferences.
iii) Measurements at 186 keV of ^{235}U deposits that include reactor returns require a maximum ROI setting of 210 keV with NaI (Table VII.3) to avoid negative bias from the peak at 238 keV.
iv) Measurements at186 keV of ^{235}U deposits that include reactor returns require a maximum ROI setting of 225 keV with CZT (Table VII.3) to avoid negative bias from the peak at 238 keV. Note again that the higher resolution retains use of all of the information in the analysis peak without risking bias from the interferences.
v) The possibility of subtracting interfering ^{237}Np activity at 416 keV from the 414-keV peak of ^{239}Pu and relies on energy resolution that is sufficient to resolve the intense ^{237}Np gamma ray at 300 keV from the 345 keV gamma-ray of ^{239}Pu. This is not possible with NaI but may be achievable with CZT, as indicated in Table VII.3.

A complex situation that involves choices of detectors as well as gamma rays for use in holdup applications arises for measurements of low-enriched uranium (LEU) holdup. Both NaI and CZT detect the 186-keV gamma ray of ^{235}U (produced in ~50% of ^{235}U decays) with high efficiency. Because the ^{235}U enrichment may be 1-5% in an LEU facility, large deposits common in LEU process equipment pose attenuation problems at this low energy. Therefore the 1001-keV peak from the ^{238}U/^{234m}Pa equilibrium decay (produced in ~1% of ^{238}U decays) might be measured simultaneously to benefit from higher penetration of the higher-energy gamma ray, whose net yield despite a low branching ratio is more comparable to that at 186-keV for very low enrichments. The resulting detector choice focuses on the thicker NaI (5-cm, which has a 6% photoelectric interaction probability at 1001 keV) and the thickest CZT (1.5-cm, which has a 3% photoelectric interaction probability at 1001 keV) in order to optimize for measurements of the higher-energy gamma ray. Because of typically low continuum and the rarity of interferences at the high energy, the 5-cm-thick NaI detector is the likely choice.

Nonetheless, a significant portion of the same LEU measurement need may focus on (sub-floor or overhead) ventilation equipment where deposits may be very thin. Ventilation equipment is bathed in 1001-keV room background from the process as a whole, and the sensitivity to thin deposits will be low at 1001 keV because a 1-cm-thick lead shield transmits half of the gamma rays at this high energy. The 186-keV gamma ray, which a few mm of lead fully shields from room background, is a better choice for equipment with thin deposits. Returning to detector considerations, a 1.25-cm-thick NaI crystal is a better choice than the 5-cm-thick crystal for thin deposits because reduced continuum at the low energy will improve the measurement sensitivity at 186 keV. Use the thicker crystal if both thick and thin deposits abound in measurement areas. Figure VII.2 shows NaI spectra of thick and thin LEU deposits in varying room backgrounds.[49]

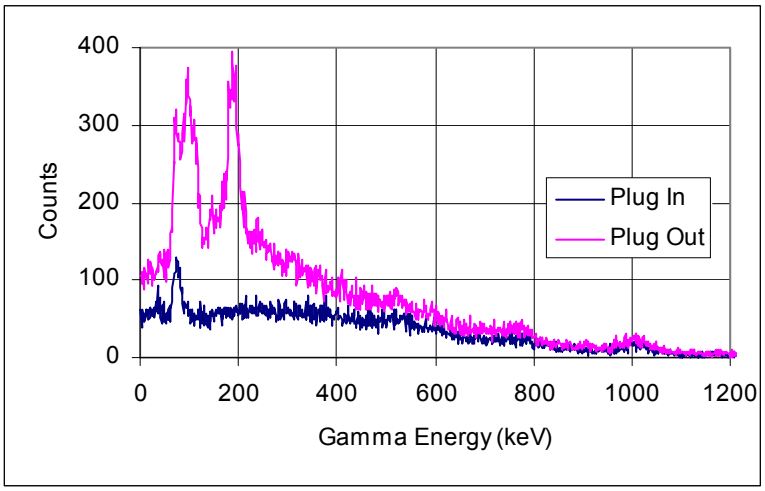

a.

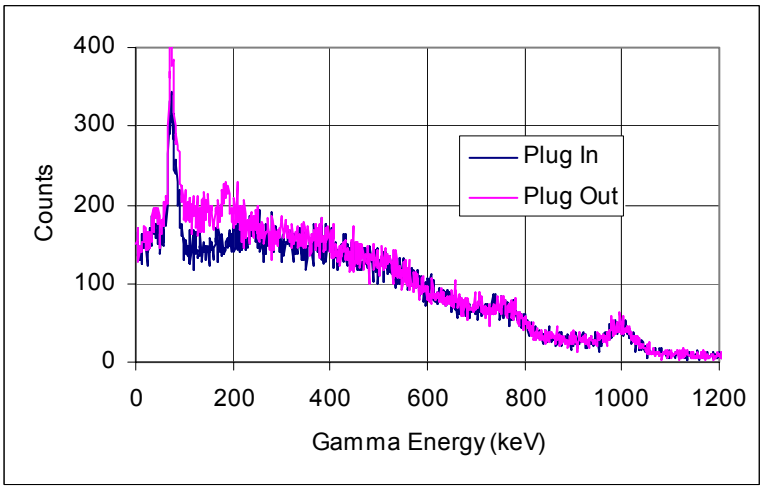

b.

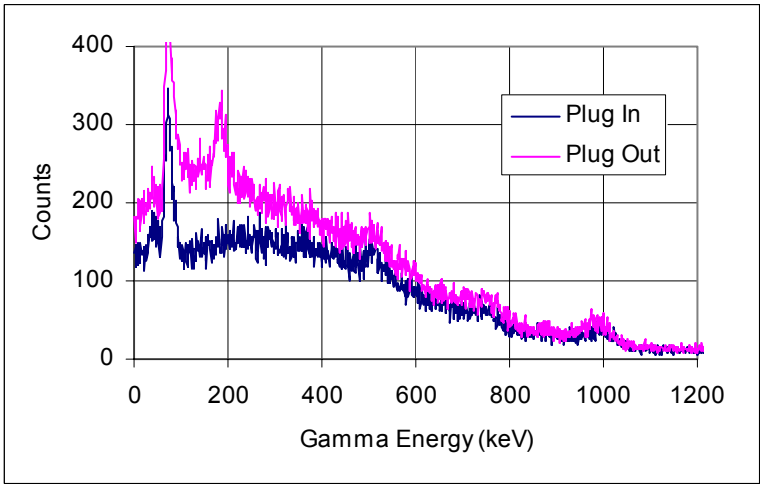

c.

Figure VII.2. Spectra of LEU (~3% ^{235}U) duct-holdup deposits were measured with short count times using a 5-cm-thick NaI detector and a tungsten plug inserted into the collimator to count room background ("Plug In"). Deposits exceed the maximum thickness for 186-keV gammas in* a *and* c*. The random uncertainty in the net 1001-keV rate is 20% in both* a *and* c *despite higher room-background continuum in* c*. Note evidence of the 238-keV gamma ray in* a*, indicating reactor-return material. The deposit measured in* b *is too thin to analyze at 1001

keV, and random uncertainty in the net 186-keV rate is 90% because of the high continuum from room background.

Use of CZT for measurements of thin deposits at 186 keV cleanly avoids negative bias from the peak at 238 keV in reactor-return materials. Figure VII.2 shows spectral evidence of 238 keV.

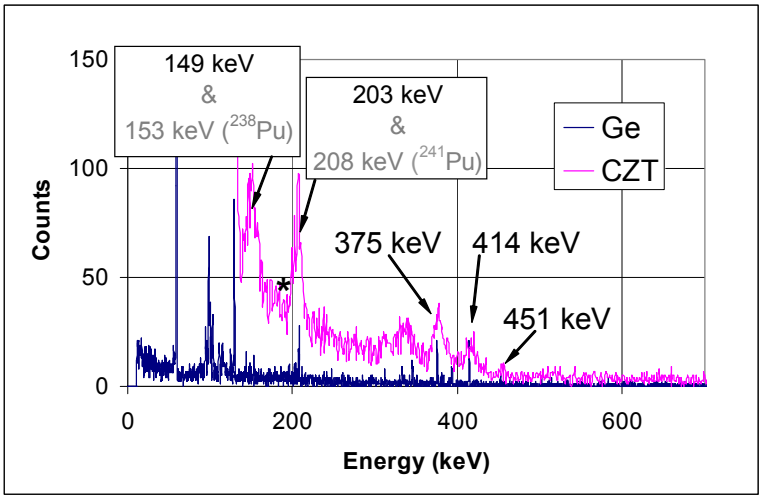

Figure VII.3. Gamma-ray spectra of deposits in the exhaust ductwork in one wing of a multimission research facility measured with Ge and CZT. The asterisk marks the expected position of the 186-keV gamma ray of ^{235}U.

Figure VII.3 shows Ge and CZT spectra of deposits in the exhaust ductwork in one wing of a research facility in the DOE complex.[25] Gamma-ray evidence of ^{239}Pu is clearly indicated by both Ge and CZT in the peaks at 375, 414 and 451 keV. Both detectors also indicate the presence of ^{238}Pu and ^{241}Pu with peaks at 153 and 208 keV, respectively. The asterisk at 186 keV marks the peak energy for ^{235}U that was expected but not detected by either CZT or Ge at this location. Despite an order of magnitude difference in resolution between Ge and CZT, the CZT, unlike NaI for the most part, can also resolve and quantify multiple isotopes. Figure VII.4 again shows Ge and CZT spectra of deposit in a second location of the same exhaust ductwork,[25] indicating in this case the presence of ^{238}Pu (153 keV) and the absence of ^{235}U (186 keV). The possibility of measuring ^{235}U in the presence of plutonium is illustrated in both Figures VII.3 and VII.4.

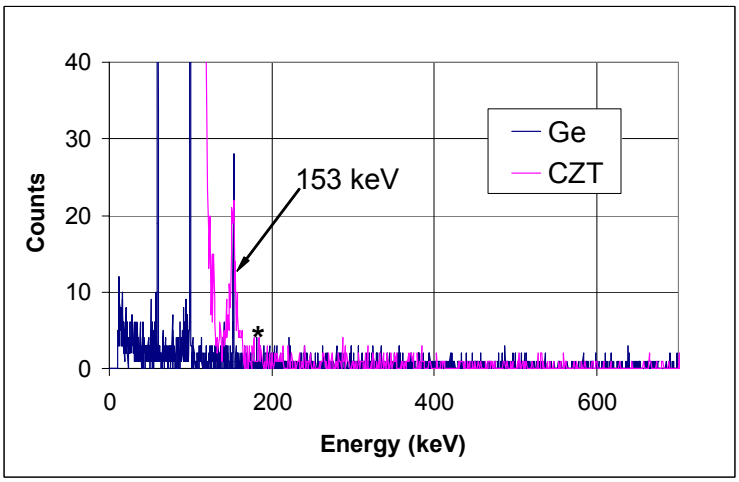

Figure VII.4 Gamma-ray spectra of deposits at a second location (see Fig. VII.3) in the exhaust ductwork in one wing of a multimission research facility measured with Ge and CZT. An asterisk is positioned at 186 keV.

Figure VII.5 shows NaI and CZT spectra of deposits of high-enriched uranium in the process equipment of a DOE facility that recovers uranium from scrap.[58] Labeled with dashed vertical lines are the 186-keV peak of ^{235}U, present for both ^{235}U enrichments in the spectra of both detectors, and the 238-keV peak produced (after ^{212}Pb beta emission) near the bottom of the ^{232}U/^{232}Th decay chain. The 238-keV activity, along with prominent higher-energy gamma rays at 583 and 510 keV of similar origin, appear in gamma-ray spectra of uranium that has been recycled from spent fuel. The capability, illustrated in Figure VII.5, of the CZT detector to resolve the ^{235}U peaks at 143 163 and 203 keV is not generally utilized for measurements of holdup. The capability to resolve the 238-keV peak from the 186-keV peak and its continuum background has been a key to measuring ^{235}U in deposits that contain recycled material, such as that illustrated by the spectrum for the 61% enriched uranium in Figure VII.5. Avoiding negative bias in the holdup result for ^{235}U from reactor-recycle materials when NaI measurements are performed requires a conservative setting (Table VII.3) of the continuum ROI for 186 keV.

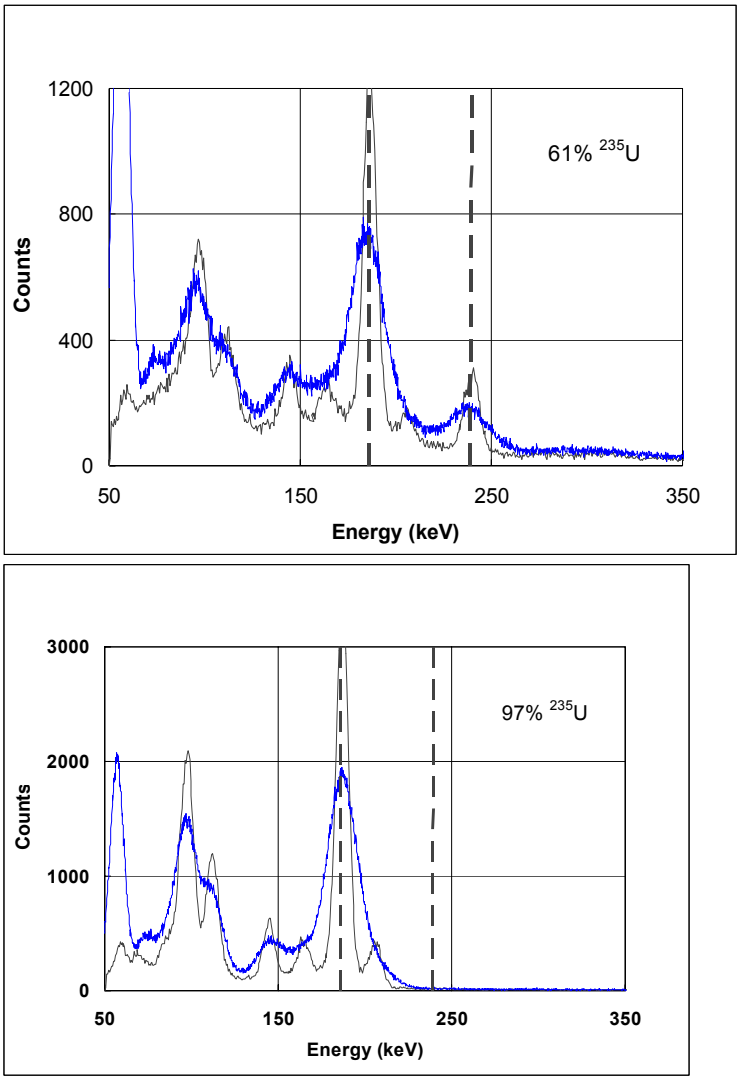

Figure VII.5. NaI and CZT spectra of ^{235}U in HEU deposits that include recycled material. The 186-keV analysis peak has a potential interference at 238 keV for the 61% enrichment. Dashed vertical lines mark both energies.

Figure VII.6 shows the spectrum of deposits of low-enriched (3% ^{235}U) uranium in the process equipment of a fuel production facility.[49] The measurements were performed with the 2.5-cm-diameter by 5-cm-thick NaI detector. The 238-keV gamma ray along with the higher-energy gamma rays at 583 and 510 keV of similar origin appear in this gamma-ray spectrum, indicating that the uranium that has been recycled. Dashed vertical lines label the regions of interest on the 186-keV peak of ^{235}U and the 1001-keV from equilibrium-daughter of ^{238}U decay. The ROIs on the 186-keV peak and continuum background are set below 210 keV, consistent with the guidance provided in Table VII.3, to avoid bias from the peak at 238 keV.

The calibration for quantifying holdup is much more vulnerable to bias from gain drift at 186 keV than at 1001 keV using the ROIs indicated in Figure VII.6. Measurements with the same NaI detector using the ROI settings shown in Figure VII.6 indicate a bias-drift coefficient (% bias per % gain drift) of 22 at 186-keV and -0.2 at 1001 keV for negative gain drift. Holdup of LEU measured at 1001 keV by five different groups using these ROI settings, short counts, and the 2.5-cm-by-5-cm NaI agrees to ±12.6%, 1σ (within measurement uncertainty). The same techniques give results for an extended line-source working standard composed of this process material and measured in the plant that agree with the reference value within statistics.[49] An encouraging note for measurements at 186 keV is that gain-drift compensation based on the 60-keV reference peak of ^{241}Am effectively stabilizes the gain to within 0.2% of the setup value.[54]

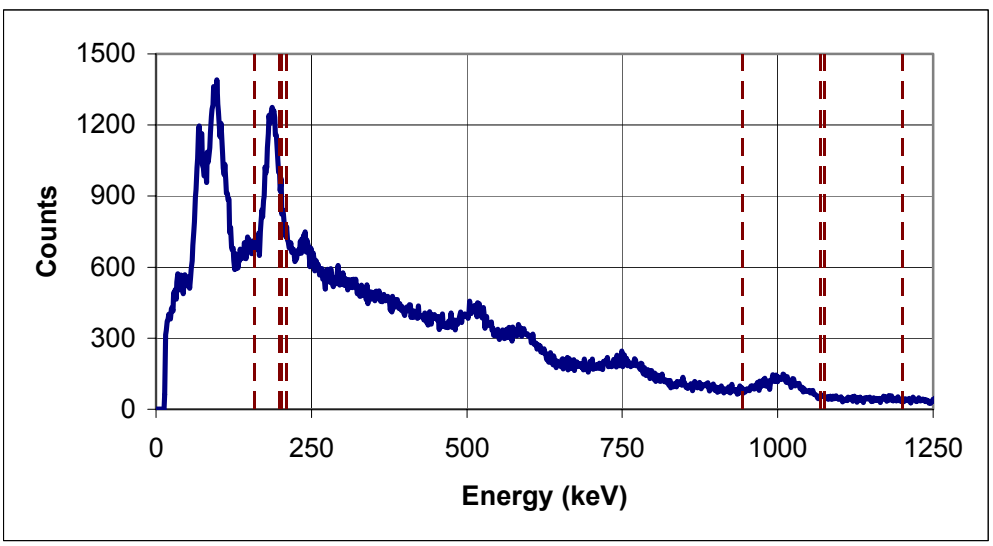

Figure VII.6. This spectrum of uranium in LEU deposits that include recycled material was measured with the 2.5-cm-diameter by 5-cm-thick NaI detector in a 300-s count. The 186 keV peak has a potential interference at 238 keV. Dashed vertical lines mark peak and high-energy continuum ROIs at both 186 and 1001 keV.

Figure VII.7 is a photograph showing the portable measurements of ^{235}U deposits in process filter systems in progress using a portable Ge detector weighing ~10 kg with its tungsten collimator-shield (top) and both CZT and NaI detectors weighing ~1 kg each with their respective tungsten and lead shields (bottom). The greater portability of the room-temperature detectors is essential for the bulk of measurements of holdup. Figure VII.8 shows the NaI detector of the same design in use for portable measurements of plutonium deposits that are located, more typically, in overhead ducts and other equipment that is difficult to access except on ladders or catwalks or with detectors mounted on telescoping poles.

Figure VII.7. Top: Portable measurements of ^{235}U deposits in a process filter system are performed with a portable Ge detector weighing ~10 kg with its tungsten collimator-shield. Bottom: CZT and NaI also in use for measurements of process filters weigh ~1 kg each with their respective tungsten and lead shields.

Figure VII.8. The compact NaI detector (see Fig. VII.6) is shown during measurements of plutonium deposits in overhead ducts. The detector is mounted on a telescoping pole. The bottom-frame exploded view from the middle frame shows a wooden meter stick used as a positioning standoff from the duct.

Table VII.4. Gamma-Ray Peak Data for BGO and $LaCl_3$

BGO (FW.5M = 12% at 662 keV)

E_γ	Isotope	% $FW.5M_\gamma$	E_γ - $FW.5M_\gamma$	E_γ + $FW.5M_\gamma$
153	^{238}Pu	25.0%	115	191
186	^{235}U	22.6%	144	228
203	^{239}Pu	21.7%	159	247
208	^{241}Pu - ^{237}U	21.4%	163	253
238	^{232}U decay	20.0%	190	286
300	^{237}Np	17.8%	247	353
345	^{239}Pu	16.6%	288	402
376	^{241}Am	15.9%	316	436
414	^{239}Pu	15.2%	351	477
416	^{237}Np	15.1%	353	479
662	^{241}Am	12.0%	583	741
1001	^{238}U - -	9.8%	903	1099

$LaCl_3$ (FW.5M = 3.2% at 662 keV)

E_γ	Isotope	% $FW.5M_\gamma$	E_γ - $FW.5M_\gamma$	E_γ + $FW.5M_\gamma$
153	^{238}Pu	6.7%	143	163
186	^{235}U	6.0%	175	197
203	^{239}Pu	5.8%	191	215
208	^{241}Pu - ^{237}U	5.7%	196	220
238	^{232}U decay	5.3%	225	251
300	^{237}Np	4.8%	286	314
345	^{239}Pu	4.4%	330	360
376	^{241}Am	4.2%	360	392
414	^{239}Pu	4.0%	397	431
416	^{237}Np	4.0%	399	433
662	^{241}Am	3.2%	641	683
1001	^{238}U - -	2.6%	975	1027

Because of its high density and Z, bismuth germinate (BGO) has been used for measurements of plutonium holdup to further reduce the detector weight with a thinner crystal. The energy resolution is so much worse than that of NaI that many common measurement problems must be addressed with a higher resolution detector.

Notwithstanding the benefits of its superior energy resolution, the cost of the large CZT detector remains very high, and its availability is still limited after a decade of commercial development. However, a new intermediate-resolution 10%-cerium-activated lanthanum-chloride scintillator has resolution equivalent to that of the large CZT detector. The $LaCl_3$ crystals are larger than those of CZT, the scintillator material is now available, and the costs are moderate.

Table VII.4, analogous to VII.2, lists common actinide peaks, including those from Table VII.1 frequently used to quantify holdup and others that can cause discrete interferences. Table VII.3 also gives the nominal FW.5M for BGO and $LaCl_3$ at each peak energy E_γ, along with the energies corresponding to one FW.5M below and above E_γ. The BGO detector addresses none of the interference situations listed as bullets above. The $LaCl_3$ is an alternative to Ge because, like CZT, it can be used in situations of limited access for portable NDA measurements and because it addresses all of the common interference situations listed above. Its resolution is not sufficient for measurements of deposits contaminated with fission products.

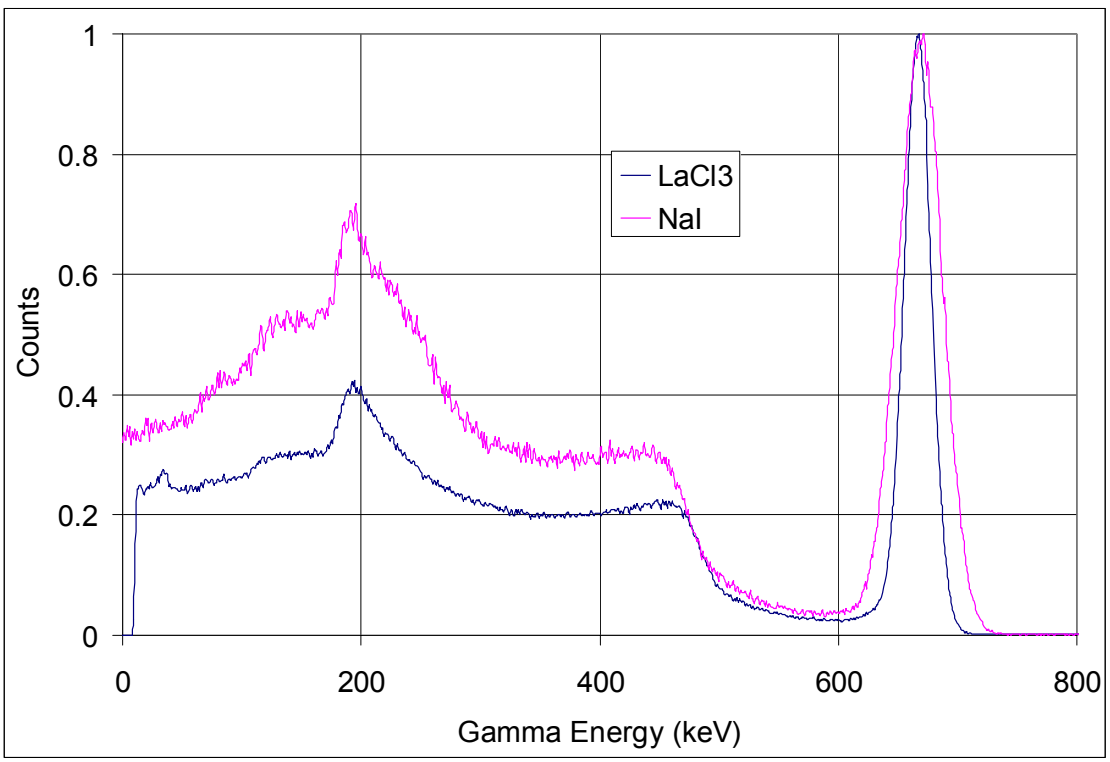

Figure VII.9. Gamma-ray spectra of ^{137}Cs measured with a 5-cm^2 by 2.54-cm thick $LaCl_3$ scintillator and with the same-size NaI scintillator. The energy resolution (FW.5M) at 662 keV is 4.0 and 6.9%, respectively.

Figure VII.9 shows gamma-ray spectra of ^{137}Cs measured with a 5-cm^2 by 2.54-cm thick $LaCl_3$ scintillator and with the same-size NaI.[59] Both spectra in Figure VII.9 were measured with a glass-window PMT. The relative FW.5M at 662 keV is 3.9% for the $LaCl_3$ scintillator, not as good as the expectation of 3.2%. This is caused by the significant loss of the scintillation light

from $LaCl_3$ by the glass window (glass absorbs wavelengths below 350 ηm) of the PMT. The emission peak for $LaCl_3$ with 10% cerium doping is 340-ηm. Nonetheless, $LaCl_3$ performance at 414 keV is substantially improved over that of NaI and is similar to that of CZT at this energy.

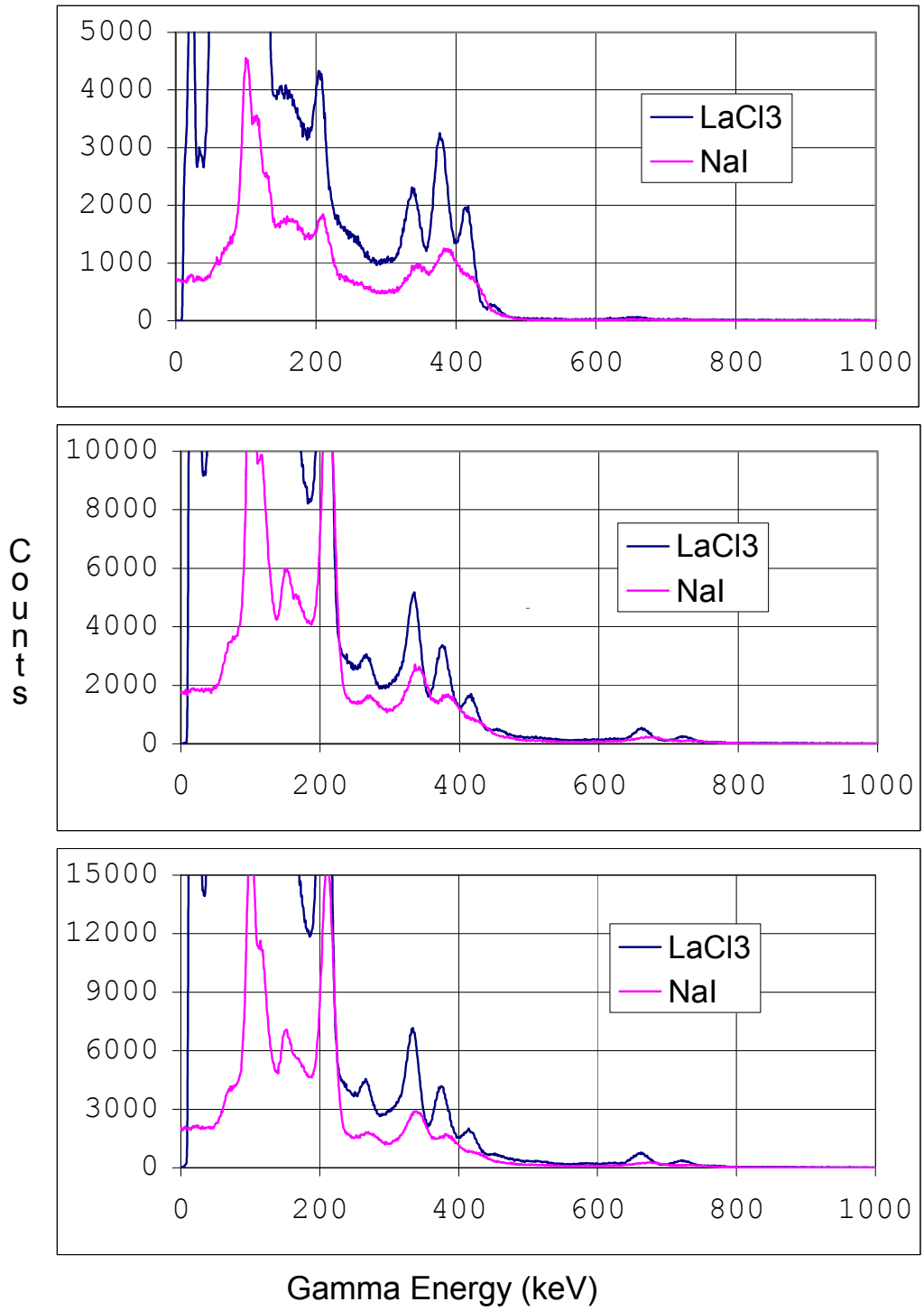

Figure VII.10. The gamma-ray spectra, top to bottom, are those of low-, medium- and high-burnup plutonium (6%, 18% and 24% ^{240}Pu, respectively), measured with a 5-cm^2 by 2.54-cm thick $LaCl_3$ scintillator and with the same-size NaI scintillator. The improved energy resolution at 414 keV is illustrated by the distinct peak in the $LaCl_3$ spectrum at this energy in the full range of isotopics.

Figure VII.10 shows the gamma-ray spectra of three 5-gram plutonium oxide samples of low-, medium- and high burnup, measured with $LaCl_3$ and NaI detectors using crystals of the same size and identical electronics.[59] The improved resolution at the 414-keV analysis energy for ^{239}Pu with this large crystal will contribute substantially to eliminating bias in measurements of high-americium deposits. The detectors will be available relatively low in cost, compared to CZT, and will incur very little sacrifice in detection efficiency relative to the compact (5 cm^2 by 5 cm) NaI detector. Table VII.5 is a summary of the properties and performance of the room-temperature gamma-ray detectors discussed above for use in portable measurements of holdup. The expectations are high that $LaCl_3$ (and possibly other higher-density lanthanum halides) will replace CZT, NaI and BGO in their current applications for measurements of plutonium holdup, for an overall improvement in versatility, measurement quality and cost-effective hardware.

Table VII.5. Portable Gamma-Ray Detectors for Holdup Measurements

DETECTOR	**BGO** ($Bi_4Ge_3O_{12}$)	**NaI** (Tl-doped)	**CZT** (CPG; Cd:Zn::9:1)	**$LaCl_3$** (10% Ce by weight)
TYPE	scintillator	scintillator	solid-state	**scintillator**
DIMENSIONS: area (cm^2) x thick. (cm)	5 cm^2 x 5 cm (or much larger)	5 cm^2 x 5 cm (or much larger)	2.3 cm^2 x 1.5 cm **(the largest)**	**5 cm^2 x 2.5 cm (current*)**
VOLUME (cm^3)	24	24	1.7	**12**
AVERAGE Z	28	32	49	**28**
DENSITY (g/cm^3)	7.1	3.7	6.1	**3.9**
RESOLUTION: % fwhm @ 662 keV	12%	**7.0%**	3.2%	**3.2% (literature)**
PHOTON λ (ηm)**	480	**415**	NA	**340**
DECAYτ (ηs)	0.3	230	NA	**20 (70%) 210 (30%) (literature)**
AVAILABILITY	6 wks after order	2 wks after order	**1 yr after order**	**8 wks after order (current)**

** Glass transmits down to 350ηm. Quartz transmits down to 180ηm.

*** Commercial detectors using $LaCl_3$ crystals with areas of 5.0 cm^2 by 3.8-cm thick, 11.4 cm^2 by 3.8-cm thick, and 20.3 cm^2 by 5.1-cm thick – as well as large crystals of $LaBr_3$ – are available as this report is published.**

VII.2. Peltier-Cooled CdTe Detectors for Isotopics and Mass

The recent availability of Peltier-cooled CdTe detectors with crystals larger than 1 cm^2 has made gamma-ray isotopics for uranium and plutonium truly portable for the first time.[55-57] Figure VII.1 illustrates the high energy resolution of CdTe. The energy resolution of Ge is only three times better. The photographs in Figure VII.11 illustrate the compact dimensions of the CdTe detector, shown in use for portable isotopics measurements of plutonium in a process glove box.

The capability of CdTe for full analysis of the isotopic distribution covers wide-range plutonium (3%- to 30%-^{240}Pu material has been tested, and the technique applies to the higher-burnup material as well), uranium (0.1 to 50% has been tested, and the technique applies up to enrichments of ~80% as well), and MOX. A count time of 15 m with the new CdTe detector measures the ^{240}Pu fraction to 2% and the ^{235}U fraction to 3%.[57]

Measurements of holdup deposits of plutonium or uranium may rely on stream isotopics if 1) process material types have been relatively constant, or 2) process knowledge of historical data for complex operations can be shown to predict residual isotopics. Many facilities have enrichments that vary widely from variable fuel burnup or multiple missions, or are intrinsically variable (enrichment plants). Because of trends toward expanded missions and more recent downsizing, reliance on stream isotopics will be less possible in the future. Studies in progress to "map" the isotopics based on history in multimission processes may alleviate needs,[15] but the ability to measure isotopics on line will likely remain an important component of NDA verification technology for holdup measurements.

Figure VII.11. The Peltier-cooled portable CdTe detector is shown in use for portable isotopics measurements of plutonium in a process glove box.

The need to know the isotopic composition in order to quantify holdup deposits is two-fold. Gamma-ray measurements of holdup, like any NDA measurement based on a nuclear technique, use a signal from a specific isotope, but the measurement must provide both the mass of the SNM isotopes (typically ^{239}Pu or ^{235}U) and that of the corresponding element (plutonium or uranium). The isotopic distribution is needed to determine the mass of the element. A second

reason is that the self-attenuation of gamma rays by the deposit material is an effect of the density of the element (or total actinide) in the deposit. This is of particular importance for actinide mixtures such as mixed U-Pu oxide or MOX, especially because the attenuation is dominated by the major actinide (usually uranium in MOX) while measurements often determine the isotope specific mass of the minor-actinide isotope (^{239}Pu). The self-attenuation correction also requires knowledge of the isotopic distribution of the actinide whose isotope is measured. Refer to Section VIII.4 for discussions of the relevant attenuation corrections.

Because of its high resolution, CdTe can readily measure the order-of-magnitude more intense lower-energy gamma rays of ^{239}Pu. Therefore, despite its six-to-seven-times smaller size compared to the 2.5-cm-diameter NaI detectors, the new CdTe detector is a viable candidate for portable, interference-free holdup measurements of multiple isotopes. A limitation at lower energies is the attenuation of gamma rays by very dense process equipment. Such dense equipment in which the thickness of steel significantly exceeds one cm (typically up to three cm, which absorbs more than 99% of the 129-keV gamma rays of ^{239}Pu) is common in fuel fabrication but appears less often in scrap-recovery and enrichment facilities.

The current large-area single-crystal CdTe detector is too thin (0.15-0.25 cm) for practical measurements of holdup at higher energies where gamma rays are more penetrating of dense equipment. A CdTe thickness of 0.2 cm absorbs 36% of the ^{235}U gamma rays at 186 keV but only 12% of the ^{239}Pu gamma rays at 414 keV. New commercial efforts to develop prototypes composed of stacked CdTe[60] crystals may triple the effective CdTe thickness eventually. Higher noise will preclude use of the thick-crystal array for gamma isotopics measurements, but the possibility exists for analyzing pulses from the first layer only for isotopics while using the full stack for quantifying holdup using higher-energy gamma rays.

Holdup measurements of ^{235}U at 186 keV as well as those of ^{239}Pu, ^{241}Pu, and ^{238}Pu at 129, 149 and 153 keV, respectively, have the great advantage that they are easily shielded against room background. Low- or intermediate-resolution portable measurements of ^{239}Pu using the 414-keV gamma ray require meticulous attention to the determination of room background at each measurement location because no practical shield is thick enough to effectively eliminate gamma rays of this energy. This is not the case for the lower-energy gamma-ray region. Hence, the process of portable gamma-ray holdup measurements of plutonium using the current large-area single-crystal CdTe detector would be much simplified compared to measurements performed with low- or intermediate-resolution gamma-ray detectors, which are unable to resolve gamma rays or sensitively extract peaks from the larger continuum in the lower energy region. Applications of CdTe for holdup measurements have been proposed but are not yet tested.

The resolution of complex spectral interferences caused by fission products is not a capability of low- or intermediate-resolution gamma-ray detectors. A practical solution to unbiased holdup measurements of uranium or plutonium deposits contaminated with fission products is the portable CdTe detector. These applications too have been proposed but not tested.

VII.3. Ancillary Detection Equipment and Sources

The gamma-ray detectors used to measure holdup must also be equipped with electronics and hardware to support the measurements. Most measurements require all of the following additional equipment:

- A portable multichannel analyzer (MCA) and PC for control and readout.
- A radially symmetric collimator.
- Gamma-ray shielding on the sides and back of the detector.
- Gamma-ray filters in front of the crystal to reduce count rates at lower energies.
- A gamma-ray reference source for spectrum quality-assurance and drift compensation.
- A gamma-ray check source to verify constant calibration response.

The previous six must be implemented with the detector at the time of calibration for holdup measurements and must be retained (all but the first item must remain assembled intact with the detector) to ensure the continued validity of the holdup calibration. Additional equipment requirements include

- Detector holders, mounting fixtures and positioning devices,
- A collimator plug,
- Tape measures, permanent markers, and duct tape, and
- Utility carts, and ladders (access-permitting).

Modern commercial portable MCAs are self-contained electronics for gamma spectrometry. These battery-powered systems provide all of the power requirements for low-resolution to high-resolution gamma-ray detectors. Most require a PC for control and spectral display, but some operate fully by manual control with limited display capabilities. Fundamental capabilities for generic spectrum analysis are available only through software emulators that require a PC, which can be a laptop or palm-size.

The new commercial portable MCAs that process the detector pulse digitally (DSP) exceed analog counterparts in performance.[61] This is most apparent for operation with large Ge detectors, which are not widely used in portable applications, but is also observed – for different reasons – with noncryogenic solid-state detectors such as CdZnTe[62-65] and CdTe.[55-57] The performance of these detectors is dependent on the choice of time constants for analysis of detector pulses. The portable DSP MCAs offer a wide range of settings that define the time constants, while analog portable MCAs typically offer only two choices. The impact on energy resolution is substantial.

Detector crystals are usually cylindrical, collimated at one end of the cylinder, and shielded on the back and sides. The choice of shielding thickness can vary for lower energy gamma rays. The 186-keV gamma ray of ^{235}U is 99.9% attenuated by a half centimeter of lead, which is thin enough to limit the overall weight of the shielded portable (noncryogenic) detector to a few pounds. A full centimeter of lead, the maximum shielding thickness that is practical for a noncryogenic detector to be manually portable in the mode required for most holdup measurements, attenuates only 90% of the 414-keV gamma ray of ^{239}Pu. This practical limit to the shielding thickness places significantly greater demands on the measurements of room background in applications to plutonium based on the 414-keV gamma ray. The use of tungsten instead of lead for shielding reduces the thickness required to achieve the same shielding effect but gives only a very small reduction in weight in these applications. Tungsten shields are more costly to build, but tungsten unlike lead is nontoxic.

Radially symmetric detector collimation – a cylindrical or conical collimator – is required for consistent implementation of the holdup measurement methodology. This requirement is discussed further in Section VII. Cylindrical collimation is typical and is normally co-axial with

the axis of the cylindrical detector. Recommended exceptions to this coaxial arrangement arise when clearance space for measurements between or beneath equipment is too small to accommodate the overall length of the detector and satisfy other positioning requirements. Cylindrical collimation perpendicular to the axis of the cylindrical detector (the collimator hole penetrates the side of the detector shield) is recommended in these cases. The diameter of the typical collimator is approximately or less than that of the cylindrical crystal. The collimator aspect ratio is typically 1, but smaller ratios may be employed (by insertion of cylindrical sleeves into the ratio-1 collimator) for specific needs.

Gamma-ray filters are (usually) disks of metal foil or sheet stock that are positioned at the front of the crystal to attenuate the lower-energy portion of the gamma-ray spectrum that is unused in the holdup measurement but may otherwise contribute to high detector count rates and interfere in other ways with the reference source. Tin filters as thick as two to three millimeters have been used to filter the 60-keV gamma rays from plutonium spectra of materials with high americium content. Occasionally metal sheets are wrapped around the sides of the detector, between the detector and the shield, to filter lead or tungsten (or other materials that may be used for shielding) x rays from the gamma-ray spectrum when these x rays interfere with analysis or reference peaks. Tantalum metal sheet (0.5-mm-thick) is an effective filter of lead x rays.

The gamma-ray reference source for assurance of spectrum quality/response and for gain-drift compensation is normally positioned, as a thin disc-shaped foil laminate, between the detector and the gamma-ray filters. The reference source spectrum should be lower in energy than the regions used to measure holdup. The activity of the reference source should be sufficient for monitoring the count rate, centroid and width of the selected reference peak for every holdup spectrum including those acquired in very short count times. The choice of reference source influences the choice of radiation filters in that the spectral influence of radiation from deposits and room background in the energy region of the reference peak must be considered in selecting the filters. Common gamma-ray reference sources are ^{109}Cd and ^{241}Am with corresponding reference peaks at 60 and 88 keV, respectively. Though lower in energy, the 60-keV gamma ray is often preferred, even for the higher-energy plutonium applications. One advantage at 60 keV is the longer half-life of ^{241}Am compared with that of ^{109}Cd: approximately 450 years compared to 450 days. Despite the significant presence of ^{241}Am in all plutonium environments, the 60-keV gamma rays are also much easier to filter. The gamma-ray transmission through 2.5 mm of tin is approximately 0.001% and 2% at 60 and 88 keV, respectively. A 0.1-micro-Ci source of ^{241}Am gives a net rate of ~1000 s^{-1} in the 60 keV peak. The 60-keV reference peak measured with NaI using the nominal ^{241}Am source and appropriate filtering of low-energy gammas is very symmetric on a low continuum background with a centroid that repeats in short count times to better than 0.1 channels when the gain is adjusted to 1 keV per channel. An additional complication with the 88-keV gamma-ray reference peak when the detector is shielded with lead is the need to filter lead x rays to avoid their variable systematic effect on the measured centroid of the reference peak. Section IX.5 discusses measurement controls satisfied by the reference source.

The gamma-ray check source is, ideally, a small working standard of the material for which the holdup measurement is calibrated. More typically, it is a compact, stable form of this material such as a packaged metal foil or compressed oxide powder. The check source is equipped with a positioning holder that places it reproducibly at the end of the detector collimator. The HEU metal standards described in Table VI.1 and Figure VI.1 are used as gamma-ray check sources.[38]

Their encapsulation (Figure VI.1) allows reproducible positioning of these sources at the end of the 5.1-cm diameter detector collimator. The effective analysis result for the check source is measured at the time of calibration using the ROIs established for the calibration. The check source result is verified multiple times daily during the holdup measurement activities to ensure the continued validity of the calibration. Unlike the reference source, whose position relative to the detector is fixed, the check source result reflects any changes in the mounting of the detector within the shield, changes in collimation, or the presence of interfering background or contamination. It is also sensitive to changes in spectrum quality/response and gain, which the reference source monitors, spectrum-by-spectrum. An alternative check source such as ^{133}Ba or ^{137}Cs is sometimes used in plutonium holdup applications because of risks associated with moving plutonium sources. Section IX.5 discusses measurement controls satisfied by the check source.

Detectors for measurements of holdup may often be attached to a holder (hand-held or stand-alone) with adjustable positioning capability. Examples are the telescoping poles shown in use in Figure VII.8. Other portable options with less positioning flexibility that require less manual effort are extendable-leg tripods and counterweighted lifts. Attachment to any of these holders requires a fixture that clamps to the detector shield as well as a mating fixture on each holder. The detector fixture may be designed to also hold a positioning device such as a standoff ruler, as shown in Figure VII.8, or a laser pointer. If multiple holder options (poles, tripods, *etc*.) are planned, adapting each to the same detector fixture design is beneficial.

Collimator plugs are cylinders (or truncated cones if the collimator is conical) of lead or tungsten or other dense shielding material that insert snugly into the collimator for measurements of room background. A tungsten plug was used to obtain the room background spectra shown in Figure VII.2. A plug is especially important for measurements of room background at higher energies such as 414 and 1001 keV because these gamma rays penetrate the collimator and detector shielding. Additional rationale for the plug and further guidance on measurements of room background are discussed in Section IX.3.

It is best to determine equipment dimensions and mark the measurement positions in advance of the measurement campaign. This is not always possible, and such efforts are not always complete. Therefore, tape measures and permanent markers are essential supplies. The need for duct tape – to stabilize awkward detector positions, hold the plug inside the inverted collimator, or effect makeshift repairs, for example – is inevitable in a measurement campaign.

When measurements take place on a single accessible floor for extended periods, the use of utility carts can speed up the measurement process and sometimes eliminate the need for additional personnel. Elevated levels accessed via narrow staircases or atop catwalks are the common exceptions. The use of ladders, combined with elevation of the detector on a telescoping pole, is often necessary to reach overhead equipment.

VIII. MODELS, METHODOLOGIES, AND ALGORITHMS

Generalized procedures to quantify holdup using passive gamma measurements have been in use for decades. Recent improvements eliminate the two major sources of bias – finite source dimensions and self-attenuation – inherent in these procedures without sacrificing the generality of the approach.[66, 67] The improvements rely on a common empirical parameter that self-consistently limits the total error incurred (from uncertain knowledge of this parameter) in the combined correction process. This describes the generalized models and the methods to calibrate, measure and analyze holdup using these models. All algorithms required for implementation – including those addressing the effects of the finite source dimensions, self-attenuation, and corresponding expressions for random uncertainty – are presented. Spreadsheet automation of the complete analysis is straightforward.

VIII.1. Generalized Geometry Holdup (GGH) Method

The Generalized Geometry Holdup (GGH) analysis method was developed to simplify the quantitative analysis of holdup by measurements performed using portable gamma-ray spectroscopy. One extreme viewpoint on holdup measurements is that the geometry of each individual holdup deposit is unique. Because holdup is measured with portable radiation detectors, variable measurement geometry adds another dimension to the geometric uniqueness of each holdup measurement. The variable radiological environment for each deposit location is yet another. Therefore, the analysis of holdup data, which necessarily involves many measurements (hundreds or thousands), is only practical with constraints applied to the variables.

VIII.1.1. Assumptions and constraints.

Four constraints that simplify the models used to interpret holdup measurements were defined in regulatory guides published by the Nuclear Regulatory Commission approximately 25 years ago[6, 7] and were revised at Los Alamos approximately 15 years ago. Two of the four constraints are achieved mechanically.

1) Heavy metal shielding on the back and sides of the crystal limits efficient detection to gammas that impinge on the front of the crystal.
2) A cylindrical collimator concentric with the crystal, installed on the front of the crystal, defines the field of view and maintains a symmetric response about the detector axis.

The other two requirements enforce the measurement geometry.

3) Position the detector relative to the deposit so that the two-dimensional spatial distribution of the deposit in its planar field of view at the measurement distance can be described as one of the following with respect to the field of view:
   i) A small point at its center.
   ii) A narrow, uniform line through its center whose length extends beyond its width.
   iii) A uniform distribution whose length and width extend beyond its length and width.
4) Each measurement is performed with an associated, known measurement distance $\boldsymbol{r}$ between the detector (crystal) and the deposit plane. Section IX.1 and Tables IX.1 and IX.2 give the components of $\boldsymbol{r}$.

Figure VIII.1 illustrates the four constraints for a point source.

Knowledge of an additional parameter that specifies the deposit width is a fifth constraint on the measurement geometry that will be required in order to perform the new corrections for finite source dimensions and gamma-ray self-attenuation. This requirement is discussed in depth throughout Sections VIII.3.1-3 and VIII.4.1-4.

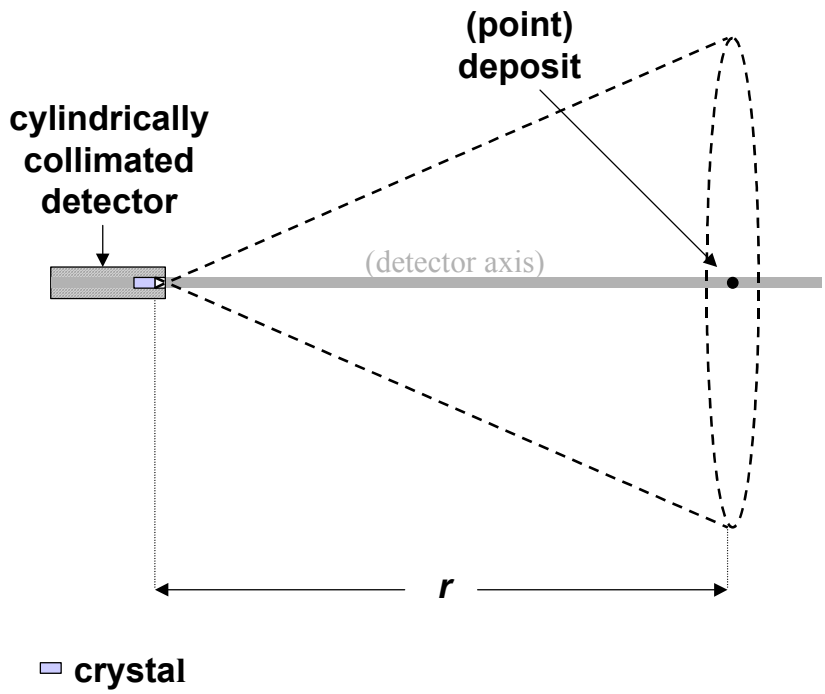

Figure VIII.1. A point source is positioned on the axis of the cylindrically collimated detector at distance r from the crystal. The field of view (dashed circle) is in the source plane perpendicular to the detector axis.

VIII.1.2. Calibration.

Calibration of the quantitative analysis of a point, line or area deposit of a given isotope is accomplished with a single point source standard of known attenuation. The reference mass m_0 of the isotope in the standard is corrected for self-attenuation before it is applied in the calibration.[8] The response for each gamma-ray peak is measured with this source positioned on the detector axis at a known distance r_0 from the crystal. (Section IX.1 and Tables IX.1 and IX.2 give the components of r_0.) Measurements are also performed with the source displaced at fixed intervals from the axial position on a line that is perpendicular to it. These data are used to obtain the two-dimensional radial response of the collimated detector. Because the collimation is cylindrical, few measurements are needed to determine the radial response.

Figure VIII.2. illustrates nine off-axis positions for a point source used to determine the two-dimensional radial response of a collimated detector at the fixed distance. The axial position is at the center of nine concentric circles that intersect each of the nine measurement points indicated with integers. The response of the detector to a source at any point on the circle equals the

corresponding measured response at the fixed measurement distance r_0 because of rotational symmetry.

Figure VIII.3 shows the normalized radial response data (room-background-subtracted, net peak count rate C_i *vs*. axial displacement i of the source) obtained in this way for the 414-keV gamma ray of ^{239}Pu using a 2.54-cm diameter by 5-cm thick NaI detector. The length and diameter of the collimator are both 2.54 cm. The distance between the calibration source and crystal, r_0, is 40 cm. Data for this example were obtained with the point source positioned on both sides of the axial position.

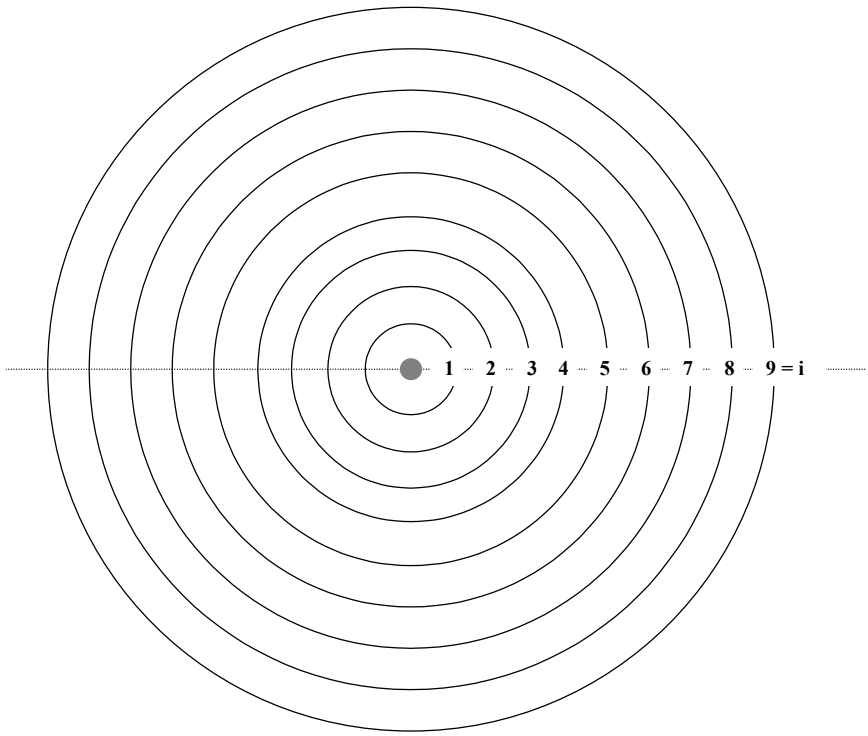

Figure VIII.2. Nine, equally spaced off-axis positions of the point source used to measure the two-dimensional radial response of the gamma-ray detector at a fixed distance r_0 are illustrated. The axial position (center) is the source position illustrated in Figure VIII.1. The detector response is constant for a source at any point along each concentric circle. Because of this radial symmetry, the two-dimensional response can be determined with a small number of measurements.

The data in Figure VIII.3 are used to calibrate of the quantitative analysis of specific isotope mass in a point, line or area deposit. The point calibration uses only the un-normalized axial response C_0 (s^{-1}) because model assumes that a point deposit has no finite width in either dimension of the detector's two-dimensional field of view. The point calibration constant is:

$$K_P\ (\mathrm{g} \bullet \mathrm{s} \bullet \mathrm{cm}^{-2}) = m_0 \div (C_0 \bullet r_0^2) \quad . \qquad (1)$$

The specific mass of the isotope measured with this detector at a distance r (to obtain a room-background-subtracted net count rate C for the analysis peak) and analyzed as a point deposit depends on the square of the measurement distance:

$$m_P\,(\mathrm{g}) = K_P \bullet C \bullet r^2 \quad . \qquad (2)$$

The measured specific mass of a point deposit is identical to the mass of the deposit. The random relative uncertainty in the mass, assuming only random (statistical) error in ***C*** is:

$$\sigma_R(m_P) = \sigma_R(C) \quad , \qquad (3)$$

where relative uncertainty $\boldsymbol{\sigma_R(C)}$ is propagated from counting statistics.[8]

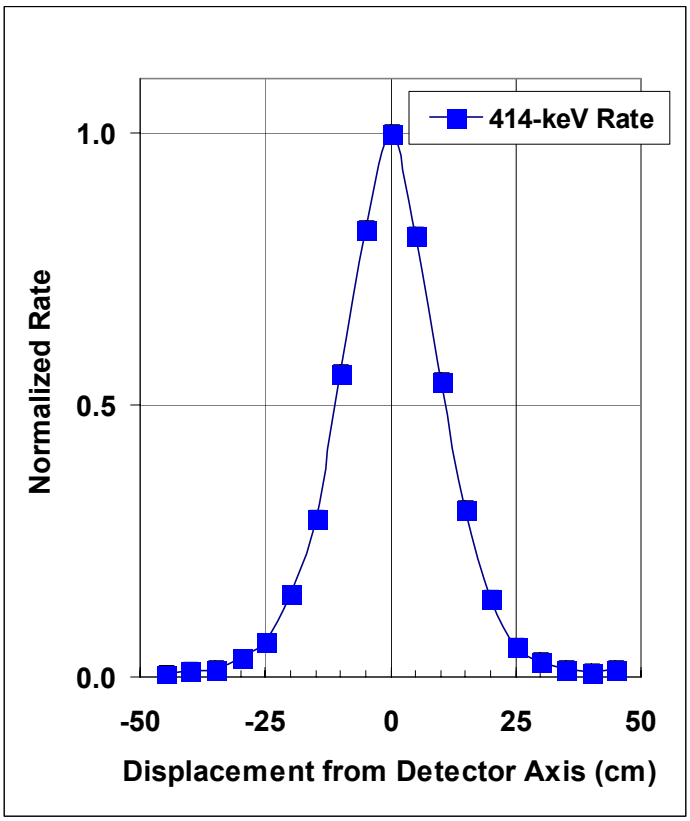

Figure VIII.3. Normalized net, room-background-subtracted rate of the ^{239}Pu 414-keV peak vs. displacement of the point source from the detector axis. A smooth curve connects the data points. This one-dimensional radial response was measured at a distance r_0 of 40 cm with a collimated NaI detector (2.54-cm diameter by 5-cm long crystal). Collimator depth and diameter were both 2.54 cm. Data obtained on both (positive and negative) sides of the detector axis confirm the radial symmetry.

The line calibration uses both the un-normalized axial response $\boldsymbol{C_0}$ (s^{-1}) and a geometric response parameter ***L*** (cm) that is evaluated from a sum of the normalized radial responses $\boldsymbol{C_i}$ weighted by the distance between the measurement positions.[8-10] The geometric model assumes line deposit exceeds the width of (fills) the detector's field of view in length and has no finite width in the second dimension of the two-dimensional field of view. The line calibration constant is:

$$K_L\ (\mathrm{g \bullet s \bullet cm^{-2}}) = m_0 \div (L \bullet C_0 \bullet r_0) \quad . \tag{4}$$

The specific mass of the isotope measured with this detector at a distance ***r*** (to obtain a room-background-subtracted net count rate ***C*** for the analysis peak) and analyzed as a line deposit depends on the measurement distance to the first power:

$$m_L\ (\mathrm{g/cm}) = K_L \bullet C \bullet r \quad . \tag{5}$$

This is also called the measured linear density of the deposit. The random relative uncertainty in the linear density, assuming only random error in ***C*** is:

$$\sigma_R(m_L) = \sigma_R(C) \quad , \tag{6}$$

where relative uncertainty $\boldsymbol{\sigma_R(C)}$ is propagated from counting statistics.[8]

The area calibration uses both the un-normalized axial response $\boldsymbol{C_0}$ (s^{-1}) and a geometric response parameter ***A*** (cm^2) that is evaluated from a sum of the normalized radial responses $\boldsymbol{C_i}$ weighted by the area between the axially concentric circles that intersect the measurement positions.[8-10] The geometric model assumes that the length and width of an area deposit exceeds the length and width of (fills) the detector's two-dimensional field of view. The area calibration constant is:

$$K_A\ (\mathrm{g \bullet s \bullet cm^{-2}}) = m_0 \div (A \bullet C_0) \quad . \tag{7}$$

The specific mass of the isotope measured with this detector at a distance ***r*** (to obtain a room-background-subtracted net count rate ***C*** for the analysis peak) and analyzed as an area deposit is independent of the measurement distance:

$$m_A\ (\mathrm{g/cm^2}) = K_A \bullet C \quad . \tag{8}$$

This is also called the measured areal density of the deposit. The relative uncertainty in specific mass, assuming only random error in ***C*** is:

$$\sigma_R(m_A) = \sigma_R(C) \quad , \tag{9}$$

where the relative uncertainty $\sigma_R\ (C)$ is propagated from counting statistics.[8]

By adhering to the four constraints listed above, calibration for a breadth of deposit geometries is achieved simply with a point source standard of the isotope. This approach circumvents the great difficulties of fabricating reference samples of special nuclear materials configured in special geometric distributions. Validation of the holdup measurements calibrated by such techniques is nevertheless essential. Refer to Section VI.3.

Refer to Section VI for specific requirements on calibration standards and Section IX.2 for alternative reference materials suitable for measurements of the radial response. Procedures for calibration measurements are discussed in Sections IX.1 and IX.2.

VIII.1.3. Obtaining and analyzing specific mass: overview.

Using the GGH analysis method to determine quantities of uranium or plutonium holdup by portable gamma-ray spectroscopy requires portable gamma spectroscopy electronics, a collimated/shielded gamma-ray detector, and other hardware as described throughout Section VII. The spectrometer system must be calibrated as described in Section VIII.1.2. A user must understand the assumptions in the two-dimensional point, line and area deposit models in order to make the best choice for positioning the collimated detector for measurement at each holdup location. The distance $\boldsymbol{r}$ between deposit and detector must be recorded for each measurement. Section IX.4 gives recommendations on measurements that are of great importance to ensuring the validity of the models. Section IX.1 and Tables IX.1 and IX.2 give the components of $\boldsymbol{r}$.

A spectrum of the room background is required for each deposit measurement. This is particularly important for ^{239}Pu measurements because the 414-keV γ rays penetrate the detector shield more readily than the 186-keV gamma rays of ^{235}U. Procedures for obtaining the room-background spectrum and using the associated reduced spectral data vary according to the gamma-ray energy (or energies), measurement geometry, and plant environment. Refer to Section IX.3 for recommendations on measurements of room background.

Analysis of the gamma-ray spectra of both the holdup deposit and room background gives a net count rate for the analysis peak. Subtraction of the two rates gives the room-background-subtracted net rate, $\boldsymbol{C}$. This is used along with $\boldsymbol{r}$ and the GGH calibration constants described above to obtain the specific isotope mass for point, line or area deposits using Equations (2), (5) or (8), respectively. The corresponding relative uncertainty in the specific mass is determined for each result from Equations (3), (6) and (9), respectively.

Count times for holdup measurements can be very short (5-15 s) when the acquisition of data is automated in order to perform measurements at as many locations as possible, as discussed in Section X.4. Therefore, the random uncertainty can be large for the individual measurements as a result of counting statistics alone, especially when the deposit is thin and/or room background is high. The random uncertainty in specific mass propagates nonlinearly through the self-attenuation correction (Sections VIII.4.1-VIII.4.3) causing the random uncertainty to increase for thick deposits for which the correction is large. Propagating the uncertainties of the many measurements that are normally performed and averaged to get the total holdup in an extended piece of equipment considerably reduces the relative random error in the final result for mass. However, the random uncertainty of each individual measurement must be preserved through the final correction step i) in order to propagate this uncertainty through the nonlinear expressions, and ii) for use in tests described in Section VIII.4.3 to validate that measurements are in the range applicable to self-attenuation corrections.

The initial analysis result provides the specific mass $\boldsymbol{m_P}$ (g), $\boldsymbol{m_L}$ (g/cm), or $\boldsymbol{m_A}$ (g/cm^2) – for a point, line, or area deposit, respectively. Each deposit is measured and analyzed as one of three, generalized, two-dimensional geometries. Each analysis includes subtraction of the room background signal. However, three additional corrections to the measured specific mass are required to improve the accuracy of every measurement result. Each of the three corresponding effects contributes to a negative bias in the holdup analysis result for specific mass if the effect goes uncorrected. The first effect is that of equipment attenuation. The corresponding correction has been carried out routinely for decades. The correction approach is reviewed briefly in Section VIII.2 because it is this result that must be corrected further for two effects that have

been ignored in GGH analysis in the past. The two additional effects are that of the finite source dimension and self-attenuation. The corresponding generalized correction procedures are treated in depth in Sections VIII.3.1-VIII.3.3 and VIII.4.1-VIII.4.3. The corrections must be performed in the sequence in which they are treated below because of the nonlinearity of the self-attenuation correction.

VIII.2. Correcting Specific Mass for Effect of Equipment Attenuation

Correcting the specific mass of a point, line or area deposit, $\boldsymbol{m_P}$ (g), $\boldsymbol{m_L}$ (g/cm) or $\boldsymbol{m_A}$ (g/cm^2) for equipment attenuation effects gives $\boldsymbol{m_{P,EQ}}$ (g), $\boldsymbol{m_{L,EQ}}$ (g/cm) or $\boldsymbol{m_{A,EQ}}$ (g/cm^2) for a point, line or area source. The correction factor for equipment attenuation is always greater than 1. It is expressed by the formula:

$$CF_{EQ}(Z, E\gamma) = e^{\mu\rho t} \quad , \tag{10}$$

where, ρ (g/cm^3) and **t** (cm) are the density and thickness of the equipment. Wall thickness will underestimate **t** for curved or extended equipment. The corresponding systematic effects should be quantified as described in Section IX.8. The mass attenuation coefficient μ (cm^2/g) depends on the $\boldsymbol{Z}$ of the equipment and on the gamma-ray energy $\mathbf{E_\gamma}$. The correction for equipment attenuation is applied linearly to the room-background-subtracted specific mass of a point, line or area deposit, Equation (2), (5)and (8), respectively. The corrected specific masses are:

$$m_{P,EQ}\ (\text{g}) = m_P \cdot CF_{EQ}(Z, E\gamma) \quad , \tag{11}$$

$$m_{L,EQ}\ (\text{g/cm}) = m_L \cdot CF_{EQ}(Z, E\gamma) \quad , \tag{12}$$

and

$$m_{A,EQ}\ (\text{g/cm}^2) = m_A \cdot CF_{EQ}(Z, E\gamma) \quad , \tag{13}$$

respectively. Because the correction is applied linearly to the uncorrected specific masses, the relative uncertainties in $\boldsymbol{m_{P,EQ}}$, $\boldsymbol{m_{L,EQ}}$ or $\boldsymbol{m_{A,EQ}}$ are unchanged from those given in Equations (3), (6) and (9), respectively.

The analysis gamma ray for measurements of ^{239}Pu holdup is usually 414 keV. The 414-keV gamma ray is much more penetrating of process equipment than the 186 keV gamma ray used to measure ^{235}U holdup. Therefore, the primary equipment-attenuation correction factors for ^{239}Pu holdup measurements will be closer to 1 than those for ^{235}U holdup measurements for the same type of process equipment. However, many holdup measurements of ^{239}Pu are performed on equipment that is housed within a secondary containment (glovebox, *etc*.), which can result in a larger overall correction factor for equipment attenuation of the higher energy gamma ray.

Net room-background count rates may require correction for equipment attenuation before being subtracted from the net count rates of the deposits. This occurs when the equipment that contains the deposit shields the detector from room background that reaches the detector through the collimator when the deposit is being measured. The detector may be displaced laterally from this equipment in order to measure the room background. The correction factor is the inverse of

Equation (10) and is less than 1 in this case. Refer to Section IX.3 for discussions of approaches to measuring room background.

Lack of knowledge of the process equipment affects the accuracy of equipment attenuation corrections. Process equipment may not be visible in some cases. Because the distribution of deposits on surfaces of complex equipment may be unknown and because of the complexity itself, it may be difficult to judge the applicable thickness dimension ***t***. Nonetheless, determining a best estimate of the type of material in the equipment and its thickness ***t*** is recommended. If no correction for equipment attenuation is performed, the individual specific mass and total holdup mass results will always be biased low. While a bias of 10% is generally not important for an individual deposit, a 10% bias in total holdup mass is a serious problem. An estimate of the equipment attenuation effects based on the best information available will give a result that may sometimes be high or low for the individual measurements, but the overall result for holdup mass that is based on many measurements of specific mass is likely to be unbiased.

Measurements of ^{239}Pu holdup in bulk-processing equipment in glove boxes[68] used values of $\boldsymbol{CF_{EQ}}(\boldsymbol{Z}$, 414 keV) that varied from 1.1 (lead-lined gloves) to 6.2 (steel plates on a glove box floor). Equipment attenuation corrections are implemented in most holdup measurements.

VIII.3. Correcting Specific Mass for Effect of Finite Source Dimension *w*

VIII.3.1. Concept of the finite source in holdup measurements.

Correcting for the finite dimension of a point or line deposit analyzed by the GGH method necessary because the deposit width ***w*** is a finite fraction of the field of view of the detector at the deposit distance. Finite-source corrections are not used for area deposits, whose dimensions fill the detector's field of view at the measurement distance ***r***.

It is rarely possible to position the detector such that the finite-source effect is negligible, and some situations arise that cause the effect to be large. These include physical barriers that limit the measurement distance. Areas with high room background rates relative to the count rates from holdup deposits, which may be small, also cause measurements to be performed at smaller distances. This is more common for measurements of ^{239}Pu holdup because the 414-keV gamma ray penetrates the detector shield more readily than the 186-keV gamma ray of ^{235}U. Finally, a smaller measurement distance might be required for holdup in closely spaced equipment to avoid collecting spectral data from more than one piece of equipment in a given measurement for cases in which the deposits must be quantified separately.

Figure VIII.4.a) shows a holdup measurement situation in which the measurement distance ***r*** and field of view are relatively large compared with the width of the deposit in the vertical pipe. Figure VIII.4.b) illustrates a measurement with the same detector at a similar measurement distance. The diameter of the horizontal overhead duct in Figure VIII.4.b) is four times that of the vertical pipe in Figure VIII.4.a). Furthermore, adjacent overhead equipment in Figure VIII.4.b), which may also contain holdup deposits, is in proximity to the horizontal duct being measured. A larger measurement distance may cause deposits from the adjacent ducts to be included in the field of view. The horizontal duct appears as a broad line in the detector's somewhat wider field of view at the measurement distance pictured in Figure VIII.4.b) whereas the vertical pipe is a narrow line in a relatively wide field of view in Figure VIII.4.a). Depending

on the width of the actual deposit in the horizontal overhead duct, a large finite-source effect might be expected for the case illustrated in Figure VIII.4.b) if the deposit is measured as a line source.

Figure VIII.5 shows a very large overhead duct being measured from below with a portable, collimated Ge detector. The measurement distance for any detector positioned beneath this duct will be comparable to the duct diameter because of the limited height of the equipment above the floor. The duct width is always a significant fraction of the width of the field of view of the detector for common ventilation ducts such as these. A large finite-source effect might be expected for such equipment if holdup deposits are measured as line sources.

The small measurement distance illustrated in Figure VIII.5 may have been selected to fill the field of view of the collimated detector with the deposit within the duct. Adjusting the measurement geometry to satisfy requirements for an area deposit eliminates finite-source effects but increases the probability of systematic sampling effects because a smaller fraction of the total deposit is included in the field of view. A larger measurement distance will improve the quantitative result from the standpoint of sampling, finite source dimensions, and positioning uncertainties. However, the measurement distance must be optimized rather than maximized because the (degrading) effects of deposits in adjacent equipment and the decreasing signal-to-background ratio of the gamma-ray peak are enhanced at greater measurement distances. Section X.3 discusses simple approaches to optimizing measurement distance.

Figure VIII.4. a). A collimated NaI detector (radial response described by Figure VIII.3) measures the gamma-ray spectrum of holdup in the pipe at the location marked by the white bar-coded label. This vertical pipe appears as a narrow line in the detector's relatively wide field of view at this measurement distance. The finite-source effect on the specific mass for the line deposit is small in this case. b). The same detector is positioned at the same measurement distance from a second bar-coded measurement location on a horizontal duct whose diameter is four times that of the vertical pipe in a). Proximity of the neighboring overhead equipment may prevent use of a larger measurement distance without including additional deposits in the field of view. The horizontal duct appears as a broad line in the detector's somewhat wider field of view at this measurement distance. The finite-source effect on the specific mass for the line source is much larger in this case.

Figure VIII.5. A very large overhead duct is measured from below with a portable collimated Ge detector. The largest measurement distance for any detector positioned beneath this duct is comparable to the duct diameter because of the proximity of the equipment to the floor. The duct width is always a significant fraction of the width of the field of view of the collimated gamma-ray detector for common ventilation ducts such as this. The duct surface completely fills the field of view of this collimated detector, a geometry that is most likely (depending on the dimensions of the deposit) best-suited to analysis of the holdup as an area deposit.

The correction for the finite source dimension of a point, line, or area deposit is applied linearly to the respective specific mass, Equation (11), (12) or (13) that has been corrected for equipment attenuation. The correction factor for a finite-source effect is always 1 or greater. The respective specific mass corrected for finite-source effect is:

$$m_{P,FIN}\ (\mathrm{g}) = m_{P,EQ} \cdot CF_{FIN,P} \quad , \tag{14}$$

$$m_{L,FIN}\ (\mathrm{g/cm}) = m_{L,EQ} \cdot CF_{FIN,L} \quad , \tag{15}$$

or

$$m_{A,FIN}\ (\mathrm{g/cm^2}) = m_{A,EQ} \tag{16}$$

because

$$CF_{FIN,\mathrm{A}} = 1 \quad . \tag{17}$$

Because the finite-source correction is applied linearly to the specific masses, the relative uncertainties in $\boldsymbol{m_{P,FIN}}$, $\boldsymbol{m_{L,FIN}}$ or $\boldsymbol{m_{A,FIN}}$ are unchanged from those given in Equations (3), (6) and (9), respectively.

VIII.3.2. Models of finite sources.

Figures VIII.6-8 are sketches that illustrate two-dimensional finite area, line, and point deposits with diagonal shading. The illustrated shading is uniform, unlike the thickness distribution of most actual deposits. However, deposit nonuniformity as a departure from the assumptions of the two-dimensional geometric model has a random effect on the result of each holdup measurement if detector positioning at successive locations has constant spacing and is random with respect to deposit locations. No bias is incurred in the total measured holdup from nonuniformities in the deposit when dozens (hundreds, thousands) of individual holdup measurements are performed per campaign.

Like the systematic effects of equipment attenuation, those of finite-source effects cause a negative bias in each individual holdup measurement. If finite-source effects are ignored in the analysis of the holdup data, the total measured holdup will also be biased low. Controls may be implemented to minimize the effects of finite source dimensions by choosing the largest practical measurement distance ***r***. While a bias of several percent is generally not important for an individual measurement point, a several-percent bias in a facility's total holdup is a problem.

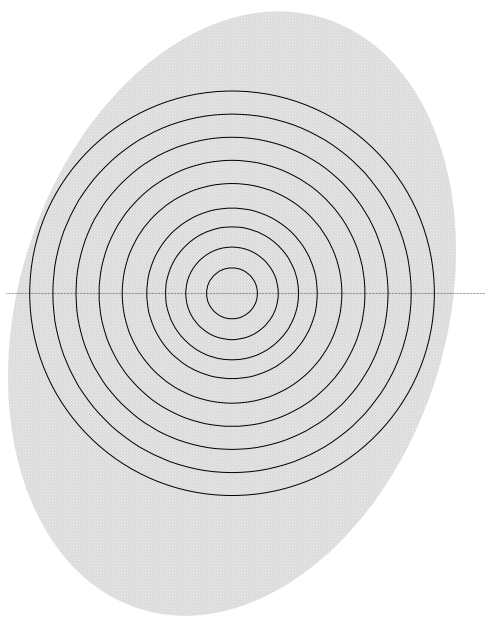

Figure VIII.6. The diagonally shaded area represents a finite area deposit superimposed on the field of view of the cylindrically collimated detector. Concentric circles indicate equally spaced loci of constant response. The radial positions defined by these circles mark the axial source displacements used to obtain the radial response plotted in one dimension in Figure VIII.3. The finite area deposit fills the field of view in two dimensions, as prescribed by the two-dimensional model for the area deposit.

The finite area deposit in Figure VIII.6 fills the field of view of the detector, in accordance with the two-dimensional model for the area source. Because the model of the area deposit does not constrain the dimension of the deposit, the finite area source introduces no bias.

The finite line deposit in Figure VIII.7 is centered in the circular field of view, and its length exceeds the width of the field of view, as required by the line source model. However, although its width ***w*** is less than the width of the field of view, it is a considerable fraction of it. The generalized line-source model constrains the geometry of the line deposit in one dimension by assuming that the line width is very small compared with the width of the field of view, as illustrated by the narrow solid horizontal line. If the response of the detector to a source at any position on the line deposit is less than the peak of the response at the horizontal displacement (from the axial position), a model-dependent negative bias is incurred. The diagonally shaded line in Figure VIII.7 and most line deposits of holdup have finite widths, in this sense. Assuming that the concentric circles in Figure VIII.7 correspond to the measurement positions in Figure VIII.3, the detector response varies between 80% and 100% of its peak response across the width (***w***, the vertical dimension labeled in Figure VIII.7) of the diagonally shaded line. The response of the detector to the uniform line deposit is only ~90% of the expectation of the model in one of the two dimensions in this example. If the measurement is analyzed as a line deposit in this case, the result would be biased by -10% and a correction factor of 0.9^{-1} or 1.11 would be needed.

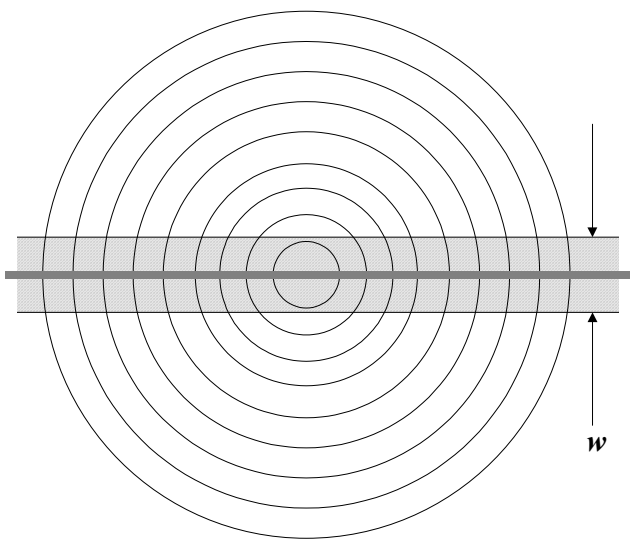

Figure VIII.7. The diagonally shaded area represents a finite line deposit superimposed on the field of view of the cylindrically collimated detector. Concentric circles indicate equally spaced loci of constant response. The radial positions defined by these circles mark the axial source displacements used to obtain the radial response plotted in one dimension in Figure VIII.3. The finite line deposit is centered in the field of view with a length that exceeds the width of the field of view in one dimension, as prescribed by the two-dimensional line model. The finite width w exceeds that prescribed by the one-dimensional constraint for the line deposit (narrow, solid line).

The finite point deposit in Figure VIII.8 is centered in the circular field of view, as required by the point-source model. The width, ***w***, of the finite point deposit is less than the width of the field of view in Figure VIII.8, but is a considerable fraction of it nonetheless. The model for a point deposit assumes that the point diameter (width) is very small compared with the width of the field of view, as illustrated by the small solid point. If the response of the detector to a source at any position on the point deposit is less than the peak of the response at the center of the field of view, a model-dependent negative bias is incurred. The diagonally shaded point in Figure VIII.8 as well as most point holdup deposits has finite width in this sense. Assuming that the concentric

circles in Figure VIII.8 mark the axial source displacements in Figure VIII.3, the detector response varies from ~80-100 % of its 'peak' across both (vertical and horizontal) width dimensions of the diagonally shaded point in Figure VIII.8. The average response for this example is ~90% of the expectation of the model in both of the two dimensions. If the measurement is analyzed as a point deposit in this case – and note that the width ***w*** of the finite point in Figure VIII.8 is the same as that of the finite line in Figure VIII.7 – the result would also be biased but by -20% in the case of the point deposit. A correction factor of 0.9^{-2} or 1.23 is required. The point-source correction factor is the square of that for the line source because the model constrains the geometry of the point deposit in two dimensions rather than one.

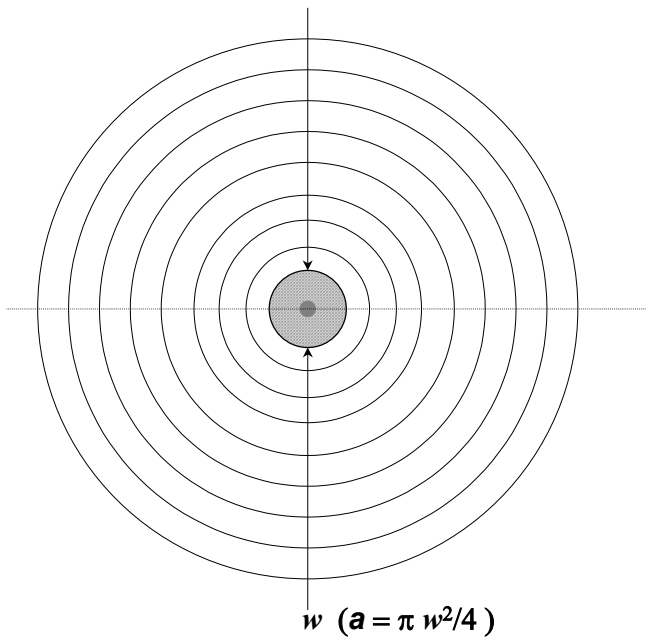

Figure VIII.8. The diagonally shaded area represents a finite point deposit superimposed on the field of view of the cylindrically collimated detector. The concentric circles indicate equally spaced loci of constant response. The intersections of the circles with a diameter mark the axial source displacements in the one-dimensional radial response plotted in Figure VIII. 3. The finite point deposit is centered in the field of view, as prescribed by the two-dimensional model for the point source. Its finite width w (which gives its area a) exceeds that prescribed by the two-dimensional constraint for the point deposit (small, solid point).

VIII.3.3. Correct measured specific mass for finite source dimension *w*.

Correcting for the finite dimension of a deposit begins with a decision on the width ***w*** of the deposit. An over- or underestimate of ***w*** leads to over- or undercorrection for the effect of the finite source dimension. However, as described previously, this characteristic is preferable to a persistent negative bias caused by uncorrected finite-source effects because the total holdup will tend to be unbiased. To minimize the magnitude of the over- or undercorrection of the individual holdup measurements, the choice of the finite source dimension must be a best estimate based on knowledge of the equipment and process and, if possible, on a scanning of the gamma-ray count rate across the surface of the equipment with a collimated detector. If a duct is oriented vertically, for example, it is reasonable to assume that the deposit width is the inner diameter of

the duct. If it is horizontal and cylindrical, a scan of the equipment may be a better approach to estimating ***w***.

Defining ***w*** uses known parameters of holdup deposits. Using ***w*** in a general manner to correct for the finite dimensions of holdup deposits is a new approach.[67, 68]

An aspect of ***w*** that should be addressed at this point in the derivation of the correction algorithms is that the same experimental width parameter ***w*** required for the finite-source corrections is also required in the corrections for self- attenuation, as described in Section VIII.4.1-3. Furthermore, Section VIII.5 demonstrates that there is actually a compensating effect between the finite-source and self-attenuation corrections in the sensitivity of the experimental result for specific isotope mass to the uncertainty in the experimental width parameter ***w***. Therefore, it is very important to perform both corrections, in order to i) avoid a negative bias in the measured holdup (that results both from the effects of the finite source dimensions and self attenuation) and ii) reduce the magnitude of the (positive or negative) systematic effects associated with over- or underestimates of the experimental width parameter ***w***.

The corrections for the finite dimensions of a holdup deposit can be performed in six steps. The emphasis is on generality. The procedure is the same for and applicable to all measurements. Previous efforts to address the finite dimensions of deposits have viewed the geometry of the particular type of holdup deposit uniquely in an approach that does not extend generally to other geometries.[26-28] The emphasis is also on formality and simplicity so that process for any measurement application can be documented and also automated by software.

The following six steps describe the method and algorithms for the finite-source corrections.

1) Plot the normalized radial response data C_i for the analysis gamma ray (the 414-keV ^{239}Pu peak or the 186-keV ^{235}U peak, for example) measured with the point source at the positions ***i*** along a line at a fixed distance r_0 from a particular detector. Figure VIII.3 shows this plot, with a smooth curve ***C(x)*** drawn through the data points, for the ^{239}Pu gamma ray at 414 keV. Evaluate **C(x)** from the numerical data or, alternatively, fit the data to a normalized Gaussian ***G(x)***, or another form that represents the shape of the radial response curve. The Gaussian example is

$$C(x) = G(x) = \exp[-0.5(2.354x/\mathrm{FW.5M})^2] \quad , \qquad (18)$$

where ***x*** is the displacement of the source from the detector axis. Figure VIII.9 is a plot of the fit of Equation (18) to the data from Figure VIII.3. The data points are also plotted. The curve ***C(x)*** is used to obtain all corrections for the finite dimensions of point or line deposits measured with this particular detector.

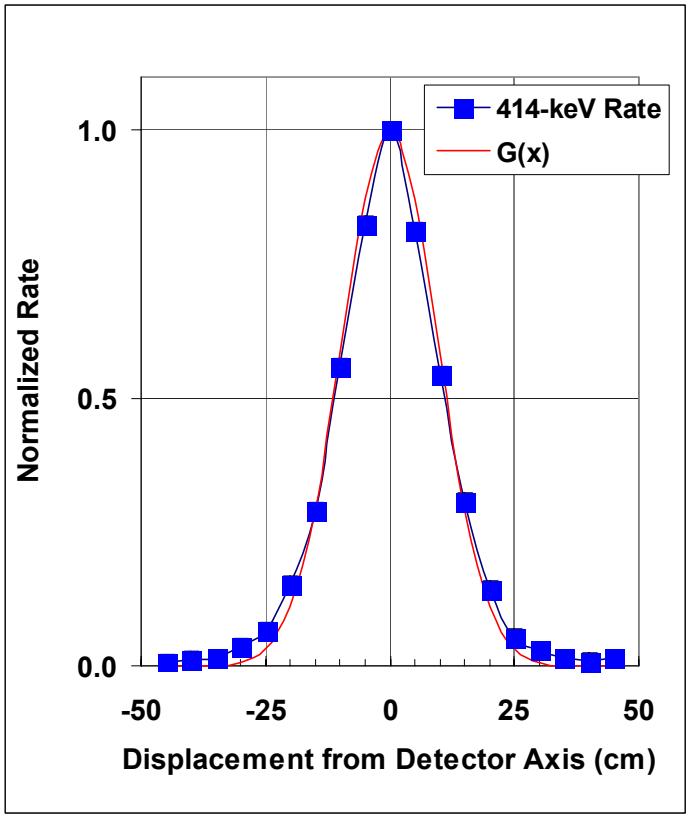

Figure VIII.9. The data from Figure VIII.3 (normalized net, room-background-subtracted count rate of the ^{239}Pu 414-keV gamma-ray peak vs. displacement of the point source from the detector axis) are shown in blue. The measurements were performed at a distance r_0 of 40 cm with a collimated NaI detector. The red curve is the fit of Equation 18 (normalized Gaussian) to these data. The FW.5M of the fit is 22 cm.

2) Measure a holdup deposit at distance $\boldsymbol{r}$ with finite dimension $\boldsymbol{w}$ (width of a line or diameter of a point source). Use the ratio $\boldsymbol{r}/\boldsymbol{r_0}$ to adjust $\boldsymbol{w}$ for the difference between $\boldsymbol{r}$ and the calibration distance $\boldsymbol{r_0}$.

$$w_0 = w \cdot (r/r_0)^{-1} \quad . \tag{19}$$

3) Determine the normalized radial response $\boldsymbol{C}(\boldsymbol{w_0}/2)$ at the outer edge ($\boldsymbol{x} = \boldsymbol{w_0}/2$) of the line or point by reading it from the plot (Figure VIII.9) or evaluating it from the fit.

4) Obtain the average of $\boldsymbol{C}(\boldsymbol{w_0}/2)$, the normalized response at the edge of the deposit, and 1, the normalized response at the center of the deposit, to get the effective radial response

$$C_{EFF} = [\ 1 + C(w_0/2)\ ] / 2 \tag{20}$$

for the source of finite dimension $\boldsymbol{w}$.

5) Compute the finite-source correction factor for a line deposit.

$$CF_{FIN,L} = (C_{EFF})^{-1} \ , \tag{21}$$

or a point deposit

$$CF_{FIN,P} = (C_{EFF})^{-2} \ . \tag{22}$$

6) Apply the finite-source correction to the equipment-attenuation corrected specific mass for a point deposit using Equation (14). Apply the finite-source correction to the equipment-attenuation corrected specific mass for a line deposit using Equation (15). Recall that the finite dimensions of the area deposit complies with the model for this geometry so that there is no correction to the equipment-attenuation corrected specific mass. See Equation (16).

Advantages of using an analytical form such as a Gaussian fit to the radial response data $\boldsymbol{C_i}$ rather than a smooth curve drawn through the data include simplicity of implementation and automation. A disadvantage is that the shape of the radial response depends on the collimator dimensions and changes with the energy of the gamma ray for a given detector. A given analytical form may represent the measured response better at one energy than another. The Gaussian, for example, gives a better fit to the radial response measured with a lead-collimated NaI detector (2.54-cm-diameter crystal and collimator) for the ^{235}U gamma ray at 186 keV than for the ^{239}Pu gamma ray at 414 keV (Figure 9). Refer to Section IX.1 for further discussion.

A sample calculation showing the effect of a finite-source correction is presented below. It is based on using the detector described in Figure VIII.9 to measure the 414-keV gamma ray of ^{239}Pu in a 24-cm-wide vertical duct viewed as a (wide) line at $\boldsymbol{r}$ = 80 cm. Assuming that $\boldsymbol{r_0}$ = 40 cm, Equation 19 gives

$$w_0 = 12 \text{ cm} \quad ,$$

and Equation (18) – or Figure VIII.9 – gives

$$C(w_0/2) = 0.8 \quad .$$

Therefore, the effective normalized radial response to deposits in the duct, Equation (20), is

$$C_{EFF} = (1 + 0.8)/2 = 0.9 \quad .$$

The correction factor from Equation (21) for the finite line source, which multiplies the specific mass $\boldsymbol{m_{L,EQ}}$ for the finite line deposit, Equation (15), is

$$CF_{FIN,L} = (0.9)^{-1} = 1.11 \quad .$$

Measurements of plutonium holdup[68] in high-throughput bulk-processing equipment inside of glove boxes used the 414-keV gamma ray and the GGH formalism. The values of $CF_{FIN,L}$ obtained varied from 1 (for area deposits on glove box surfaces) to 1.25 (for line deposits of powder accumulated in troughs on the glove box floor).

The six-step procedure for finite-source corrections described and illustrated above applies to holdup deposits measured with a cylindrically collimated gamma-ray detector of any type. It applies to holdup measurements that are set up and analyzed as point or line deposits consistent with the geometric requirements of the generalized models. Like the GGH procedure itself, the corrections may be implemented for any gamma-ray spectrometer detector (NaI, BGO, Ge, CZT, *etc*.) and any gamma-ray peak chosen for the quantitative analysis. Because of certain choices made during the holdup measurements that are based on the radiological characteristics of ^{235}U and ^{239}Pu, corrections for the effects of finite source dimensions may tend to be larger for measurements of ^{239}Pu than for ^{235}U. This can be the case because the 414-keV gamma ray of ^{239}Pu is more penetrating of the background shielding on the detectors than is the 186-keV gamma ray of ^{235}U. A smaller measurement distance $\boldsymbol{r}$ may be necessary for measurements of ^{239}Pu or LEU to improve the ratio of signal to background to achieve the required detection sensitivity. Refer to Section IX.3 for guidance on choosing $\boldsymbol{r}$ and IX.1 for components of $\boldsymbol{r}$.

The six-step procedure for finite-source corrections described and illustrated above is readily implemented with a spreadsheet. It is also part of the *HMS4* analysis software, which automates the plant-wide portable measurement, analysis, and tracking of holdup using the GGH formalism.[13] Automation for rapid measurements in the plant is, in fact, possible because of the simplicity and generality of the GGH approach.

VIII.4. Correcting Specific Mass for Effect of Self-Attenuation

VIII.4.1. Self-attenuation in holdup measurements.

Characteristic of bulk quantities of special nuclear materials is the self-absorption of gamma rays emitted by the material. A detailed treatment of these effects[39] includes descriptions of the experimental methods used to correct for self-attenuation when quantitative analysis relies on a gamma ray emitted by the material. The corrections are important when a quantitative gamma-ray measurement is based on the net counts in a spectral region, which is the case in the GGH approach to measurements of holdup. If self-attenuation is ignored, every measurement result will again (as with equipment-attenuation and finite-source effects) be biased low.

The two approaches used routinely in gamma-ray NDA measurements to correct for self-attenuation involve determining the i) intensities of gamma rays transmitted through the material from external (transmission) sources, and ii) relative intensities of multiple gamma rays emitted from the bulk material. Both of these techniques have been explored for holdup measurements. Neither is satisfactory in these applications.

Transmission sources are difficult to use in portable measurements that characteristically lack fixed or well controlled geometries and a good definition/knowledge of the materials (other than the nuclear material deposits) in the transmission path. Implementing the use of transmission sources for holdup measurements is also cumbersome procedurally because the implementation of a transmission source hinders the rapid performance of measurements at a large number of locations. There are also safety restrictions on carrying a gamma-ray source of sufficient intensity to perform the transmission measurements at relatively large distances and through dense equipment. Attempts to use transmission sources to obtain corrections for self-attenuation in the measurement of holdup typically lead to systematic biases of 100% or more.[22]

Measurements of the relative intensities of multiple gamma rays emitted from the bulk material require the use of Ge detectors, which are difficult to use for routine measurements of holdup because of the large size and weight of such detectors, especially when fitted with shielding against gamma-ray backgrounds. Efforts to perform such measurements to correct for self-attenuation of gamma rays by the holdup deposits have not been successful.[22] Weak signals that are typical of holdup measurements limit the statistics of the net counts in useful gamma-ray peaks. Very long count times are not practical in these circumstances.

Typical holdup deposits tend to be thin. Therefore, for a given facility, the average self-attenuation effect may be as large as a few percent, depending on the energy of the assay gamma ray. While a bias of several percent is generally not important for an individual measurement point, a several-percent bias in a facility's total holdup is a serious problem.

The magnitude of the effect of gamma-ray self-attenuation for a measured holdup deposit can be determined if the areal density of the deposit, uncorrected for self-attenuation (but corrected for room-background, equipment-attenuation and finite-source effects), is known. Because the actinide content of a holdup deposit dominates the attenuation of gamma rays, the actinide areal density is sufficient to perform the correction for a specific deposit geometry. The key to the self-attenuation correction is converting the specific mass of the actinide isotope obtained from the holdup measurement to the uncorrected areal density of the actinide. The conversion uses the experimental width parameter ***w*** in the cases of line or point deposits,

The holdup measurement of an area deposit gives the areal density of the actinide isotope directly. This can be readily converted to the areal density of the actinide element using the known isotopic fraction. This in turn is used directly to determine the effect of self-attenuation. The holdup measurement of a line deposit gives the uncorrected linear density of the actinide isotope. This can be converted to an uncorrected areal density by dividing by the experimental width parameter ***w*** of the line deposit. Subsequently, the effect of gamma-ray self-attenuation for the line deposit is determined as for the area deposit. The holdup measurement of a point deposit gives the uncorrected mass of the actinide isotope. This can be converted to an uncorrected areal density by dividing by the area ***a*** of the point deposit, which is related simply to the experimental width parameter ***w***:

$$a = \pi \bullet (w/2)^2 \quad . \tag{23}$$

Subsequently, the effect of gamma-ray self-attenuation for the point deposit is determined as for the area deposit. Defining ***w*** uses known parameters of holdup deposits. Using ***w*** to infer the measured areal density is new approach.[67, 68] Determining the self-attenuation effect directly from the measured areal density differs from all previous approaches.

VIII.4.2. Determine self-attenuation from the measured areal density.

The areal density of an actinide deposit is its mass per unit area (typically in g/cm^2). The measurement of holdup as a generalized deposit geometry gives the measured actinide areal density, $\mathbf{(\rho x)_{MEAS}}$, as described above. The true areal density, $\mathbf{(\rho x)}$, is corrected for the effect of self-attenuation on the gamma ray used to perform the measurement. The far-field correction for self-attenuation[39] is redefined as the ratio of the true to the measured areal densities of a slab deposit of the total actinide:

$$(\rho x)/(\rho x)_{MEAS} = \mu(\rho x)/[1-e^{-\mu(\rho x)}] \quad , \qquad (24)$$

where μ is the mass attenuation coefficient (in cm^2/g) of the actinide at the energy of the gamma ray used to perform the measurement. Rearranging Equation (24) gives the true result (corrected for self-attenuation) for the areal density as a function of the measured:

$$(\rho x) = - (\ln[1 - \mu(\rho x)_{MEAS}])/\mu \quad . \qquad (25)$$

Equation (25) is a nonlinear conversion of the measured actinide areal density to the quantity corrected for self-attenuation. It uses the mass attenuation coefficient of the actinide. However, most holdup deposits are not elements but compounds and probably mixtures of compounds.

The mass attenuation coefficient can be obtained for any element or for particular compounds or mixtures. Knowledge of the process and perhaps its history is required to identify the elements, compounds and mixtures representing the holdup deposit. Strictly speaking, corrections for self-attenuation by actinide oxide deposits must be performed using mass attenuation coefficients for the actinide oxide. However, if μ for an actinide oxide is used to perform the correction, then the actinide areal density $\mathbf{(\rho x)_{MEAS}}$ must be converted to the oxide areal density. This complicates notation for the measured results unnecessarily for two reasons: i) A simple ratio of formula weights is conversion factor between areal density of the actinide and that of a specified compound or mixture containing the actinide. ii) The areal density is always multiplied by the corresponding mass attenuation coefficient, so it is straightforward to re-define mass attenuation coefficient μ as a "normalizing" mass attenuation coefficient $\boldsymbol{\mu}$ to preserve areal density as a property of the elemental actinide.

Column 4 of Table VIII.1 gives the mass attenuation coefficients μ for elemental uranium and plutonium and for several common compounds encountered in the processing of these actinides. The two sets of results for uranium give the mass attenuation coefficients for 186-keV gamma rays (used to measure ^{235}U) and 1001-keV gamma rays (used, for low-enriched uranium primarily, to measure ^{238}U). The mass attenuation coefficients for plutonium materials correspond to 414-keV gamma rays, those used to measure ^{239}Pu. Column 2 of Table VIII.1 is the assay of the actinide element (mass element per unit mass of material), which is a ratio of formula weights and is identically 1 for the elemental material. The normalizing mass attenuation coefficient (μ_{NORM} or $\boldsymbol{\mu}$) is the ratio of the mass attenuation coefficient to the assay. The exclusive use of $\boldsymbol{\mu}$ instead of μ eliminates the need to redefine areal density regardless of the assumption about the deposit material. Equations (24) and (25) are rewritten accordingly:

$$(\rho x)/(\rho x)_{MEAS} = \boldsymbol{\mu}(\rho x)/[1-e^{-\boldsymbol{\mu}(\rho x)}] \quad , \qquad (24a)$$

and

$$(\rho x) = - (\ln[1 - \boldsymbol{\mu}(\rho x)_{MEAS}])/\boldsymbol{\mu} \quad . \qquad (25a)$$

The normalizing mass attenuation coefficient $\boldsymbol{\mu}$ as defined in Table VIII.1 appears below in the algorithms for the self-attenuation correction.

Table VIII.1
Gamma-Ray Mass Attenuation Coefficients

Deposit Material	Assay* ($g_{ELEMENT}/g$)	E_γ (keV)	μ (cm^2/g)	$\mu = \mu_{NORM}$ = μ / Assay* (cm^2/g)	$\mu / \mu_{ELEMENT}$
U	1.00	186	1.47	1.47	1.00
UO_2	0.88	186	1.31	1.49	1.01
U_3O_8	0.85	186	1.26	1.49	1.02
$UO_2(NO_3)_2{\bullet}6H_2O$	0.47	186	0.76	1.62	1.11
Pu	1.00	414	0.27	0.27	1.00
PuO_2	0.88	414	0.25	0.28	1.05
PuO3	0.83	414	0.24	0.29	1.07
U	1.00	1001	0.075	0.075	1.00
UO_2	0.88	1001	0.074	0.084	1.11
U_3O_8	0.85	1001	0.073	0.087	1.15
$UO_2(NO_3)_2{\bullet}6H_2O$	0.47	1001	0.071	0.149	1.98

* Assay is determined assuming the following:

- 93% ^{235}U at 186 keV
- 94% ^{239}Pu at 414 keV
- 97% ^{238}U at 1001 keV

Column 6 of Table VIII.1, the ratio of each μ to the μ for the element, shows that the sensitivity to different deposit formulas is much weaker at 186 keV than that determined by the ratio of their μ values (Column 4). Although the μ values for U and $UO_2(NO_3)_2{\bullet}6H_2O$ differ by a factor of two, the relevant normalizing mass attenuation coefficients (Table VIII.1) differ by only 10%. The reason is the compensating effect of the decreasing assay as μ increases. It is tempting to assume that lower energy gamma rays should have the greatest sensitivity to the deposit formula because the corresponding mass attenuation coefficients μ are so much larger, but Column 6 of Table VIII.1 indicates otherwise. That is, the μ value for UO_2 when used for analysis of all data despite the possible presence of U_3O_8 at some locations in the process equipment could be in error by ~1% for measurements of HEU deposits (possibly) at 186 keV and by ~4% for measurements of LEU deposits (probably) at 1001 keV. The higher sensitivity at higher gamma-ray energy comes from the continuously decreasing energy dependence of the mass attenuation coefficient for actinides while that for oxygen and other low-Z materials is relatively unchanging above 200 keV and is comparable to that of actinides at 1001 keV. Figure VIII.10 illustrates this trend. Nonetheless, an incorrect assumption about the deposit composition will have a relatively small impact on the quantitative result, even for most measurements at 1001 keV, as discussed in Section IX.8.

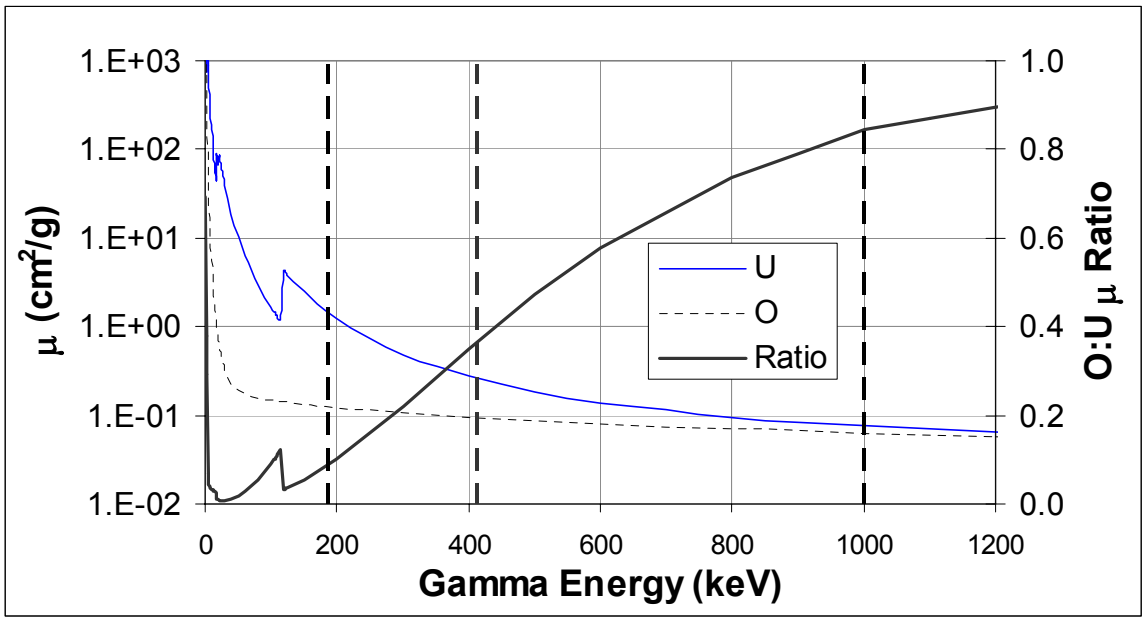

Figure VIII.10. The mass attenuation coefficients for uranium and oxygen are plotted vs. gamma-ray energy up to 1200 keV. The ratio of the mass attenuation coefficient of oxygen to that of uranium increases by an order of magnitude between 186 and 1001 keV so that the values are nearly comparable at 1001 keV.

Figure VIII.11 plots the relationship between **(ρx)** and $\mathbf{(\rho x)_{MEAS}}$ defined by Equation (25a) representing three forms of plutonium (Pu metal, PuO_2 and PuO_3) for the 414-keV gamma ray of ^{239}Pu. The μ values at 414-keV for these three materials come from Table VIII.1. The straight line in each graph has a slope of 1. Therefore, the ratio of the **(ρx)** values on the curved line to those on the straight line is the correction factor for self-attenuation. The correction factors are hardly distinguishable among the different materials for **(ρx)** less than 5 g/cm^2 (most holdup deposits are well below this limit). Equation (25) shows that the product $\mu\mathbf{(\rho x)_{MEAS}}$ must be less than 1. The apparent singularity in each plot in Figure VIII.11 is the approach of the product $\mu\mathbf{(\rho x)_{MEAS}}$ to 1, corresponding to a deposit that exceeds a maximum correctable thickness. Deposits near this thickness for a given gamma-ray energy cannot be measured by these strictly passive methods. Furthermore, as the product $\mu\mathbf{(\rho x)_{MEAS}}$ approaches 1 the uncertainty in the corrected value is increasingly magnified compared to the measured uncertainty, as follows:

$$\sigma(\rho x) = \sigma(\rho x)_{MEAS} / [1 - \mu(\rho x)_{MEAS}] \quad , \qquad (26)$$

making the corrected results of such measurements unrealistic. Plutonium deposits that approach the maximum correctable (or "maximum") thickness within the measurement uncertainty, which gets larger for thicker deposits, as indicated in Equation (26), cannot be quantified using the 414-keV gamma ray. The large random uncertainty in each measurement of holdup limits the thickness of deposits that can be corrected by this approach.

An iterative approach to solving Equation 24 or 24a is possible. The number of iterations to achieve convergence varies with $\mathbf{(\rho x)_{MEAS}}$ and can be large, judging maximum deposit thickness can be difficult, and evaluating the uncertainty is more complex than solving Equation 26. Defining maximum thickness for a given objective on data quality (Section IX.6) is also difficult.

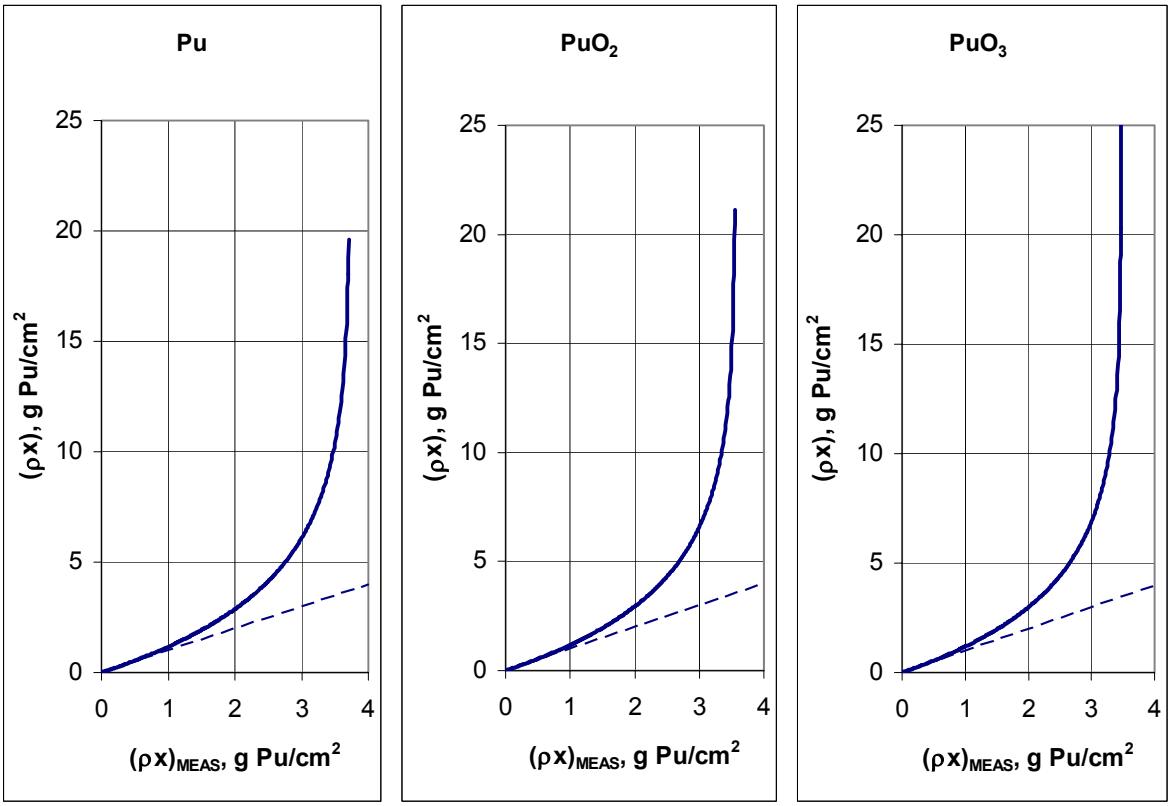

Figure VIII.11. True vs. measured thickness (areal density of plutonium, g/cm^2) is plotted for 414-keV gamma rays from plutonium metal, PuO_2 and PuO_3 as determined by Equation 25a. The measured thickness corresponds to that determined experimentally from the specific holdup mass corrected for the effects of room background, equipment attenuation, and the finite source dimension. The straight line has a slope of 1. Therefore, the correction factor for self-attenuation is the ratio of the curved line to the straight line.

Figures VIII.12-13 graphically indicate corresponding corresponding maxima in the correctable areal density of uranium measured at 186 and 1001 keV, respectively. A discussion analogous to that above for 414-keV gamma rays applies for 186-keV gammas as well and to all but $UO_2(NO_3)_2{\cdot}6H_2O$ at 1001 keV. The large random uncertainty in each measurement of holdup limits the thickness of deposits, particularly those measured at low-energies like 186 keV, that can be corrected by this approach. Unlike approaches that measure transmission through oxides of uranium at high gamma-ray energies and extrapolate to 186-keV,[39] using the direct measurement of areal density to obtain the correction for self-attenuation is limited to relatively thin deposits for holdup measurements at 186 keV. Section IX.6 describes a method for defining a practical maximum thickness for thick holdup deposits of uranium, plutonium and other materials based on the uncertainty in the measured areal density.

The uncertainty in the measured result, $\boldsymbol{\sigma(\rho x)_{MEAS}}$, can be large for plant-wide measurements of holdup because the count times must be minimized, as discussed in Section X.4. Conservative approaches can identify those deposits whose product $\boldsymbol{\mu(\rho x)_{MEAS}}$ approaches 1, such that the deposit is statistically equivalent to a maximum thickness. A screening algorithm such as

$$\mu(\rho x)_{MEAS} + K{\bullet}\mu{\bullet}\sigma(\rho x)_{MEAS} \geq 1 \quad , \qquad (27)$$

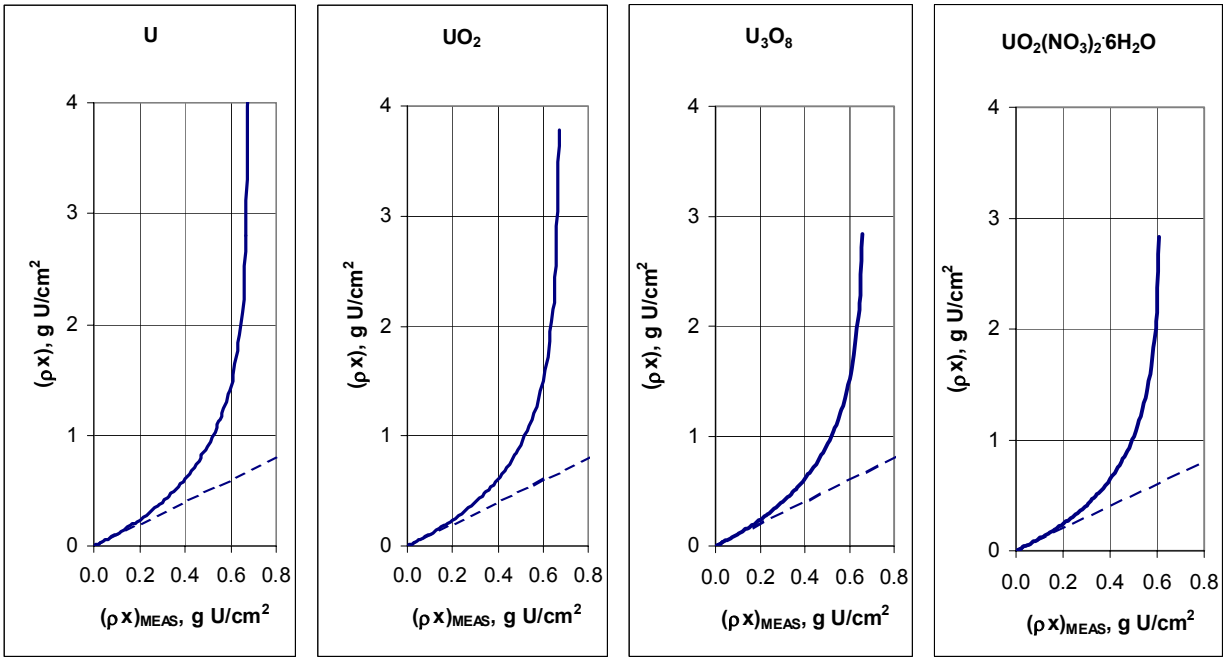

Figure VIII.12. True vs. measured thickness (areal density of uranium, g/cm^2) is plotted for 186-keV gamma rays from uranium metal, UO_2,U_3O_8, and $UO_2(NO_3)_2{\cdot}6H_2O$ as determined by Equation 25a. The measured thickness corresponds to that determined experimentally from the specific holdup mass corrected for the effects of room background, equipment attenuation, and the finite source dimension. The straight line has a slope of 1. Therefore, the correction factor for self-attenuation is the ratio of the curved line to the straight line.

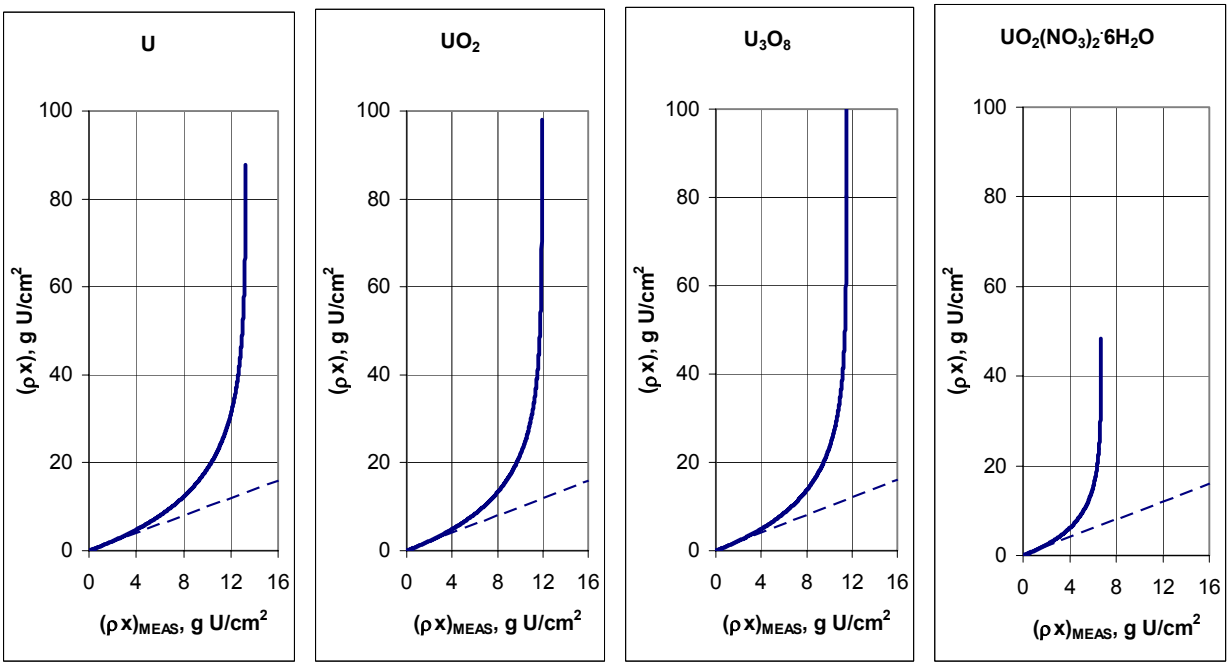

Figure VIII.13. True vs. measured thickness (areal density of uranium, g/cm^2) is plotted for 1001-keV gamma rays from uranium metal, UO_2,U_3O_8, and $UO_2(NO_3)_2{\cdot}6H_2O$ as determined by Equation 25a. The measured thickness is that determined experimentally from the specific holdup mass corrected for the effects of room background, equipment attenuation, and the finite source dimension. The straight line has a slope of 1. Therefore, the correction factor for self-attenuation is the ratio of the curved line to the straight line.

gives a criterion (where **K** may be set to 3, as suggested by the treatment in Section IX.6) for rejecting a measurement. Equation (26) indicates that measurements failing the initial thick-deposit screening may pass if measured again with improved statistics. (Refer to Section IX.6.) Alternative approaches (use of higher-energy gamma rays, transmission measurements, or neutron measurements as appropriate) may be pursued if improved statistics fail to satisfy the screening criterion of Equation (27). Even if equipment dimensions are critically safe, the chance that deposits fill the interior cavity of the equipment may raise concerns for processing. Cleanout of deposits too thick for self-attenuation corrections to be reliable (when effective alternative measurements are not available) may be considered for enhanced safety and productivity.

VIII.4.3. Correct measured specific mass for self-attenuation

Correcting for gamma-ray self-attenuation in a holdup deposit also begins with a decision on the width $\boldsymbol{w}$ of the deposit, except that this decision has already been made in the previous correction procedure for finite-source effects. An over- or underestimate of $\boldsymbol{w}$ leads, respectively, to under- or overcorrection for the effect of self-attenuation. This is opposite to the result of over- or underestimating $\boldsymbol{w}$ in the case of the finite-source correction. It is for this reason that, in a limited range of deposit thickness, the effects of errors in the estimates of $\boldsymbol{w}$ tend to compensate for each other when both corrections are performed. Section VIII.6 illustrates the compensating tendency.

The correction for finite source dimensions, like the self-attenuation correction, addresses an additional persistent negative bias that propagates to the total holdup. The correction factor for self-attenuation is always greater than 1. As discussed in the previous correction procedure for finite-source effects, the correction process leads to a total holdup result that will tend to be unbiased, because the result is sometimes high or low for an individual measurement.

Unlike the previous corrections for equipment attenuation, Equations (11)-(13), and finite-source effects, Equations (14)-(16), the correction formula for self attenuation, Equation (24a), is a nonlinear function of the specific mass (converted to areal density) of the deposit. Therefore, it *must* be applied after all the other corrections have been made. Furthermore, for the same reason of nonlinearity and because the self-attenuation effect is determined by the areal density of the total actinide deposit, the isotope fraction must be used to convert the measured areal density of the isotope to that of the element if only one actinide is present. If more than one actinide is present in significant amounts, both the element and isotope fractions are multiplied for use in this conversion step.

The relative uncertainty in the specific mass corrected for equipment attenuation and finite dimensions of a point, line or area deposit remain unchanged from the respective uncorrected values, Equations (3), (6) or (9), because these corrections are linear. The areal density (and, therefore, specific mass) corrected for self-attenuation using Equation (25a) varies nonlinearly with the deposit thickness. Therefore, Equation (26) must be used to derive the propagated relative uncertainty in the specific mass of a (point, line or area) deposit corrected for self-attenuation.

The correction for self-attenuation of gamma rays by a holdup deposit can be performed in six steps. The emphasis is on generality. The procedure is the same for and applicable to all measurements, which is unlike previous efforts to address the effects of self-attenuation in

holdup measurements.[22] Emphasis on formality and simplicity also enable generic documentation and automated implementation of the analysis procedures.

The six steps to self-attenuation corrections are:

1) Convert the specific isotope mass of a point, line or area source obtained in Equations (14)-(16), respectively, to the specific actinide (***AC***) mass as follows:

$$m_{P,FIN\,AC}\ (\mathrm{g}) = m_{P,FIN} / \varepsilon \quad , \tag{28}$$

$$m_{L,FIN\,AC}\ (\mathrm{g/cm}) = m_{L,FIN} / \varepsilon \quad , \tag{29}$$

and

$$m_{A,FIN\,AC}\ (\mathrm{g/cm^2}) = m_{A,FIN} / \varepsilon \quad . \tag{30}$$

The parameter, **ε**, is a product:

$$\varepsilon = f_I \bullet f_E \quad , \tag{31}$$

where $\mathbf{f_I}$ is the fraction of the actinide isotope relative to the element total and $\mathbf{f_E}$ is the fraction of the element relative to the actinide total. (The value of $\mathbf{f_E}$ for a single-element actinide deposit is 1.)

2) Convert the specific actinide mass to the measured actinide areal density $\mathbf{(\rho x)_{MEAS}}$ as follows

i) for a point deposit:

$$(\rho x)_{MEAS,P}\ (\mathrm{g/cm^2}) = m_{P,FIN\,AC} / a \quad , \tag{32}$$

ii) for a line deposit:

$$(\rho x)_{MEAS,L}\ (\mathrm{g/cm^2}) = m_{L,FIN\,AC} / w \quad , \tag{33}$$

and iii) for an area deposit:

$$(\rho x)_{MEAS,A}\ (\mathrm{g/cm^2}) = m_{A,FIN\,AC} \quad , \tag{34}$$

where ***w*** (in cm) is the finite width of the line (or point) deposit and ***a*** (in $\mathrm{cm^2}$) is the area of the point deposit, as defined by Equation (23).

3) Use this measured actinide areal density of a point, line, or area deposit to test if it is in a range that is valid for self-attenuation corrections. Equation (25a) limits measurable values of the true areal density **(ρx)** by the requirement that $\mathbf{\mu(\rho x)_{MEAS}}$ may not approach 1. The respective relative uncertainties in the values of $\mathbf{(\rho x)_{MEAS,P}}$, $\mathbf{(\rho x)_{MEAS,L}}$, and $\mathbf{(\rho x)_{MEAS,A}}$ are $\mathbf{\sigma_R(m_P)}$, $\mathbf{\sigma_R(m_L)}$, and $\mathbf{\sigma_R(m_A)}$, determined from Equations (3), (6) and (9). These apply up to, but not through, the process of correcting for self-attenuation because all prior conversions and corrections have been

linear. Using these uncertainties and Equation (27) implemented with a value of 3 for **K** (refer to Section IX.6 for justification of this choice), the screening of thick deposits can be accomplished with simple algorithmic tests. If a screening test fails, consider a repeat of the screening test after re-measurement of the deposit with improved statistics, or the other alternatives discussed in Section VIII.4.2. The three proposed screening tests for thick point, line, or area deposits, respectively, are

$$\mu(\rho x)_{MEAS,P} + 3 \bullet \mu \bullet [\sigma_R(m_P)] \bullet (\rho x)_{MEAS,P} < 1 \quad , \qquad (35)$$

$$\mu(\rho x)_{MEAS,L} + 3 \bullet \mu \bullet [\sigma_R(m_L)] \bullet (\rho x)_{MEAS,L} < 1 \quad , \qquad (36)$$

or

$$\mu(\rho x)_{MEAS,A} + 3 \bullet \mu \bullet [\sigma_R(m_A)] \bullet (\rho x)_{MEAS,A} < 1 \qquad (37)$$

for a point, line or area deposit, respectively, precede the self-attenuation corrections. A more conservative approach (**K** > 3) than these tests may be required if the random measurement uncertainty is very large (see Section IX.6). Holdup deposits normally do not approach the maximum correctable thickness, so failures of these tests will be infrequent unless equipment cleanouts are not performed regularly.

4) Use the relationship of Equation (25a) and the measured actinide areal density of a point, line or area deposit to obtain the respective areal density of a point, line, or area deposit corrected nonlinearly for self-attenuation:

$$(\rho x)_P = -(1/\mu) \bullet \ln[1 - \mu(\rho x)_{MEAS,P}] \quad , \qquad (38)$$

$$(\rho x)_L = -(1/\mu) \bullet \ln[1 - \mu(\rho x)_{MEAS,L}] \quad , \qquad (39)$$

and

$$(\rho x)_A = -(1/\mu) \bullet \ln[1 - \mu(\rho x)_{MEAS,A}] \quad . \qquad (40)$$

Note that the correction for self-attenuation is independent of deposit type because the specific mass, whose measured magnitude is geometry-dependent, has been converted to areal density for all deposit geometries. The absolute uncertainties in the corrected areal densities $\mathbf{(\rho x)_P}$, $\mathbf{(\rho x)_L}$ and $\mathbf{(\rho x)_A}$ are propagated nonlinearly using Equation (26) as follows:

$$\sigma(\rho x)_P = [\sigma_R(m_P) \bullet (\rho x)_{MEAS,P}] / [1 - \mu(\rho x)_{MEAS,P}] \quad , \qquad (41)$$

$$\sigma(\rho x)_L = [\sigma_R(m_L) \bullet (\rho x)_{MEAS,L}] / [1 - \mu(\rho x)_{MEAS,L}] \qquad (42)$$

and

$$\sigma(\rho x)_A = [\sigma_R(m_A) \bullet (\rho x)_{MEAS,A}] / [1 - \mu(\rho x)_{MEAS,A}] \quad . \qquad (43)$$

The respective relative uncertainties in the values of $\mathbf{(\rho x)_{MEAS,P}}$, $\mathbf{(\rho x)_{MEAS,L}}$, and $\mathbf{(\rho x)_{MEAS,A}}$ are $\boldsymbol{\sigma_R(m_P)}$, $\boldsymbol{\sigma_R(m_L)}$, and $\boldsymbol{\sigma_R(m_A)}$, determined from Equations (3), (6) and (9). Typically, a test of relative uncertainty in the corrected areal density is justified at this point because the denominator in Equations (41)-(43) magnifies it compared to the relative uncertainty in the uncorrected areal density. An upper limit, **T**, that is less than 1 (0.25, for example) may be chosen for the test, such that, if

$$\sigma_R(\rho x)_P = \sigma(\rho x)_P / (\rho x)_P > T \quad , \tag{44}$$

or

$$\sigma_R(\rho x)_L = \sigma(\rho x)_L / (\rho x)_L > T \quad , \tag{45}$$

or

$$\sigma_R(\rho x)_A = \sigma(\rho x)_A / (\rho x)_A > T \quad , \tag{46}$$

re-measurement of the deposit with improved statistics followed by a repeat of this test, Equations (44)-(46), would be recommended. Choosing **T** is not arbitrary. It relates to establishing formal criteria for thick deposits, as discussed in Section IX.6.

5) Convert the corrected areal density to the respective specific mass for the point, line, or area actinide deposit, corrected for self-attenuation effects, as follows:

$$m_{P,SELF\ AC}\ (\mathrm{g}) = a \bullet (\rho x)_P \quad , \tag{47}$$

$$m_{L,SELF\ AC}\ (\mathrm{g/cm}) = w \bullet (\rho x)_L \quad , \tag{48}$$

and

$$m_{A,SELF\ AC}\ (\mathrm{g/cm^2}) = (\rho x)_A \quad . \tag{49}$$

6) Convert the self-attenuation corrected specific actinide mass of the point, line, or area deposit to the respective corrected specific isotope mass:

$$m_{P,SELF}\ (\mathrm{g}) = \varepsilon \bullet m_{P,SELF\ AC} \quad , \tag{50}$$

$$m_{L,SELF}\ (\mathrm{g/cm}) = \varepsilon \bullet m_{L,SELF\ AC} \quad , \tag{51}$$

and

$$m_{A,SELF}\ (\mathrm{g/cm^2}) = \varepsilon \bullet m_{A,SELF\ AC} \quad , \tag{52}$$

The relative uncertainties of these three self-attenuation-corrected results for specific isotope mass are given by Equations (44)-(46), respectively.

Although there is little that a measurement practitioner can do to minimize the effects of self-attenuation, administrative controls may both prescribe a cleanout of the process equipment for safety or optimization of operation and stipulate the mitigation of self-attenuation during the cleanout. Such controls may rely on the measured holdup results. The self-attenuation effects are much larger for measurements of ^{235}U holdup based on the 186-keV gamma ray than for measurements of ^{239}Pu holdup based on the 414-keV gamma ray for the same elemental deposit thickness. This is because the mass attenuation coefficient is over five times larger for the lower energy gamma ray, as indicated in Table VIII.1. The decision between using the 186- or 1001-keV gamma ray for measurements of LEU deposits is simplified by mass attenuation coefficients that are smaller by factors of ten to twenty for the higher energy gamma ray (refer to Table VIII.1) and the likelihood of much larger deposits accumulated in the process equipment of LEU facilities.

Measurements of plutonium holdup[68] in high-throughput bulk-processing equipment inside of glove boxes used the 414-keV gamma-ray and the GGH formalism. The magnitude of the correction for self-attenuation determined by the ratio $(\rho x) / (\rho x)_{MEAS}$, Equation (24a), was as large as 1.11 for powder deposits on the glove box floor.

The six-step procedure for self-attenuation corrections described and illustrated above can be readily implemented with a spreadsheet. The procedure is also part of the *HMS4* analysis software, which automates the plant-wide portable measurement, analysis, and tracking of holdup using the GGH formalism.[13] Automation for rapid measurements in the plant is, in fact, possible because of the simplicity and generality of the GGH approach.

VIII.5. Computing Total Isotope Mass in the Extended Equipment

The total isotope mass contained in the extended equipment is a product of the corrected specific isotope mass that represents the extended equipment and the physical dimension (1 for a point deposit, the equipment length $\mathbf{L_{TOT}}$ for a line deposit, or the equipment area $\mathbf{A_{TOT}}$ for an area deposit) of the equipment. Frequently, an average of the multiple measurements of corrected specific isotope mass performed at different locations on the equipment represents the equipment. The average specific mass for point, line or area deposits is $\boldsymbol{m_{P,SELF,AVG}}$ (g), $\boldsymbol{m_{L,SELF,AVG}}$ (g/cm) or $\boldsymbol{m_{A,SELF,AVG}}$ (g/cm^2), respectively, as follows:

$$m_{P,SELF,AVG} = (w_1 \cdot m_{P,SELF,1} + w_2 \cdot m_{P,SELF,1} + \ldots w_N \cdot m_{P,SELF,N})/(\Sigma w_i) \quad , \quad (53)$$

$$m_{L,SELF,AVG} = (w_1 \cdot m_{L,SELF,1} + w_2 \cdot m_{L,SELF,1} + \ldots w_N \cdot m_{L,SELF,N})/(\Sigma w_i) \quad , \quad (54)$$

and

$$m_{A,SELF,AVG} = (w_1 \cdot m_{A,SELF,1} + w_2 \cdot m_{A,SELF,1} + \ldots w_N \cdot m_{A,SELF,N})/(\Sigma w_i) \quad , \quad (55)$$

where

$$(\Sigma w_i) = w_1 + w_2 + \ldots w_N \quad . \quad (56)$$

The corresponding result for the total isotope mass in the extended equipment is:

$$m\ (\mathrm{g}) = m_{P,SELF,AVG} \quad , \tag{57}$$

$$m\ (\mathrm{g}) = (\mathrm{L_{TOT}}) \bullet m_{L,SELF,AVG} \quad , \tag{58}$$

or

$$m\ (\mathrm{g}) = (\mathrm{A_{TOT}}) \bullet m_{A,SELF,AVG} \quad , \tag{59}$$

for measurements of point, line or area deposits, respectively. Dividing Equations (57)-(59) by the isotope fraction $\mathbf{f_I}$ gives the total mass of the element.

The relative uncertainty in $\boldsymbol{m}$ is the relative uncertainty in the corresponding average:

$$\sigma_R(m) = \sigma_R(m_{P,SELF,AVG}) \quad , \tag{60}$$

$$\sigma_R(m) = \sigma_R(m_{L,SELF,AVG}) \quad , \tag{61}$$

or

$$\sigma_R(m) = \sigma_R(m_{A,SELF,AVG}) \quad , \tag{62}$$

where

$$\sigma_R(m_{P,SELF,AVG}) = (w_1 \cdot \sigma^2(m_{P,SELF,1}) + w_2 \cdot \sigma^2(m_{P,SELF,1}) + \ldots\ w_N \cdot \sigma^2(m_{P,SELF,N}))^{1/2}/(m_{P,SELF,AVG} \cdot \Sigma w_i), \tag{63}$$

$$\sigma_R(m_{L,SELF,AVG}) = (w_1 \cdot \sigma^2(m_{L,SELF,1}) + w_2 \cdot \sigma^2(m_{L,SELF,1}) + \ldots\ w_N \cdot \sigma^2(m_{L,SELF,N}))^{1/2}/(m_{L,SELF,AVG} \cdot \Sigma w_i), \tag{64}$$

and

$$\sigma_R(m_{A,SELF,AVG}) = (w_1 \cdot \sigma^2(m_{A,SELF,1}) + w_2 \cdot \sigma^2(m_{A,SELF,1}) + \ldots\ w_N \cdot \sigma^2(m_{A,SELF,N}))^{1/2}/(m_{A,SELF,AVG} \cdot \Sigma w_i). \tag{65}$$

The absolute uncertainty in each specific mass term in Equations (63)-(65) comes from the relative uncertainty in the corresponding areal density as defined in Equations (44)-(46):

$$\sigma(m_{P,SELF,i}) = \sigma_R(\rho x)_{P,i} \cdot m_{P,SELF,i}\ (\mathrm{g}) \quad , \tag{66}$$

$$\sigma(m_{L,SELF,i}) = \sigma_R(\rho x)_{L,i} \cdot m_{L,SELF,i}\ (\mathrm{g/cm}) \quad , \tag{66}$$

and

$$\sigma(m_{A,SELF,i}) = \sigma_R(\rho x)_{A,i} \cdot m_{A,SELF,i}\ (\mathrm{g/cm^2}) \quad . \tag{66}$$

The contribution of counting statistics to the measurement uncertainty diminishes in the averaging process as indicated in Equations (63)-65). Nonetheless, statistics dominate the uncertainty when deposits are thick because the uncertainty is magnified in its nonlinear propagation through the mass attenuation correction, Equations (41)-(43), as discussed above and in Section IX.6.

The use of very short count times at many locations on a given piece of equipment enables the result obtained in Equation (57), (58) or (59) to be more representative of the deposits throughout the equipment, despite the typically nonuniform deposit thickness. Systematic approaches to choosing the shortest practical count time t_P are described in Section X.4. There is no loss of precision, statistically, in the optimized approach in which many short counts replace fewer long counts. However, the choice of short counts would not be practical, as described in Section IX.6, without automation of the measurement process.

Weighting the averaged terms (assigning coefficients $\mathbf{w_i} \neq 1$) requires detailed knowledge of the experimental methodology. Weighting is appropriate when measurement spacing is not constant such that the absolute dimension of the process equipment represented by each measurement is unique and significantly different from that of other measurements. However, the recommended approach for plant-wide measurements of holdup is constant spacing $\boldsymbol{l}$ (see Section X.4) to achieve random sampling of deposits of variable magnitude. The recommended shortest practical count time for plant-wide measurements, t_P, is a constant count time (see Section X.4). Weighting is not appropriate in this circumstance, for three reasons. i) Weighting overturns the randomness of the nonweighted ($\mathbf{w_i} = 1$) average. ii) Weighting according to measurement uncertainty when holdup deposits are thin biases the measurement results high because statistics are worst for the smallest deposits. iii) Weighting according to measurement uncertainty when holdup deposits are thick biases the measurement results high because statistics are worst for the thickest deposits as a consequence of the nonlinear self-attenuation correction.

The recommended guidance for measurements of holdup plant-wide includes constant spacing $\boldsymbol{l}$ and the shortest practical count time t_P, both determined as described in Section IX.6. Only a nonweighted average, such that $\mathbf{w_i} = 1$ in Equations (53)-(56) and (63)-(65), is suitable for this recommended methodology.

VIII.6. Sensitivity of Specific Mass and Total Mass to Uncertainty in *w*

VIII.6.1. Introduction.

The choice of a width parameter $\boldsymbol{w}$ is the first step in the process of correcting for the negative bias caused by the finite dimensions of a holdup deposit and self-attenuation of its gamma rays. These corrections are key to eliminating the negative bias in gamma-ray holdup measurements. Uncertain knowledge of $\boldsymbol{w}$ should not deter the use of these corrections. If the corrections are performed with the best information available on $\boldsymbol{w}$, bias is eliminated on average because the result for holdup is sometimes low and sometimes high rather than always low.

Error in the experimental width parameter $\boldsymbol{w}$ chosen by the user will introduce a systematic effect in the correction for finite source dimension and, subsequently, in that for self-attenuation. However, $\boldsymbol{w}$ is the same parameter used to perform both corrections, and the sign of the systematic effect on the measurement caused by an error in $\boldsymbol{w}$ is opposite for the two corrections. Self-attenuation dominates the corrections for very thick deposits, and the systematic effect of the uncertainty in $\boldsymbol{w}$ is effectively determined by this correction for thick deposits. The systematic effect of the uncertainty in $\boldsymbol{w}$ is influenced by both the finite source and self-attenuation corrections for thinner deposits more typical of holdup, which tends to reduce the overall error incurred in the measured holdup mass from errors in $\boldsymbol{w}$.

This section examines the magnitude of the correction for finite-source and self-attenuation effects (individually and combined) as a function of deposit thickness for the collimator (diameter and depth of 2.54 cm), measurement geometry (measurement distance ***r*** of 40 cm), and geometric response described by Figures VIII.1 and VIII.3. It demonstrates the magnitude and systematics of the inherent negative bias incurred when the corrections are ignored. It also illustrates self-consistent limitation in the total error in the measured holdup despite uncertain knowledge of the common parameter ***w*** used to describe the width of holdup deposits for both types of corrections.

The true value ***w*** for the examples calculated below is 10 cm, a common duct dimension and significant fraction of the dimension of the field of view at the 40-cm measurement distance ***r***. If the concentric circles in Figures VIII.7 and VIII.8 are spaced by 5 cm, then these two sketches correspond dimensionally to the experimental setup used to obtain Figure VIII.3, and their shaded areas conform to the proposed dimension of 10 cm for ***w***. Figures VIII.7 and VIII.8 and represent finite (10-cm wide, in this example) hypothetical line and point sources, respectively.

The corrections calculated as examples below are for measurements of 186-keV gamma rays of ^{235}U from deposits of U_3O_8. The calculations assume that $\mathbf{f_I}$ = 93%. The units on the horizontal axes of all plots are those of specific mass of ^{235}U for point (g), line (g/cm) and area (g/cm^2) deposits. The shapes of the corresponding curves for other gamma-ray energies and deposit materials are similar to those shown below for 186-keV gamma rays from ^{235}U in U_3O_8, but the useful range of the corrections differs because the mass attenuation coefficients are different.

The compensating effects of the two corrections for finite source dimensions and self-attenuation when ***w*** is in error are apparent up to actinide areal densities of about 0.3 g /cm^2 for measurements at 186 keV, as Figures VIII.14-VIII.17 will demonstrate. This compensating range increases by a factor of approximately five and ten-to-twenty, respectively, for measurements at 414 and 1001 keV because of correspondingly smaller μ values (see Table VIII.1). These compensating ranges are also consistent with the practical limits for application of self-attenuation corrections to thick deposits. These limitations are discussed in Section IX.6.

VIII.6.2. Point deposits.

Figure VIII.14.a) shows the corrected *vs*. measured specific mass of ^{235}U in the finite point deposit of U_3O_8 measured at 186 keV. The deposit width parameter ***w*** of 10 cm corresponds to an area parameter ***a*** of 79 cm^2, as indicated in Equation 23, for the point deposit. The dashed line is drawn through the origin with a slope of 1 (effectively plotting an uncorrected result) for visualizing the magnitude of the corrections. The middle (solid) curve, determined from Equations (14) and (22), is the specific mass of the finite point deposit corrected for the finite source dimension ***w*** only. The top (heavy solid) curve includes the additional correction for self-attenuation, Equations (38), (47) and (50). The self-attenuation correction dominates for the thickest deposits. Figure VIII.14.b) plots the percent difference between the corrected and measured specific mass *vs*. the measured value of the point deposit. The relative finite-source correction (bottom line) is constant and the relative self-attenuation correction (top line) increases nonlinearly with deposit thickness. Below ~10 g ^{235}U for the measured specific mass (actual deposit thickness of ~0.15 g U/cm^2), the finite-source effect exceeds the self-attenuation effect. The measured result is biased low for any thickness before applying the corrections.

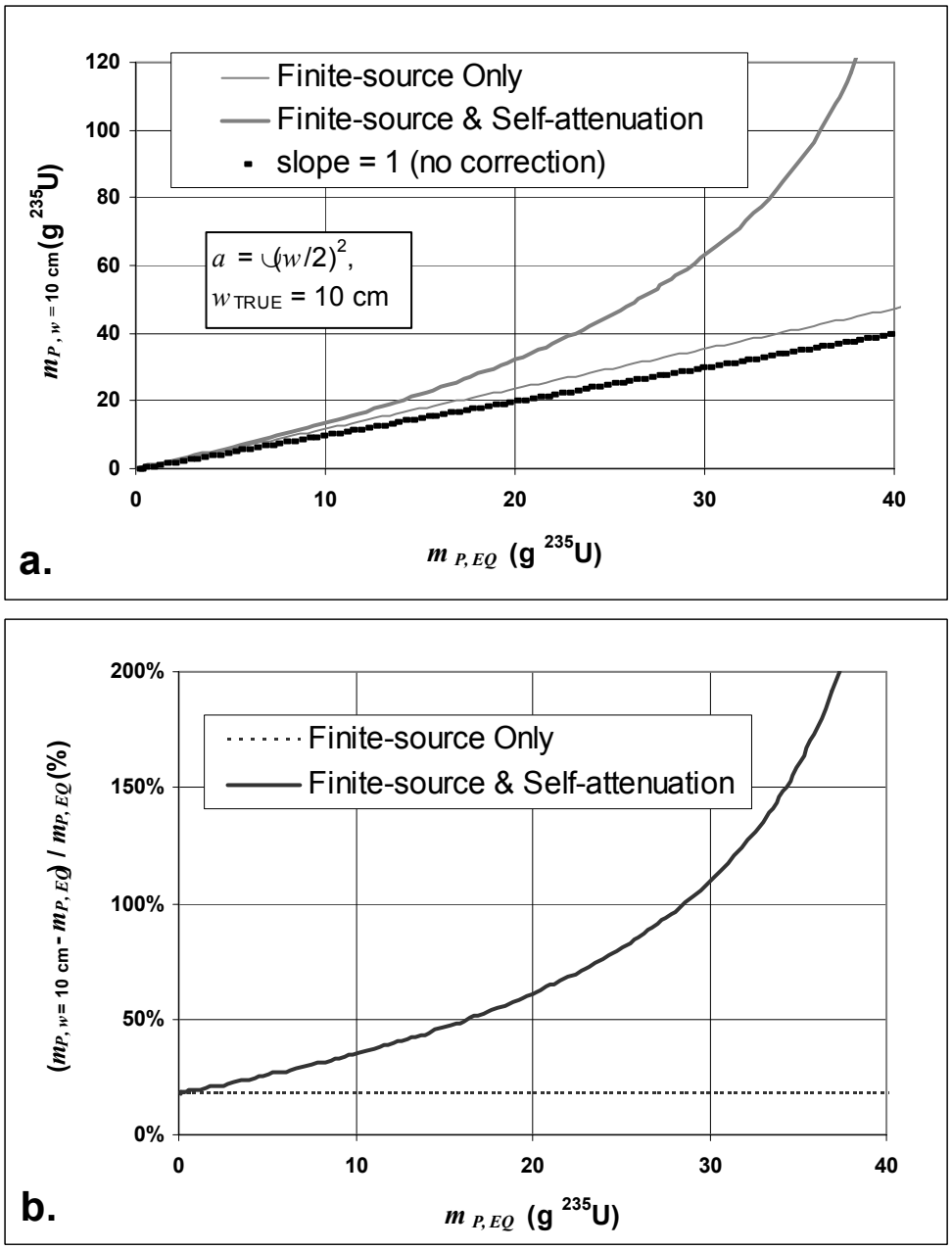

Figure VIII.14. Calculated results for point deposit of ^{235}U in U_3O_8 measured at 186 keV and r = 40 cm using a 2.5-cm by 2.5-cm cylindrical collimator: a) Corrected specific mass vs. measured, Equation (11), is plotted for the finite point source. The true deposit width w of 10 cm corresponds to an area a of 79 cm^2 for the point source. The dashed line drawn for reference passes through the origin with a slope of 1. The middle (solid) line is the specific mass of the finite point source corrected by Equations (14) and (22) for the finite-source effect only. The top (heavy solid) line is the specific mass also corrected for self-attenuation: Equations (38), (47), and (50). b) Percent difference between corrected and measured specific mass vs. measured value is plotted for the point deposit. The relative finite-source correction (dashed line) is constant, and the relative total correction including self-attenuation (top solid line) increases nonlinearly with areal density. Note: Point areal density is m_P/a.

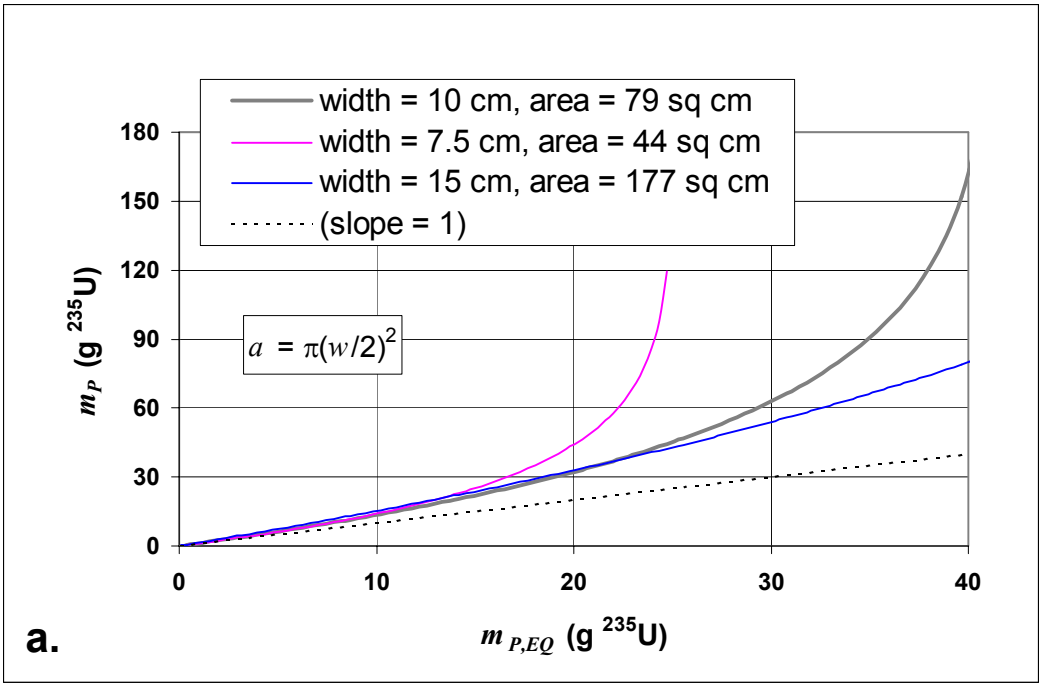

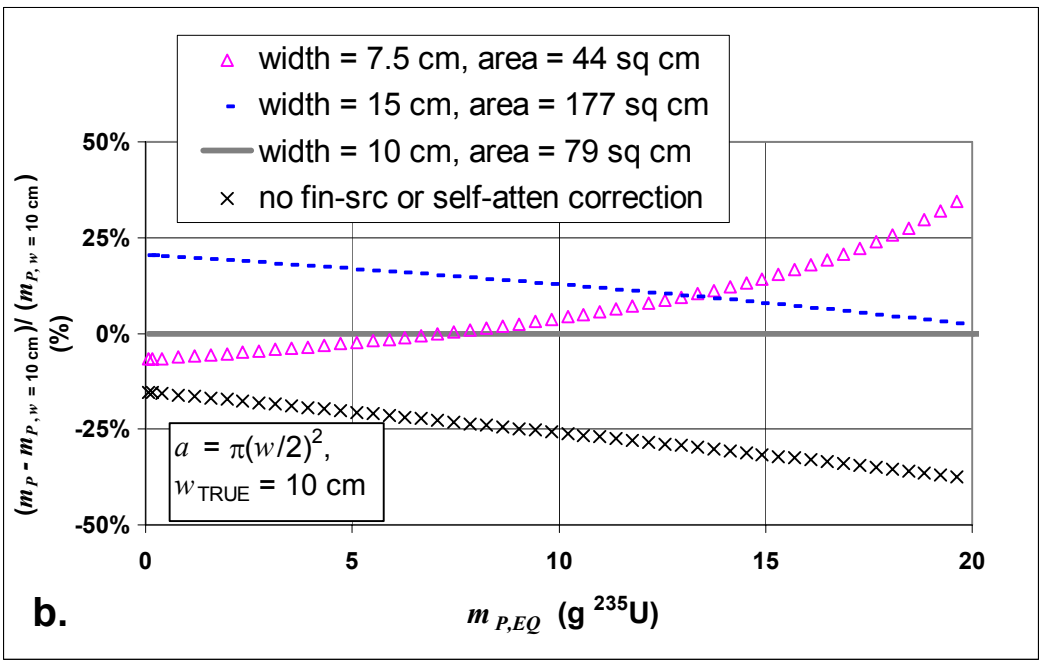

Figure VIII.15. Calculated results for point deposit of ^{235}U in U_3O_8 measured at 186 keV and r = 40 cm using a 2.5-cm by 2.5 cm cylindrical collimator: a) Fully corrected (Equations (38), (47), and (50)) vs. measured (Equation (11)) specific mass is plotted for three values of the point-deposit width parameter w. The true deposit width of 10 cm (gray, middle curve) corresponds to a point-source area of 79 cm^2. The true width parameter w is lower and higher by one third than a width of 7.5 cm (pink, upper curve) and 15 cm (blue, lower curve), respectively. The dashed line through the origin with slope of 1 is for reference. b) Percent difference between the corrected and true specific mass of the point deposit with w = 10 cm vs. the measured value is plotted in a practical mass range (up to a true deposit thickness of 0.35 g U/cm^2 in this case; see Section IX.6) for holdup measured at 186 keV. Corrected results are the solid gray line at 0% obtained using the true (w = 10 cm) width, triangles (pink) for the underestimate (w = 7.5 cm) of true width, and dashes (pink) for the overestimate (w = 15 cm) of true width. Crosses (gray, lowest curve) mark the uncorrected result. Note: Point areal density is m_P/a.

Figure VIII.15.a) shows data analogous to the heavy solid curve in Figure VIII.14.a), the fully corrected (for finite-source and self-attenuation effects both) *vs*. the measured specific mass of the U_3O_8 point deposit, but the correction is performed for three values of the deposit width parameter. If 10 cm is the true deposit width, then the true width is a third larger and a third smaller, respectively, than a possible low estimate of 7.5 cm and high estimate of 15 cm for the parameter ***w***. Above an uncorrected mass of 20 g ^{235}U, which corresponds to a fully corrected areal density of 0.35 g U/cm^2 the curves diverge significantly. Here, where self-attenuation dominates the correction, the overestimated ***w*** (***w*** = 15 cm) gives a result that is increasingly low with increasing thickness, and the underestimated ***w*** (***w*** = 7.5 cm) gives a result that is increasingly high with increasing thickness. However, the behavior below 20 g ^{235}U (below the fully corrected result of 0.35 g U/cm^2) is similar for the three values of ***w***. Section IX.6 indicates practical, statistically defined range of ~0.3-0.8 g U/cm^2 for the true areal density of deposits measured at 186 keV to be eligible for self-attenuation correction.

Figure VIII.15.b) magnifies the detail of a.) for uncorrected deposits up to 20 g ^{235}U (actual deposit thickness of ~0.35 g U/cm^2) with a plot of the percent difference between the corrected and true (***w*** = 10 cm) specific mass *vs*. the measured value. The solid (gray) horizontal line at 0% difference is the plot for the true (***w*** = 10 cm) result. The crosses (gray, lowest curve) show the uncorrected (measured) result, which always has a negative bias that increases with deposit thickness. The curve marked by triangles (pink, upward curve), corresponding to an underestimate of ***w*** (***w*** = 7.5 cm), starts out negatively biased (where finite-source effects dominate) and gradually becomes positively biased (where self-attenuation effects dominate), but the bias shrinks with increasing thickness (because of the compensating effect of the two corrections) and is always smaller than that of the uncorrected result. The curve marked by dashes (blue, downward curve), corresponding to an overestimate of ***w*** (***w*** = 15 cm), starts out with a positive bias (where finite-source effects dominate) that shrinks with increasing thickness as the self-attenuation effect grows (because of the compensating effect of the two corrections). Except for the very thinnest deposits where the bias represents a very small holdup quantity, the overall bias is always smaller than the bias in the uncorrected result for the point deposit.

Figure VIII.15 demonstrates the trends for point deposits corrected in a range practical for 186-keV holdup measurements. Over- or underestimates of ***w*** cause errors in the corrected result that 1.) are respectively opposite in sign, 2.) decrease with increasing thickness, and 3.) are smaller than the always negative and monotonically increasing (with deposit thickness) bias in the uncorrected result. Figure VIII.15 presents a strong argument in favor of performing corrections for finite-source and self-attenuation effects for all point deposits of holdup. The practical range for holdup measurements at 414- and 1001-keV increases relative to that shown for 186 keV by factors of five and ten-to-twenty, respectively, as indicated in Table VIII.1 and Section IX.6.

VIII.6.3. Line deposits.

Figure VIII.16.a) shows the corrected *vs*. measured specific mass of ^{235}U in the finite line deposit of U_3O_8 measured at 186 keV. The deposit width parameter ***w*** of 10 cm corresponds to the true width of the line deposit. The dashed line is drawn through the origin with a slope of 1 (effectively plotting an uncorrected result) for visualizing the magnitude of the corrections. The middle (solid) curve, determined from Equations (15) and (21), is the specific mass of the finite line deposit corrected for the finite source dimension ***w*** only. The top (heavy solid) curve

includes the additional correction for self-attenuation, Equations (39), (48) and (51). The self-attenuation correction dominates for the thickest deposits. Figure VIII.16.b) plots the percent difference between the corrected and measured specific mass *vs*. the measured value of the point deposit. The relative finite-source correction (bottom line) is constant and the relative self-attenuation correction (top line) increases nonlinearly with deposit thickness. Below ~1 g ^{235}U/cm for the measured specific mass (actual deposit thickness of ~0.12 g U/cm^2), the finite-source effect exceeds the self-attenuation effect. The measured result is biased low for any thickness before the corrections are applied.

Figure VIII.17.a) shows data analogous to the heavy solid curve in Figure VIII.16.a), the fully corrected (for finite-source and self-attenuation effects both) *vs*. the measured specific mass of the U_3O_8 line deposit, but the correction is performed for three values of the deposit width parameter. If 10 cm is the true deposit width, then the true width is a third larger and a third smaller, respectively, than a possible low estimate of 7.5 cm and high estimate of 15 cm for the parameter ***w***. Above an uncorrected specific mass of 3 g ^{235}U/cm, which corresponds to a fully corrected areal density of 0.45 g U/cm^2, the curves diverge significantly. Here, where self-attenuation dominates the correction, the overestimated ***w*** (***w*** = 15 cm) gives a result that is increasingly low with increasing thickness, and the underestimated ***w*** (***w*** = 7.5 cm) gives a result that is increasingly high with increasing thickness. However, the behavior below 4 g ^{235}U/cm (below the fully corrected result of ~0.7 g U/cm^2) is similar for the three values of ***w***. Section IX.6 indicates practical, statistically defined range of ~0.3-0.8 g U/cm^2 for the true areal density of deposits measured at 186 keV to be eligible for self-attenuation correction.

Figure VIII.17.b) magnifies the detail of a) for uncorrected deposits up to 4 g ^{235}U (actual deposit thickness of ~0.7 g U/cm^2) with a plot of the percent difference between the corrected and true (***w*** = 10 cm) specific mass *vs*. the measured value. The solid (gray) horizontal line at 0% difference is the plot for the true (***w*** = 10 cm) result. The crosses (gray, lowest curve) show the uncorrected (measured) result, which always has a negative bias that increases with deposit thickness. The curve marked by triangles (pink, upward curve), corresponding to an underestimate of ***w*** (***w*** = 7.5 cm), starts out negatively biased (where finite-source effects dominate) and gradually becomes positively biased (where self-attenuation effects dominate), but the bias shrinks with increasing thickness (because of the compensating effect of the two corrections) and is always smaller than that of the uncorrected result. The curve marked by dashes (blue, downward curve), corresponding to an overestimate of ***w*** (***w*** = 15 cm), starts out with a positive bias (where finite-source effects dominate) that shrinks with increasing thickness as the self-attenuation effect grows (because of the compensating effect of the two corrections). Except for the very thinnest deposits where the bias represents a very small holdup quantity, the overall bias is always smaller than the bias in the uncorrected result for the line deposit.

Figure VIII.17 demonstrates the trends for line deposits corrected in a range practical for 186-keV holdup measurements. Over- or underestimates of ***w*** cause errors in the corrected result that 1) are respectively opposite in sign, 2) decrease with increasing thickness, and 3) are smaller than the always negative and monotonically increasing (with deposit thickness) bias in the uncorrected result. Figure VIII.17 presents a strong argument in favor of performing corrections for finite-source and self-attenuation effects for all line deposits of holdup. The practical range for holdup measurements at 414- and 1001-keV increases relative to that shown for 186 keV by factors of five and ten-to-twenty, respectively, as indicated in Table VIII.1 and Section IX.6.

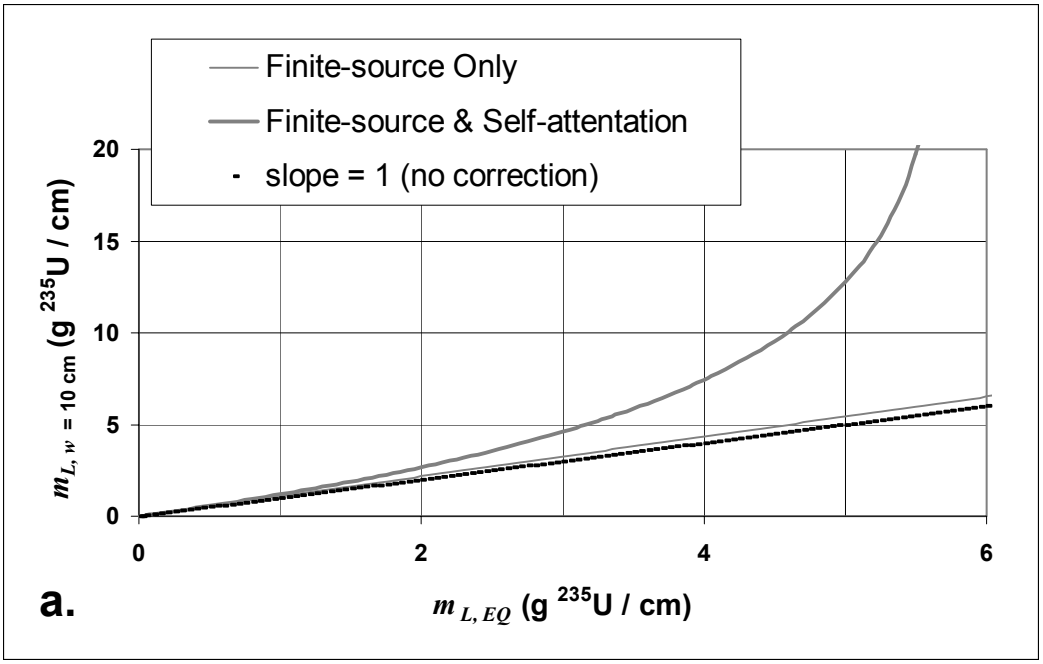

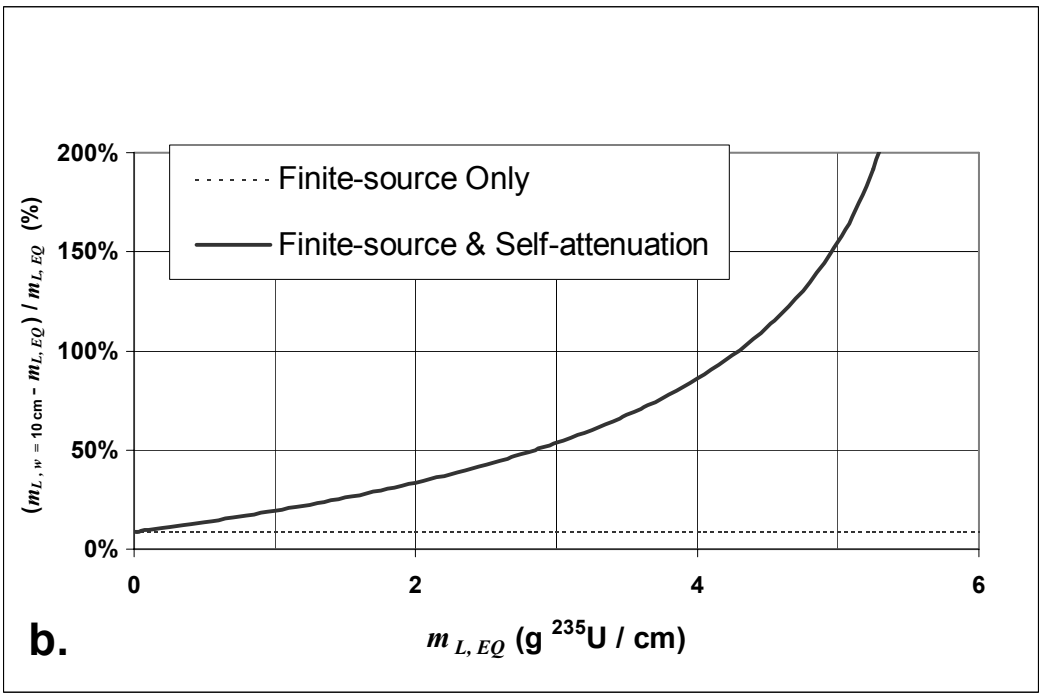

Figure VIII.16. Calculated results for line deposit of ^{235}U in U_3O_8 measured at 186 keV and r = 40 cm using a 2.5-cm by 2.5-cm cylindrical collimator: a) Corrected specific mass vs. measured, Equation (12), is plotted for the finite line source. The true deposit width w is 10 cm. The dashed line drawn for reference passes through the origin with a slope of 1. The middle (solid) line is the specific mass of the finite line source corrected by Equations (15) and (21) for the finite-source effect only. The top (heavy solid) line is the specific mass also corrected for self-attenuation, Equations (39), (48), and (51). b) Percent difference between the corrected and measured specific mass vs. the measured value is plotted for the line deposit. The relative finite-source correction (bottom dashed line) is constant, and the relative total correction including self-attenuation (top solid line) increases nonlinearly with areal density. Note: Line areal density is m_L/w.

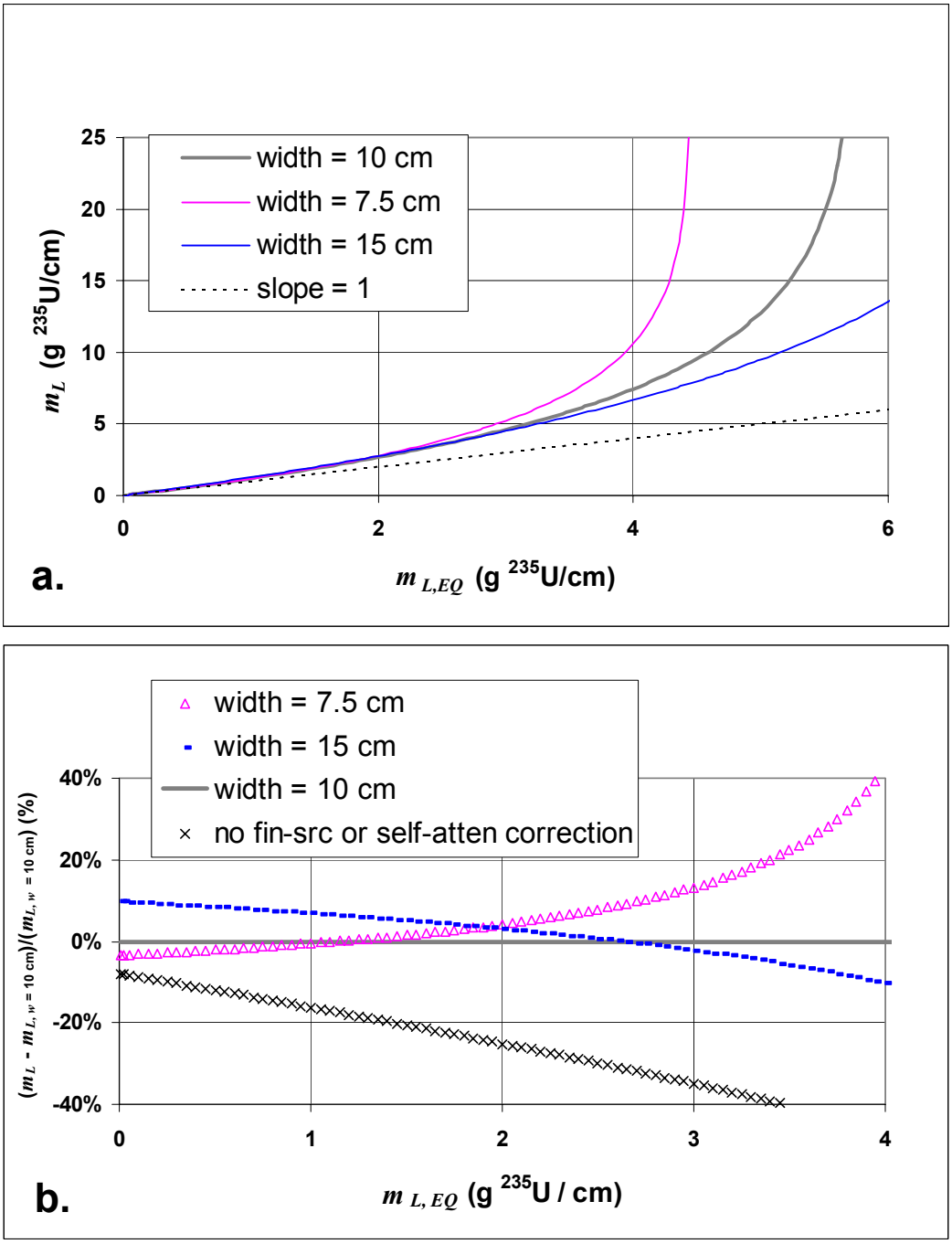

Figure VIII.17. Calculated results for line deposit of ^{235}U in U_3O_8 measured at 186 keV and r = 40 cm using a 2.5-cm by 2.5 cm cylindrical collimator: a) Fully corrected (Equations (39), (48) and (51)) vs. measured (Equation (11)) specific mass is plotted for three values of the line-deposit width parameter w. The true deposit width is 10 cm (gray, middle curve). The true width parameter is lower and higher by one third than a width of 7.5 cm (pink, upper curve) and 15 cm (blue, lower curve), respectively. The dashed line through the origin with slope of 1 is for reference. b) Percent difference between corrected and true specific mass of the line deposit with w = 10 cm vs. the measured value is plotted in a practical mass range (up to a true deposit thickness of 0.7 g U/cm^2 in this case; see Section IX.6) for holdup measured at 186 keV. Corrected results are the solid gray line at 0% obtained using the true (w = 10 cm) width, triangles (pink) for the underestimate (w = 7.5 cm) of true width, and dashes (pink) for the overestimate (w = 15 cm). Crosses (gray, lowest curve) mark the uncorrected result. Note: Line areal density is m_L/w.

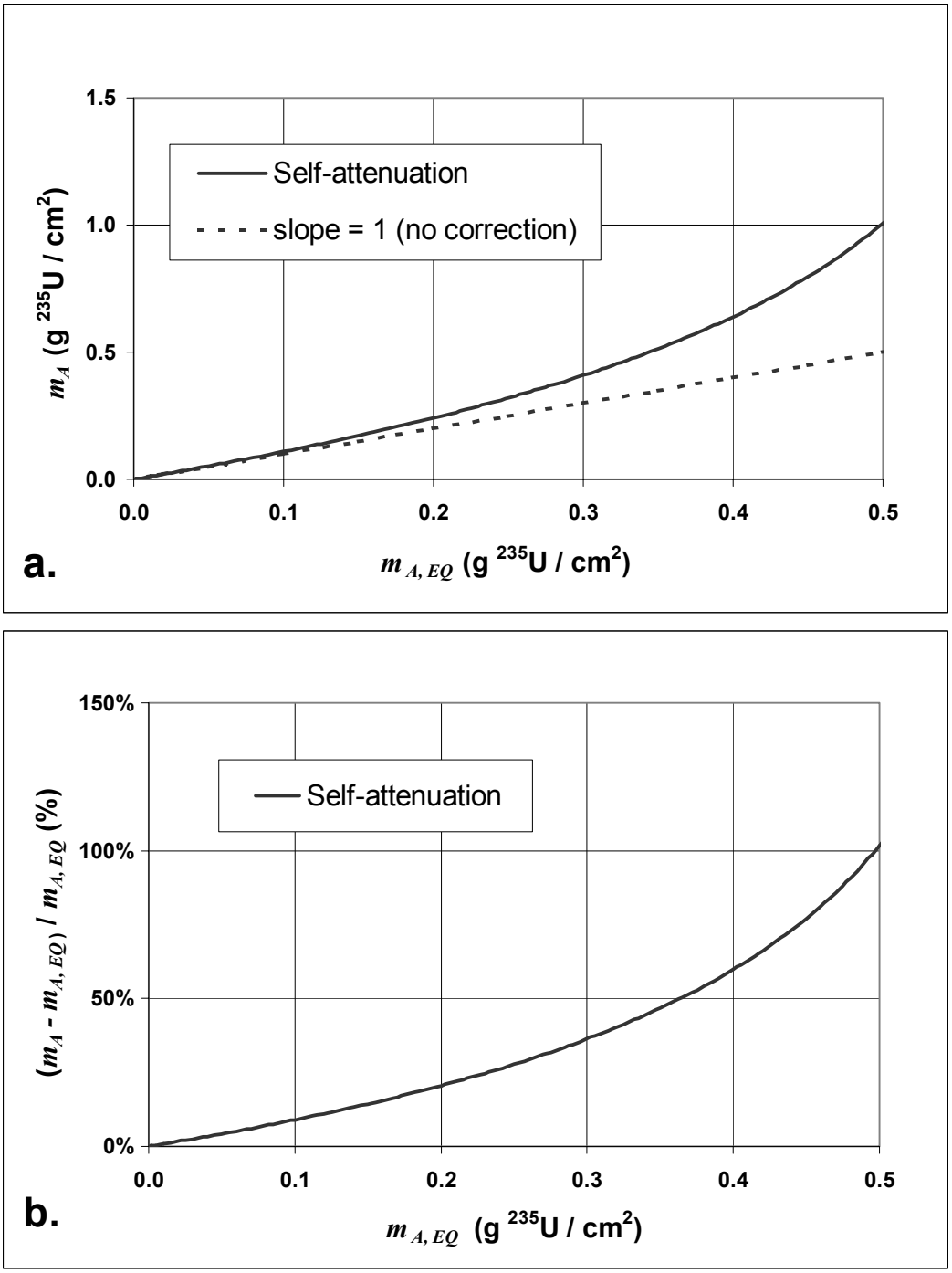

Figure VIII.18. Calculated results for area deposit of ^{235}U in U_3O_8 measured at 186 keV and r = 40 cm using a 2.5-cm by 2.5-cm cylindrical collimator: a) Corrected specific mass vs. measured, Equation (13), is plotted for the area source. The dashed line drawn for reference passes through the origin with a slope of 1. The solid line is the specific mass of the area source corrected by Equations (40), (49), and (52) for self-attenuation. b) Percent difference between the corrected and measured specific mass vs. the measured value is plotted for the area deposit. The finite-source correction does not apply to this model of the generalized area deposit. (That is, areal density for the area deposit is m_A.) The relative correction for self-attenuation increases nonlinearly with areal density.

VIII.6.4. Area deposits.

The width parameter does not apply to an area deposit because the finite area deposit fills the detector field of view. Figure VIII.18.a) shows the corrected *vs*. measured specific mass of ^{235}U in area deposits of U_3O_8 measured at 186 keV. The dashed line drawn for reference passes through the origin with a slope of 1 (effectively plotting an uncorrected result) for visualizing the magnitude of the corrections. Because the finite width exceeds the detector field of view, there is no correction for the finite dimension of an area source. The solid line includes the correction for self-attenuation only, Equations (40), (49) and (52).

Figure VIII.18.b) shows the percent difference between the corrected and measured specific mass *vs*. the measured value of the area deposit. The maximum measured specific mass plotted is the areal density, 0.5 g $^{235}U/cm^2$, which corresponds to a fully corrected areal density of >1 g U/cm^2. This exceeds the practical, statistically defined range of ~0.3-0.8 g U/cm^2 for the true areal density of deposits measured at 186 keV to be eligible for self-attenuation correction. However, for all measured thicknesses of the area deposit, the measured result is biased low before corrections for self-attenuation are applied.

The correction for self-attenuation of an area deposit does not require knowledge of an empirical width parameter. It uses only the measured value of the specific mass, which is areal density in the case of an area deposit. Figure VIII.18 demonstrates that in the entire thickness range for holdup deposits, the correction for self-attenuation by the area deposit increases with increasing deposit thickness. Unless corrected for self-attenuation, the areal density determined from the holdup measurement is biased low. This is a strong argument in favor of performing corrections for self-attenuation effects for all area deposits of holdup. The practical range for holdup measurements at 414- and 1001-keV increases relative to that shown for 186 keV by factors of five and ten-to-twenty, respectively, as indicated in Table VIII.1 and Section IX.6.

IX. MEASUREMENT PROCEDURES

IX.1. Calibration Measurements

The fundamental process of calibration for a quantitative passive gamma-ray measurement of an isotope is a determination of the relationship between the count rate of the measured gamma ray and the mass of the isotope. Section VI discusses the importance of point standards whose composition, geometry and packaging are well understood. This section summarizes other important considerations that apply to calibration measurements.

The measurement environment for calibration should be controlled radiologically such that the presence of sources other than the calibration source is minimized and unchanging. The issue of large room background is one of random uncertainty incurred from the subtraction of room background. The issue of changing room background is one of systematic uncertainty incurred from the subtraction of incorrect room background. Control of room background is easier for measurements at low energies such as 186 keV because detectors are collimated and shielded, but background sources in the field of view of the detector will still have an impact at low energy. Planning is most important in carrying out side-by-side calibrations and especially face-to-face calibrations of multiple detectors to avoid the systematic effects of the calibration standard or the reference source used by one detector on the calibration measurement of other detectors.

Knowledge of the geometry and packaging of the point-like calibration standard is most important for corrections that must be applied to the net gamma-ray count rate after subtraction of room background. The measured rate must be corrected for attenuation effects of the cladding, the finite dimension of the point standard and self-attenuation.

Minimizing the magnitude of these corrections is the first step in reducing the resulting uncertainty in the correction factors. This includes choosing an orientation for the calibration source corresponding to the thinner cladding surface. It also includes choosing a calibration distance r_0 that is large relative to the finite source dimension. It may include orienting the thinner source dimension perpendicular to the detector axis. It may also include choosing the smaller (thinner) of the available calibration standards.

Minimizing the uncertainty in the corrections includes orienting the source relative to the detector axis so that both its finite width and the form for the self-attenuation correction factor are well defined. Apply traditional expressions (see Tables VI.1-VI.3) for self-attenuation corrections for the known source to the calibration standard. This enables calibrations to be performed with standards that are isotopically well suited but are (nearly) the maximum thickness for the analysis gamma ray when no other standard is available. Use procedures described in Section VIII.3 to correct for the effects of the finite-source dimension of the calibration standard.

Positioning of the source relative to the detector will contribute to the systematic error in the holdup calibration. Minimizing the positioning uncertainty includes knowing the calibration distance r_0 very well. Equivalent knowledge of the measurement distance r is required for measurements of holdup deposits. Specifying r_0 (or r) requires a good determination of the distance between detector and calibration source (or between detector and equipment, in the case

of holdup measurements). It also requires knowing the collimator depth and any other dimensions – including the total thickness of the layers of metal (tin sheet, *etc*.) that filter low-energy gamma rays, and the recess depth between the face of the crystal and the surface of the detector – that displace the crystal from the collimator. It requires knowing, in addition, the recess distance of the source within its capsule. (The analogous parameter for measurements of holdup deposits is the spacing between the holdup deposit and the surface of the equipment.) Finally, the material-specific energy-dependent average depth of gamma-ray interaction within the crystal must be determined and included, especially for thicker crystals and higher energies.

Table IX.1.
Usual Components of Calibration and Measurement Distances, r_0 and r

Distance Component of r_0 or r	Type	Typical Range (cm)	
		r_0	r
Source-to-Detector	Meas.-Geometry	30-50	30-300
Collimator Depth	Detector	2-5	2-5
Crystal Recess	Detector	0.1-0.4	0.1-0.4
Gamma Filter Thickness	Detector	0.1-0.3	0.1-0.3
Gamma Interaction Depth	Energy	0.2-2	0.2-2
Source/Deposit Recess	Capsule/Equip.	0.2-2	0.2-200

Table IX.2.
Mean Gamma-Ray Interaction Depth in NaI Crystals

		Mean Interaction Depth (cm)	
Isotope	E_{γ} (keV)	1.25-cm NaI	5-cm NaI
^{238}Pu	153	0.22	0.25
^{235}U	186	0.32	0.51
^{241}Pu - ^{237}U	208	0.37	0.58
^{237}Np	300	0.46	1.03
^{239}Pu	414	0.50	1.35
^{241}Am	662	0.54	1.65
^{238}U - -	1001	0.56	1.81

Table IX.1 lists the components of r_0 and the analogous components of r. The entries in blue are detector and gamma-ray parameters that are constant for calibration and for the corresponding holdup measurements. Adding these dimensions to the measurement-geometry and

capsule/equipment distances during the analysis phase saves measurement personnel the time needed to enter these manually. Table IX.2 lists the average interaction depth in the 1.25- and 5-cm-thick NaI crystals for gamma rays commonly used to measure holdup.

Minimizing the positioning uncertainty also requires ensuring that the calibration standard placed at the calibration distance r_0 is centered on the detector axis. Ensuring co-linearity of the cylindrical axes of the detector and collimator is essential. The use of positioning devices can be a most important addition in that it simplifies the source/detector placement process and gives the calibration positioning better reproducibility. Figure IX.1 shows a mechanical positioning device in use for calibrating the 2.5-cm by 5.0-cm NaI detector for measurements of LEU. Though the angle of the source axis can be varied, the device fixes the required ninety-degree relationship between detector and source axis. It allows easy adjustment and fixing of the calibration position r_0 from contact with the detector to a distance approaching a meter. It also allows easy fixing of the calibration source on the detector axis and displacement of the source to the left or right of the axial position. The latter capability supports well-controlled measurements of the radial response of the detector.

Fixed-energy ROIs established at the time of calibration must be maintained for the calibration to remain valid. Uncompensated drifts in gain introduce a calibration bias that must be included as part of the systematic uncertainty. (Refer to Section IX.8.) If it is necessary to change the ROI energy (upon discovery of an interference, for example), the calibration must be re-determined. Similarly, the collimator, shielding, and gamma filtering must remain as configured at the time of calibration in order for the calibration to remain valid.

Figure IX.1. A mechanical positioning device is shown in use for calibrating the 2.5-cm by 5.0-cm compact NaI detector to measure LEU. The calibration standard is mounted on the detector axis at r_0 = 40 cm. An additional device shown at the right (nearly fully collapsed for storage) illustrates the variable position of the calibration standard, detector distance, and relative angle between source and detector axes allowed by this simple device.

IX.2. Measurements of the Radial Response

The positioning device pictured in Figure IX.1 is a particular convenience for measuring the radial response of the detector at the energy of the analysis gamma ray. Although it is tempting to consider using a single set of radial-response data for multiple analysis gamma rays because only relative response is required of these measurements (refer to Figure VIII.3), it is necessary

to obtain this data uniquely for each gamma-ray energy. Mechanical positioning devices are most useful in reproducing the source positions for such multiple measurements.

The radial response curves plotted in Figure IX.2 were measured with the same detector (2.5-cm diameter by 5-cm-thick NaI detector with 2.5-cm by 2.5-cm collimator). The measurement distance r_0 for the three gamma-ray sources was 40 cm. The FW.5M of each response curve measured at 186 keV, 414 keV, and 1001 keV is 23 cm, 22 cm, and 19 cm, respectively. The significantly more narrow response for higher energy gammas is the result of the loss of events as the off-axis displacement of the source exceeds the radius of the collimator and the direct gammas no longer impinge on the detector perpendicular to its surface. When the diameters of the detector and collimator are the same, the shortened detector thickness at these angles reduces the detection efficiency for higher-energy gammas.

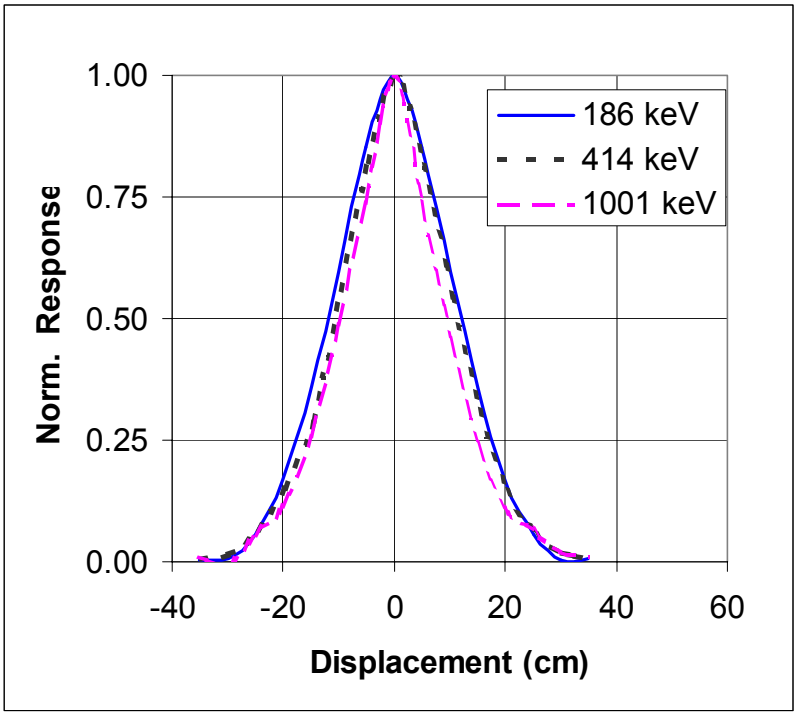

Figure IX.2. The radial response (normalized gamma-ray count rate vs. displacement of the source from the on-axis position) of the 2.5-cm diameter by 5-cm-thick NaI detector with 2.5-cm by 2.5-cm collimator is plotted for 186-, 414- and 1001-keV gamma rays. The FW.5M of each radial response curve is 23 cm, 22 cm and 19 cm, respectively.

The data in Figure IX.2 indicate that the geometric response of the detector is dependent on gamma-ray energy. Therefore, the radial response must be determined uniquely for each gamma-ray energy. This requirement is inconvenient for certain calibrations because the small solid angle for measurements at large axial displacements greatly reduces the measured count rate, as Figure IX.2 indicates. A relatively strong gamma-ray source is required in order to complete the measurements in a reasonable time. Furthermore, when the gamma-ray energy is high, a unique measurement of background with a shielding plug inserted in the collimator is required at each displacement, as discussed in Section IX.3.

The branching ratio for some actinide gamma rays important to holdup measurements is small. Self-attenuation by the high-Z material limits using a larger source to compensate for a small

branching ratio. The use of an alternative source with a gamma ray close in energy to the weaker actinide gamma ray is recommended in such cases. Because the radial response is a relative measurement, the use of a standard is not required for these measurements.

The 1001-keV gamma ray is most demanding of the radial response measurements because of its high energy and small net branching ratio (<1%) relative to the decay of ^{238}U. The recommended alternative for radial-response measurements applicable to 1001 keV is the 1064-keV gamma ray of ^{207}Bi. The ^{207}Bi source is a practical choice because of both its gamma-ray energy and its 30-year half life. A ^{207}Bi source activity of ~50 μCi is recommended for this purpose. Such sources are available commercially.

IX.3. Room Background Measurements

Room background is a net contribution to the analysis peak that arises from sources other than the holdup deposit. The discussions below address only room-background contributions of photoelectric events from the analysis gamma ray. The spectroscopic techniques required to avoid other background effects on the spectrum, including discrete photoelectric interferences (from other than the analysis gamma) and discrete (edge, *etc*.) influences of the Compton continuum are discussed in detail in Section VII.1-VII.2.

Holdup measurements benefit greatly from well-designed measurements of room background and usually fail otherwise. Background is more important in measurements of holdup than almost any other situation. Inventory may be located in interim storage or within the process equipment throughout the plant while holdup measurements are in progress. Holdup deposits can be small while other inventory is substantial. Well-planned measurements of room background can result in measurement failures if room background dominates the holdup spectrum because the measurement sensitivity diminishes from the subtraction of a large contribution from room background. Reducing room background benefits all holdup measurements. The walk-down activity described in Section X.2 is a good opportunity to discuss schedules for cleanout and plans for interim storage of materials so that the measurement schedules can be timed accordingly for lower-background periods.

The methodology best suited to measurement and subtraction of room background depends on numerous sensitivities to the particular measurement situation, choice of detector, and choice of analysis gamma ray. The following two considerations can guide a generalized approach to room background measurements.

- Room background for low-energy (<300-keV) gamma measurements with collimated shielded NaI is primarily detected through the collimator opening, originating from sources that are behind or alongside the holdup deposits.
- Room background for high-energy (>300-keV) gamma measurements with collimated NaI also includes significant background from sources behind or alongside the detector because the analysis gammas at higher energies can penetrate the detector shield.

Simple approaches can address many cases for each of the two types of background: that entering the detector through the collimator and that penetrating the shielding.

The most effective two-fold approach to background that enters the detector through the collimator is to i) know the specific sources of background and their locations, and ii) position

the detector to avoid counting this type of background. The walk-down activity described in Section X.2 also is a good opportunity to locate background sources and plan to position detectors accordingly. Viewing the deposit with the detector facing opposite the background source locations is recommended when possible. When options for alternative positioning that precludes viewing background are limited, positioning to view only distant background is a possible alternative. Distance reduces the background signal, and it also allows lower-energy background to be measured independent of radiation from the deposit by shifting the detector sideways to look past the deposit and measure the background alone. If the equipment that contains the deposit has attenuated the room background during measurement of the deposit but not during the measurement of room background, the measured room background must be corrected (reduced) by this attenuation effect. Measurements performed with the collimator in proximity to the equipment can be well served by holding a sheet of dense metal behind the equipment as a background shield. This is effective primarily at lower gamma-ray energies that are shielded by relatively thin lead (*etc*.) sheet.[20]

Collimator plugs, cylinders of lead or tungsten or other dense shielding material that insert snugly into the collimator for measurements of room background, is an effective approach to measuring room background that reaches the detector by penetrating the shielding. This approach is essential for holdup measurements at high gamma-ray energies. Unlike measurements at 186 keV, a unique measurement of room background with the tungsten plug inserted is usually required for each individual deposit measurement at 414 or 1001 keV in a working plant. The detector position for the measurement with the plug inserted is identical to that of the corresponding measurement with the plug removed. Holdup measurements of room background that rely on the use of a collimator plug must also be calibrated using the same mode of background measurement. Measurements of holdup deposits that are difficult to access except by positioning devices such as telescoping poles (Figure VII.8) are more efficient if the collimator plug is removed for measurements of holdup deposits at successive locations and then inserted for the measurement of room background at the same multiple locations. Section VII.3 has additional discussion on collimator plugs for measurements of room background.

When room background is a combination of gamma rays that enter the detector through the collimator and those that penetrate the shielding, measurement of room background can be a process of two or more measurement steps. Distant background itself could be subject to evaluation by the plug-in/plug-out process at higher energies. A major benefit to scheduling for periods when room background is minimum is avoiding multiple-step measurements of room background.

Expert use of the generalized-geometry techniques has led some teams to develop models that address more complex background effects, such as partial shielding of the room background by the equipment in which the deposit resides.[69] More detailed knowledge of equipment dimensions and positions is needed to apply these models. Such approaches may be the most practical in specific applications when positioning or scheduling is not effective in reducing the effort required to measure room background. The success of such approaches will also represent first steps toward modeling of the future facility equipped with distributed sensors in fixed networks that measure the distribution and mass of nuclear materials throughout the plant.

IX.4. Holdup Measurements

Successful application of the generalized-geometry approach to holdup measurements requires pursuing reasonable means to ensure that the measurement methodology complies with the generalized analysis models. The following partial list of good practices can guide the user's understanding on making decisions about compliance.

i) Optimize sampling
- Maximize measurement distance to improve sampling.
- Minimize count time to increase the number of measurements, improving sampling.
- Refer to Sections X.3 and X.4 for practical guidance in these areas.

ii) Reduce the magnitude of additional systematic effects by minimizing the magnitude of the corrections
- Maximize measurement distance to reduce the magnitude of the finite-source effect.
- Avoid or temporarily relocate movable barriers to the process equipment (including some types of shielding) to reduce equipment attenuation effects.
- Strive to measure a (glove box, etc.) floor from above looking down or from below looking up to minimize the magnitude of corrections for attenuation by deposit and equipment. (Use detectors collimated from the side when clearance space is limited.)
- Orient the detector to view the thin dimension of a thick deposit. (View horizontal ducts or pipes from above or beneath.)

iii) Enforce the geometric assumptions of the model.
- Maintain a 90° relationship between the deposit surface and detector/collimator axis.
- Center cavities of equipment containing point or line deposits in the field of view of the detector.
- Position the detector so that the corresponding equipment surface fills the detector field of view for measurement of an area deposit. (Use cylindrical collimator inserts to reduce the field of view if the minimum measurement distance exceeds that needed to meet the requirement.)

iv) Determine and use the best available information on deposits and equipment.
- Use a positioning standoff marked with linear dimensions to set the desired measurement distance.
- Use tape measures to determine and mark measurement positions and measure overall equipment dimensions.
- Use an ultrasonic thickness gauge to measure equipment thickness when a drawing is not available.
- Use radiation survey meters or collimated rate-meters to estimate deposit width.
- Investigate the deposit composition and choose attenuation coefficients accordingly.

The reality of the measurement environment can force departures from ideal practice. Some of these departures can be addressed readily by increasing the sophistication (and the required number of parameters) of the existing model. One example from measurements of LEU is deposits that fill the cavity of a cylindrical duct. The cylindrical line or point deposit is better treated for self-attenuation by multiplying the normalizing mass attenuation coefficient μ (Table VIII.1) by the factor $\boldsymbol{F}$ such that

$$1 < F \leq \pi/4 \quad , \tag{67}$$

where $\boldsymbol{F} = \pi/4$ is applicable for the far-field cylinder geometry, and $\boldsymbol{F} = 1$ corresponds to the slab.[39] The magnitude of the effect of such a change to the model, like many that may be considered on a case-by-case basis as each piece of equipment appears to depart somewhat from the strict assumptions of the original model, may prove to be too small to justify adding an additional geometric parameter to the analysis setup requirements. The magnitude of the effect in the case of this LEU example is evaluated numerically in Section IX.8. Users maintain, nonetheless, that frequent encounters with generic departures from the simple model reinforce needs for greater sophistication.

Successful application of the generalized-geometry approach to holdup measurements requires users who understand the model and recognize its limits. The ideal user will decrease the measurement uncertainty by pursuing reasonable means to ensure that the measurement methodology complies with the generalized analysis models. Expert users are simultaneously developing systemic improvements that extend the generalized models to geometries commonly encountered in their facilities that represent departures from the original models.[69, 70]

IX.5. Measurement Control

The prescribed implementation of an internal reference source and an external check source, and the saving of gamma-ray spectra combine for effective measurement control in quantifying holdup. Measurement control must be uniformly applied to the acquisition of all gamma-ray spectra associated with holdup measurements. This includes those obtained in calibration, verification, and holdup measurements. A great benefit of the automation of holdup measurement process is the assurance of consistent measurement control offered by the automation.[12] Measurement control performed manually is often bypassed or performed less frequently because of time constraints that limit the extent of implementing this process manually. Automation eliminates the significant additional cost in time associated with manually performing and managing measurement control. The real-time readout of measurement-control data can avoid loss of measurement data that arises when spectra analyzed after the measurement campaign is complete fail to meet quality or efficiency requirements.

Sections VII.1 and VII.3 discuss the application and choice of the gamma-ray reference source, which mounts inside the detector shield in fixed geometry relative to the crystal. This source provides gamma rays lower in energy than the analysis gamma rays. It must be installed on the detector before completing the final mechanical assembly of the detector so that it can be characterized at the time of the initial setup and calibration of the assembled detector and be put to use thereafter. Storing the net count rate, centroid, and resolution (FW.5M) of the reference peak for every spectrum requires a rate of approximately 10^3 s^{-1} for the reference gamma ray to obtain the empirical parameters with sufficient precision in the shortest (~10-s) count times used for measurement of holdup. The net count rate of the reference peak monitors constant operation and dead time, its centroid monitors the gain, and its resolution ensures the quality of gamma peaks for each spectrum. Automation of the acquisition of holdup data includes automating the evaluation, storage, readout, and testing of the empirical measurement-control parameters against stored values, as well as automating alarms that warn the user of failed tests.[13]

Use of the reference-peak centroid for automatic digital gain-drift compensation[54] or stabilization (analog or digital) is important when scintillation detectors like NaI operate in measurement environments in which temperature is not controlled. Manual compensation for gain drift is time-consuming to implement in the field. and is even costly to implement off-line with the saved gamma-ray spectra. The reference-peak M can also be used to automatically signal unacceptable loss of resolution when room-temperature detectors like CZT are used in elevated-temperature conditions.

Section VII.3 discusses the application and choice of the gamma-ray check source, which mounts at the end of the collimator, external to the detector shield, in fixed geometry relative to the crystal. This source provides gamma rays of the same energy as (or of an energy similar to) that of the analysis gamma ray. The mounting mechanism for the check source must be simple for easy, reliable, and reproducible mounting in the field. The source and mounting mechanism must be available at the time of calibration so that the source can be characterized at this time. The encapsulation of the HEU standards illustrated by the sketch in Figure VI.1 is designed with a machined cylindrical extension that inserts reproducibly into the 5.1-cm-diameter collimator of the compact, shielded NaI detectors (Figures VII.8 and IX.1). These calibration standards readily double as check sources for use in the field with the NaI detectors.

Stored parameters for the net count rate, centroid, and FW.5M of the check-source gamma peak are compared with the values obtained in the field at intervals determined administratively or enforced by automation. Unique changes (not detected in the parameters of the reference-source peak) in the net rate, FW.5M or centroid of the check-source peak can signal the presence of discrete interferences. The net count rate of the check-source gamma peak monitors the stability of the calibration more specifically than the net count rate of the reference gamma because the check-source energy is the same as (or very similar to) that of the analysis peak. Automation of the acquisition of holdup data includes prompts to use the check source as well as automated evaluation, storage, readout, and testing of the check-source parameters and alarms that warn the user of failed tests.[12] Note that the net rate of the check-source gamma peak can also uniquely signal the loss of calibration accuracy (caused, for example, by a mechanical shift in detector position within the shield) but cannot be used to correct such an effect.

Saving spectra is the best assurance that data obtained during periods of instability (electronic, environmental, radiological) can be reanalyzed with parameters that compensate for the effects of the instability. The reference source ensures the presence of well-defined spectral features for even the shortest count time to support the design of an appropriate reanalysis. Because memory is compact and low in cost, saving the hundreds or thousands of spectra acquired with short count intervals in the measurements of holdup deposits is reasonable and recommended. Saving spectra manually in the field is not practical because it is time-consuming, but this aspect of measurement control is a feature of the automated acquisition of holdup measurement data.[13]

The following list summarizes the recommended measurement controls for gamma-ray spectra acquired for the purpose of calibrating or verifying the measurement systems or quantifying holdup deposits, and indicates how each is used.

- The centroid of the gamma peak for the internal reference source, measured for every gamma-ray spectrum acquired, documents the stability and precision of the gain. The gain must remain constant within defined limits, or the analysis ROIs must be adjusted accordingly, for validity of the calibration.

- The FW.5M of the gamma peak for the internal reference source, measured for every gamma-ray spectrum acquired, documents the stability and precision of the resolution, which must remain constant within defined limits for validity of the calibration.
- The net count rate of the gamma peak for the internal reference source, measured for every gamma-ray spectrum acquired, documents the live data-acquisition time, which must be used to adjust measured count rates in some cases (including high count rates) for validity of the calibration.
- The centroid of the gamma peak for the external check source, measured at specified intervals (determined by automation or by administrative controls), documents the stability and precision of the centroid of the analysis peak. The centroid must remain constant within defined limits, or the analysis ROIs must be adjusted accordingly, for validity of the calibration.
- The FW.5M of the gamma peak for the external check source, measured at specified (by automation or administrative controls) intervals, documents the stability and precision of the width of the analysis peak, which must remain constant within defined limits for validity of the calibration.
- The net rate of the gamma peak for the external check source, measured at specified intervals (determined by automation or administrative controls), documents all instabilities in the calibration, which must remain constant within defined limits for validity. Agreement within limits with the stored value constitutes a bias check on the holdup calibration, and repeatability within a measurement period is a precision check. The net rate also uniquely senses (though it is unable to quantify) discrete gamma-ray interferences or changes in the detection solid angle.
- Saving all gamma-ray spectra enables reanalysis in most cases of uncompensated gain drift, some cases of worsening resolution, some cases of discrete interference and most cases of changing solid angle.

IX.6. Thick Deposits and Defining the Limiting Thickness

Equation (26) describes the nonlinear increase in the uncertainty in the measured areal density of holdup that arises from correcting this result for self-attenuation. The correction factor for self-attenuation, Equation (25a), is a nonlinear function of the measured areal density. Because of short count times, large background contributions, and relatively small detection solid angles, the random uncertainty in the measured areal density is typically large –10 to 20% – for holdup measurements, as illustrated by the error bars on the points in Figure VI.5. The data quality objectives (DQOs) of specific customers may stipulate count times that achieve better results for random uncertainty

The ability to perform a correction for self-attenuation is limited for thicker deposits because the measured thickness with its random uncertainty propagates to a significantly more uncertain corrected result. A measured deposit whose thickness (areal density) plus random uncertainty equals or exceeds the maximum thickness cannot be corrected for self-attenuation because its resulting uncertainty is undefined. Even a measured deposit whose thickness (areal density) plus random uncertainty approaches the maximum thickness may not be corrected when the resulting uncertainty is unacceptably large. It is possible to define the maximum deposit thickness (areal

density) using criteria derived from the random uncertainty. Note here that the following paragraphs discuss the limits for deposit thickness in the context of random uncertainty, because the relative random uncertainty in the counting statistics varies from measurement to measurement, screening for maximum thickness must be applied to each individual (short-count-time) measurement, and the counting statistics for a portable measurement performed at the largest practical distance (r_P) in the shortest practical count time (t_P) will not be good. The second set of examples discussed below assumes that for a single measurement the relative random uncertainty of 20% 1σ from counting statistics is typical for moderate deposits. The systematic uncertainty will not usually exceed this. However, if realistic estimates of the systematic effects surpass this limit (refer to Section IX.9), the examples illustrated in Table IX.4 below should be recalculated for a higher (greater than 20%) limit.

Table IX.3 lists the gamma rays commonly used to quantify holdup and the normalizing mass attenuation coefficient μ (Table VIII.1) of each for elemental deposits. The maximum areal density for the element before correction, $(\rho x)_{MEAS}$, is $1/\mu$ such that the product $\mu(\rho x)_{MEAS}$ is 1. Assuming a 10%-1σ relative random uncertainty in $(\rho x)_{MEAS}$, better than counting statistics for most holdup measurements, the *limiting* corrected areal density **(ρx)** is determined using Equation (25a) and a value of $(\rho x)_{MEAS}$ that is 1σ smaller than its maximum. The resulting relative random 1**σ** in the *limiting* value of **(ρx)** gets inflated to 39% in this case. This uncertainty is typically too large. A *practical* corrected areal density **(ρx)** is determined using Equation (25a) and a value of $(\rho x)_{MEAS}$ that is 3**σ** smaller than its maximum. The resulting random relative 1**σ** in the *practical* value of **(ρx)** is inflated to only 19%, which is usually acceptable for an individual deposit. Therefore, a 3**σ** criterion on the maximum $(\rho x)_{MEAS}$ as defined in Equations (35)-(37) defines the practical limit of the element areal density of thick deposits when the DQO stipulates a relative random measurement uncertainty of 10%.

Table IX.3
Statistical Criterion for the Practical Deposit Thickness with 10%-1σ Counting Statistics

Isotope	Gamma Energy (keV)	Deposit Material	μ (cm^2/g)	Maximum $(\rho x)_{MEAS}$ (g/cm^2)	Limiting* (ρx) (g/cm^2)	Limiting* σ(ρx) (g/cm^2)	Limiting* [σ(ρx)/(ρx)]	Practical** (ρx) (g/cm^2)	Practical** σ(ρx) (g/cm^2)	Practical** [σ(ρx)/(ρx)]
^{238}Pu	153	Pu	2.5	0.40	0.9	0.4	39%	0.5	0.1	19%
^{235}U	186	U	1.5	0.68	1.6	0.6	39%	0.8	0.2	19%
^{241}Pu	208	Pu	1.2	0.84	1.9	0.8	39%	1.0	0.2	19%
^{237}Np	300	Np	0.50	2.0	4.6	1.8	39%	2.4	0.5	19%
^{239}Pu	414	Pu	0.27	3.7	8.6	3.4	39%	4.5	0.9	19%
^{241}Am	662	Am	0.13	7.6	17	6.8	39%	9.1	1.8	19%
^{238}U	1001	U	0.075	13	31	12	39%	16	3.1	19%

* Based on applying a 1σ criterion of 10% to the Maximum $(\rho x)_{MEAS}$.

** Based on applying a 3σ criterion of 30% to the Maximum $(\rho x)_{MEAS}$.

Table IX.4 is analogous to Table IX.3 except that it assumes a realistic 20%-1σ relative random uncertainty in $(\rho x)_{MEAS}$. The resulting random relative 1**σ** in the *limiting* value of **(ρx)** is inflated to 50% in this case while the random relative 1**σ** in the *practical* value of **(ρx)** is more reasonable at 26%. Therefore, the 3**σ** criterion on the maximum $(\rho x)_{MEAS}$ as defined in Equations (35)-(37) also defines a practical limit of element areal density for thick deposits when DQO stipulates a

random measurement uncertainty of 20%. The values in Column 11 (26% for Table IX.4, 19% in Table IX.3) may be used to assign a practical limit on random relative uncertainty in the postcorrection areal density, the quantity **T** in Equations (44)-(46).

Notice that the practical value of $(\rho x)_{POST}$ for 10% measurements is more than twice that for 20% measurements (Column 9 of Tables IX.3 and IX.4). Therefore, repeated measurements with longer counts for improved relative random uncertainty is an option upon failure of thick-deposit tests described by Equations (35)-(37). Remeasurement may be elected when equipment includes variable-thickness deposits because reducing the weighting $\mathbf{w_i}$ defined in Equations (53)-(56) and (63)-(65) or sacrificing results with unacceptably large uncertainty produces negative bias in the holdup mass for extended equipment. (Refer to Section VIII.5.) The option to measure a higher-energy gamma ray should be explored in appropriate cases of thick deposits.

Table IX.4
Statistical Criterion for the Practical Deposit Thickness with 20%-1σ Counting Statistics

Isotope	Gamma Energy (keV)	Deposit Material	μ (cm^2/g)	Maximum $(\rho x)_{MEAS}$ (g/cm^2)	Limiting* (ρx) (g/cm^2)	Limiting* σ(ρx) (g/cm^2)	Limiting* [σ(ρx)/(ρx)]	Practical** (ρx) (g/cm^2)	Practical** σ(ρx) (g/cm^2)	Practical** [σ(ρx)/(ρx)]
^{238}Pu	153	Pu	2.5	0.40	0.6	0.3	50%	0.2	0.1	26%
^{235}U	186	U	1.5	0.68	1.1	0.5	50%	0.3	0.1	26%
^{241}Pu	208	Pu	1.2	0.84	1.3	0.7	50%	0.4	0.1	26%
^{237}Np	300	Np	0.50	2.0	3.2	1.6	50%	1.0	0.3	26%
^{239}Pu	414	Pu	0.27	3.7	6.0	3.0	50%	1.9	0.5	26%
^{241}Am	662	Am	0.13	7.6	12.2	6.1	50%	3.9	1.0	26%
^{238}U	1001	U	0.075	13	21.4	10.6	50%	6.8	1.8	26%

* Based on applying a 1σ criterion of 20% to the Maximum $(\rho x)_{MEAS}$.

** Based on applying a 3σ criterion of 60% to the Maximum $(\rho x)_{MEAS}$.

IX.7. Thin Deposits and Measuring Zero

Measurement uncertainty inflates for thick deposits as it propagates nonlinearly through the self-attenuation correction. The uncertainty is also large for thin deposits because the smaller net count rate and larger relative background contribution produces a relative random uncertainty in the measured areal density exceeding that for moderate-to-thick deposits. Net rates are consistent with zero at the 3σ level for these deposits. Nevertheless, the uncertainty will not inflate in the process of correcting for self-attenuation.

It is important for the following three reasons to fully analyze the thin-deposit results, despite the possibility that results will be consistent with zero holdup. 1) The overall precision in total holdup mass obtained from multiple measurements performed on the extended equipment will improve over that of individual measurements. ii) Obtaining 3σ limits on the holdup deposits is valuable to many customers of holdup measurements. iii) Assigning a smaller weighting $\mathbf{w_i}$ to an individual measurement result based on its uncertainty or sacrificing a result with unacceptably large uncertainty will positively bias the holdup mass for the extended equipment. (Refer to Section VIII.5.)

The option of a smaller measurement distance can be considered for equipment in which deposits are thin at all locations because maximized sampling is less important for thin deposits. Refer to Section X.3 for recommendations on the smallest practical measurement distance.

IX.8. Numerical Evaluation of Systematic Effects

Results for specific mass of ^{238}U in a horizontal vacuum line containing LEU oxide with well determined measurement geometry are plotted *vs*. measurement position in Figure VI.5. The LEU measurements used the 1001-keV gamma ray. The average correction factors determined as outlined in Section VIII for measurements at 73 equally spaced locations along the duct were 1.26, 1.06 and 1.18, respectively. The total uranium mass determined from these measurements is 183 ± 11 kg, where the uncertainty (6.2% relative) is the random error in the total mass, propagated as described in Section VIII. It is difficult to prescribe or program the propagation of numerous independent systematic error terms independently through the analytical expressions. The error propagation must be carried out point by -point, because of the nonlinear self-attenuation correction, and the error terms can vary with location and time. It is straightforward, however, with a spreadsheet analysis of the point-by-point generalized-geometry data to define the uncertainty limits at a specified confidence level (68% for one-sigma, for example) on each of the parameters that contribute to the analysis, vary each parameter by its uncertainty, and recalculate the total uranium mass with each variation. Combining the relative systematic errors from the individual effects gives the total relative systematic error. Combine this with the total random error that is propagated analytically.

Table IX.5 shows the results of such a numerical evaluation of the systematic error for parameters grouped in five categories: deposit composition, measurement geometry, process equipment dimensions, the calibration constant, and the self-attenuation model. The latter two categories contribute the largest effects in this case. The total relative systematic error is 10.3%, 1σ, and the total (random plus systematic) relative error is 12.0%, 1σ. Many facilities will need to carry out this type of analysis at a higher confidence level – 95% (2σ) or 99.7% (3σ) – to be responsive to the interests of criticality safety.

The relative random error in the total mass is only 6.2% because statistics were reasonable and the random error did not inflate from attenuation corrections at these deposit thicknesses, which exceed maximum thickness at 186 keV but not at 1001 keV. Shorter count times, fewer measurements or comparable 1001-keV measurements of thinner or thicker deposits than these can increase the relative random error in the total mass to equal or exceed the systematic error.

Table IX.5 includes results for only eight systematic error terms. Some of these are small enough to be omitted. An example is the uncertainty in the ^{235}U enrichment for these measurements of ^{238}U at 1001 keV. The variation in the ^{238}U that corresponds to the 10% relative uncertainty in ^{235}U enrichment given in Table IX.5 is negligible. If measurements were performed at 186 keV, however, the contribution from this effect would be large. The following ten terms contribute to systematic effects on portable gamma-ray measurements of holdup: 1) isotopic enrichment, 2) composition of deposit or value of μ, 3) deposit width, 4) measurement distance or detector positioning, 5) equipment attenuation/thickness, 6) total equipment dimension, 7) calibration uncertainty (see discussion below), 8) self-attenuation model, 9) deposit distribution (see Section IX.9 on evaluating complex systematic effects), and 10) room background. Neither term 9) nor 10) was included in Table IX.5. The large number of measurements performed on this duct

contributes to minimizing the effects of deposit distribution (9) on total deposit mass. Large LEU deposits and the specific location of this duct (periphery of process area where room background is low) minimize the systematic effects of room background (10). Neglecting the systematics of 1001-keV room background is unusual because it so readily penetrates detector shielding.

Table IX.5
Numerical Evaluation of Systematic Error in Total U Mass for 1001-keV Measurements of LEU

Parameter	Type	Best Value	Units	Best Value - 1σ	Best Value + 1σ	Measured Uranium Mass (kg) (- 1σ)	Best	(+ 1σ)	Relative Systemat. Error
^{235}U Enrichment	Depos	2.7%		2.4%	3.0%	182.7	**183.4**	184.0	0.3%
$\mu = \mu_{NORM}$	Depos	0.0753	cm^2/g		0.0838		**183.4**	188.0	2.5%
Deposit Width w	Geom	8	cm	7		186.0	**183.4**		1.4%
Meas. Distance r	Geom	42	cm	41	43	178.8	**183.4**	188.0	2.5%
Equip. Thickness t	Equip	0.5	cm	0.45	0.55	178.3	**183.4**	188.6	2.8%
Equip. Length L_{TOT}	Equip	7400	cm	7300	7500	180.9	**183.4**	185.9	1.3%
Calib. Constant, K_L	Calib	0.382	g×s/cm^2	0.363	0.401	172.4	**183.4**	194.6	6.1%
Deposit Atten. Model	Model	$F = \pi/4$			$F = 1$		**183.4**	195.5	6.6%

Total Relative Systematic Error = 10.3%
Total Relative Random Error = 6.2%
Total Relative Error = 12.0%

Although some parameters may remain relatively constant from one measurement campaign to the next, systematic effects can still vary. An example is the systematic uncertainty in the holdup calibration constant. Influenced by such effects as gain drift, the calibration constant can depend on temperature. The calibration can also be influenced by systematic radiological effects causing discrete interferences in some campaigns and not others. Cleanouts may cause both the width parameter w and the corresponding systematic effects to vary. The *best* value for w in Table IX.5 is that equal to the inner diameter of the equipment because the measurements were performed when deposits were large. Therefore, no positive variation from the *best* value is indicated for this parameter, which may not be the case after a cleanout. Instances in which nearly all analysis parameters and the associated systematic effects would change from one campaign to the next include an analysis transition from 1001 keV to 186 keV following a cleanout.

Estimating the systematic error in holdup for extended process equipment that is measured using both 1001 and 186 keV gamma rays is more complex than the simple numerical process described above. Subdividing the equipment according to the measurement energy would be necessary for purposes of analysis. Analysis results and uncertainties (random and systematic) for holdup mass in these equipment subdivisions would be recombined for purposes of reporting mass. The number of such subdivisions and their boundaries would vary from one measurement campaign to the next as deposits become thicker or cleanouts occur. Plans that include mixing analysis energies for quantifying holdup in extended equipment require automated analysis designed with significant enhancements in bookkeeping, despite the use of analytical and numerical methods that are common to those for single energy analysis.

Including numerical evaluations of systematic effects into the error analysis is straightforward with spreadsheet automation of the generalized-geometry analysis of holdup because the

multiple parameters used by the analysis are readily accessible for variation. These numerical approaches will be difficult to implement when a parameter database supports the analysis.

IX.9. Monte Carlo Evaluation of Complex Systematic Effects

Determining the realistic systematic variation of many individual parameters that influence the analysis result of portable holdup measurements is straightforward for many types of equipment. The effects tabulated in Table IX.5 (columns 5 and 6) for the cylindrical vacuum line are examples. The use of uniform spacing for the large number of measurements (73) of a nonuniform distribution such as that represented by the vacuum line greatly reduces the effects of variable deposit uniformity, which was excluded in this case but would also need to be evaluated if very few measurements were performed. The systematic effects of departure from the assumption of uniform deposit thickness can be can be difficult to quantify in some cases.

Because a nonuniform deposit distribution in the same extended vacuum line measured at only one position rather than 73 departs in a nonquantifiable way from the calibration assumption of uniformity, the magnitude of the systematic effect in a realistic range of nonuniformity must be determined as part of the systematic error in the measurement. This is complex because two effects dominate. One is the nonuniformity in the field of view of the single measurement. The second is the nonuniformity over the full 73-meter length. The complexity can be reduced by treating the two as separate and independent systematic effects using realistic assumptions about the range of deposit thickness in the particular vacuum line. It is not always possible to reduce a complex systematic effect of deposit distribution to multiple simple effects. The use of numerical techniques such as Monte Carlo can determine the complex effects in such cases. An example is taken from measurements of converters used to enrich uranium as UF_6 in gaseous diffusion.

The converter is an example of bulk processing equipment with internal deposits of variable uniformity. Variation of deposit uniformity in the axial dimension of the large cylindrical vessel can be addressed by performing gamma measurements at multiple longitudinal positions along the converter. Variations in radial uniformity – such that deposits might be uniform throughout the volume or more concentrated toward the center or more concentrated toward the surface of the cylindrical shell – that cannot be addressed by measurements must be included as systematic part of the systematic uncertainty. The variation in detector response to gammas as a function of the radial distribution of deposits from the converter is influenced by both geometry (solid angle) and attenuation by the internal equipment within the converter vessel. These cannot be evaluated independently because both are correlated with the same radial deposit distribution.

Three distributions of a fixed ^{235}U deposit mass were modeled along with detectors (both gamma and neutron detectors were used to measure the converters) and the converter.[71] Monte Carlo simulations determined the gamma and neutron responses to each of three deposit distributions illustrated in Figure IX.3. Table IX.6 gives the simulated relative response for the gamma and neutron detectors. The radially nonuniform deposit surrounding the longitudinal axis of the converter, Figure IX.3a ("axial" model), gives the smallest simulated gamma and neutron response to a given mass of ^{235}U. The simulated response to the deposit distributed uniformly throughout the converter volume, Figure IX.3b ("volume" model), is greater for both gamma and neutron, and the simulated response to the deposit distributed near the inner surface of the containment vessel, Figure IX.3c ("shell"), is greatest for both. The simulated responses are normalized to those for the deposit distributed uniformly throughout the converter volume.

Table IX.6. Monte Carlo Simulation of Complex Systematic Effects of Deposit Distribution on Gamma and Neutron Response for Converters

Response Ratio (to "Volume" Response)	Neutron	% Syst. Effect	Gamma	% Syst. Effect
"Axial"/ "Volume"	0.86	–14%	0.38	–62%
"Shell"/"Volume"	1.18	+18%	2.23	+123%

The relative neutron detector response varies moderately (+18% and –14% for "shell" and "axial" compared to "volume" distribution) while the corresponding relative gamma detector response varies greatly (+123% and –62%). Assuming that the neutron response is influenced only by geometry and not at all by the process equipment, the conclusion is that the systematic effects on the gamma response are dominated by attenuation because the effect of radial deposit distribution is so much greater. Gamma and neutron measurements of these converters reinforce the validity of the Monte Carlo simulations.[67] Unlike the validation of the gamma holdup measurements achieved by the neutron results shown in Figure VI.3, these Monte Carlo results discourage gamma measurements of holdup in converters when neutron measurements are feasible and emphasize the need to evaluate the systematic effects of the deposit distribution for either type of measurement. Monte Carlo simulations are recommended when systematic effects like those resulting from variations in deposit distribution are complex (as in this case) and large.

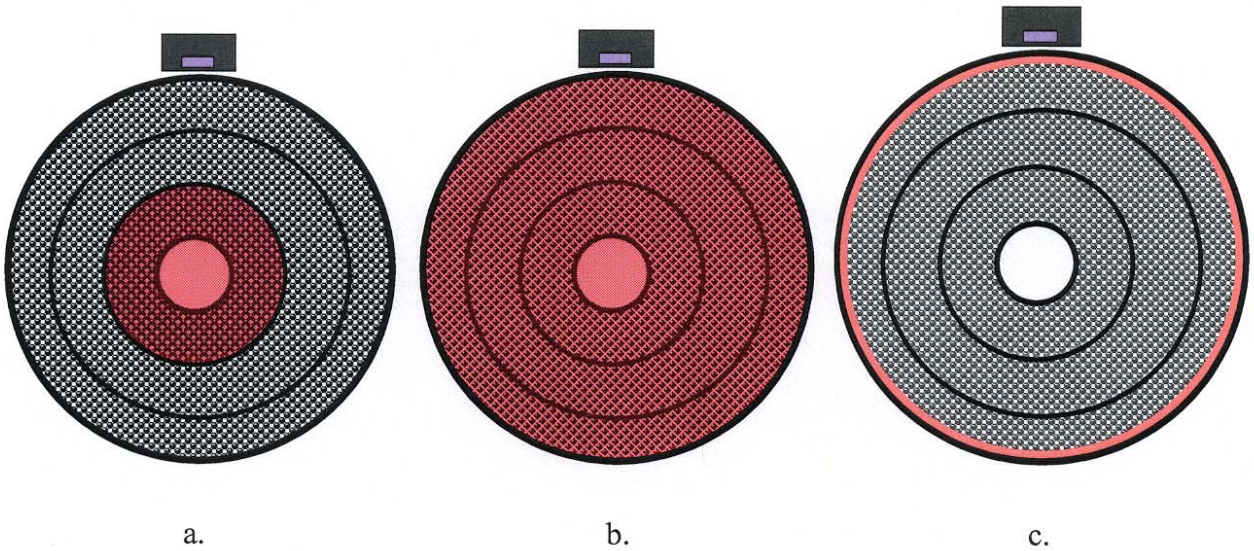

Figure IX.3. Three sketches of the transverse cross section of a converter show the a) "axial", b) "volume", and c) "shell" models for radial distribution of uranium within the converter. Red shading indicates the uranium deposit. The gamma and neutron detectors and their positions are indicated by small and large rectangles, respectively, at the top of each sketch.

IX.10. Automation of Measurements and Analysis

Automation of holdup measurements includes automating both measurements and analysis. These two functions are easy to consider separately because the ideal processor for control of

data acquisition and related functions is a palm-size unit that would not be practical for analysis for reasons of size and compatible operating systems.

The following list summarizes the benefits of automating the acquisition of holdup data.

- The tenfold decrease in t_d, the time between measurements, corresponds to a tenfold increase in the number of measurements as given by Equation (71) below.
- All gamma-ray spectrum files are saved.
- Comprehensive measurement control applies to every measurement.
- Electronically sensed measurement location is saved with measurement data.
- Active gain-drift compensation can apply to every measurement.

These benefits of automating the acquisition of data are substantial and compelling. Automation of data acquisition as described above is fully implemented, except for gain-drift compensation, for several modern portable multichannel analyzers using bar codes to sense/identify measurement location.[13] Developing the automation of the data acquisition is by far the most costly aspect of automation. It is also uniquely vulnerable to obsolescence because the software is programmed to control specific portable electronics from specific software platforms designed for handheld portable PCs. Useful lifetimes of these portable technologies are short.

The simplicity of the generalized approach is well suited to automation of the analysis because algorithms for the limited geometric models can be implemented with very few parameters. Spreadsheet automation fully supports the analysis described in Section VIII.[24, 25, 49] Software reliant in an extensive database for all parameters used for setup and analysis also fully supports the analysis described in Section VIII.[13] Both database and spreadsheet approaches offer unique advantages.

Spreadsheet implementation does not offer the following unique benefits of the database analysis.

- Analysis time is minimum because all relevant parameters are in the data base.
- Analysis is self-consistent from one campaign to the next.
- The database implements the archiving (Section XI) and enforces effective cataloging.
- Users with less expertise than that required for spreadsheet analysis can do the analysis.

Setup and maintenance of the database is costly in time and requires an expert in measurements who is also thoroughly familiar with the process and operations. This argues for its use for ongoing, routine measurement campaigns in a large facility with many hundreds or thousands of measurement locations.

However, the spreadsheet uniquely and readily supports the following:

- First-time measurements without extra overhead.
- Month-to-month changes in the analysis approach.
- Month-to-month changes in the measurement configuration.
- Optimization of the analysis approach.
- Numerical evaluation of the systematic uncertainty in holdup.

Spreadsheet users must have the expertise in measurements and be familiar with the process and operations.

The cost to automate the analysis of holdup measurement data is low compared with the cost to automate acquisition of data. Sites with a database system fully implemented can afford to implement the full spreadsheet capability as well for maximum flexibility to explore analysis alternatives and ultimately optimize the spreadsheet implementation. Evaluation of systematic uncertainty is an essential to certification of any measurement program. The numerical evaluation described above is the simplest approach that can keep up with the frequent changes that influence the systematic effects on holdup measurements. Implementing the numerical approach for evaluation of systematic uncertainty is a strong argument in favor of maintaining the spreadsheet capability for analysis of holdup measurement data.

X. PLANNING MEASUREMENTS, AND DETERMINING MEASUREMENT PARAMETERS

X.1. Dimensioned Sketches for Planning and Performing Measurements

Detailed knowledge by measurements personnel of the required scope of the measurements prior to performing measurements is an essential feature of a measurement campaign. Knowledge of the equipment dimensions and positions enables personnel to judge requirements such as the need to elevate detectors, the nominal standoff distance between detector and equipment, practical setup time between measurements, locations in which access is restricted, and areas that may be also accessible to measurements with Ge detectors. A dimensioned sketch of the full equipment layout is most important in planning the measurement locations. The sketch also allows measurements personnel to graphically mark the positions of the measurements, the number of which is limited by the total allocated time, time between measurements and the practical count time (refer to X.4). Few measurement needs, including those performed for D&D, are complete after a single measurement campaign. Therefore, time dedicated to creating an electronic sketch or scanning an existing sketch to update with measurement positions in multiple campaigns is well spent.

A hard copy of the sketch marked with measurement locations becomes part of the tool kit used during measurements of holdup. It guides measurements personnel on the practical sequence of measurement locations, and provides a template onto which the actual measurement positions can be marked and the actual measurement distances labeled. Subsequent to performing measurements, the actual positions recorded at the time of the measurements can be incorporated into the electronic file. Including measurement distances in the electronic sketch is not practical, typically. However, these empirical parameters (the dimensioned coordinates of each measurement, standoff distance, and maximum width of the deposit) are essential to the analysis of the specific and total mass of holdup and must be incorporated into the electronic files that also contain the reduced spectral data for each measurement location. Each line (measurement position) of these data files also contains the position identification recorded on the sketch.

Figures X.1 a) and X.I b) are examples of dimensioned sketches. These describe subbasement and basement sections (respectively) of belowground exhaust ductwork that serves one wing of a large multimission nuclear-materials research facility. The sketches were created for and used by several measurement teams tasked to quantify holdup in the equipment.[24, 25] The equipment consists of two parallel and identical main trunks (T1 and T2) with unique arms from individual laboratory locations, a cross-trunk section (TX), and large filters at the downstream end of each main line. Blue and black numerals/letters identify each measurement in three facility areas (filter-tower, 5034 and 5023) and mark measurements performed by NaI alone and by both NaI and Ge (respectively) at the approximate indicated positions. Overall equipment dimensions are labeled on the sketch, which also reveals a downstream increase in main-trunk diameter – by a factor of two, in this case – typical of this type of equipment. Only the approximate duct width is indicated at several locations. Both this dimension and a dimensioned linear coordinate (centimeter distance from the upstream extreme of the duct) are logged at the time of measurement and recorded in the electronic file of reduced spectral data. (See Section XI.1.) The Figure X.1.a) sketch also identifies a solid-filter arm of this exhaust equipment (SF-5) that is represented elsewhere with its own dimensioned sketch, including measurement locations.

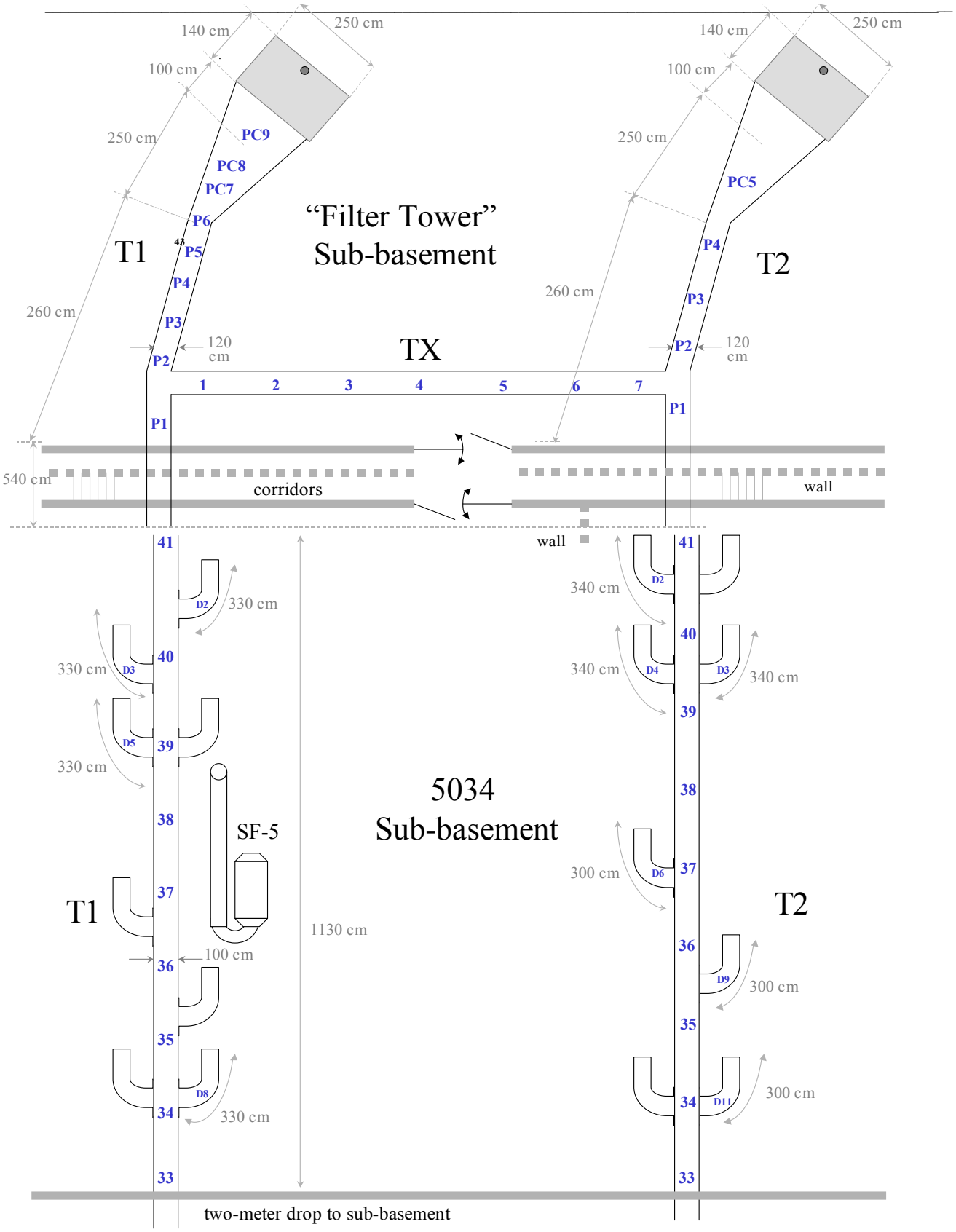

Figure X.1.a). Dimensioned sketch, not to scale, of subbasement (downstream) portion of exhaust ductwork in one wing of a large multimission nuclear-materials research facility. Blue numerals/letters indicate measurements performed with NaI at these positions. The associated solids filter (SF-5) is sketched separately.

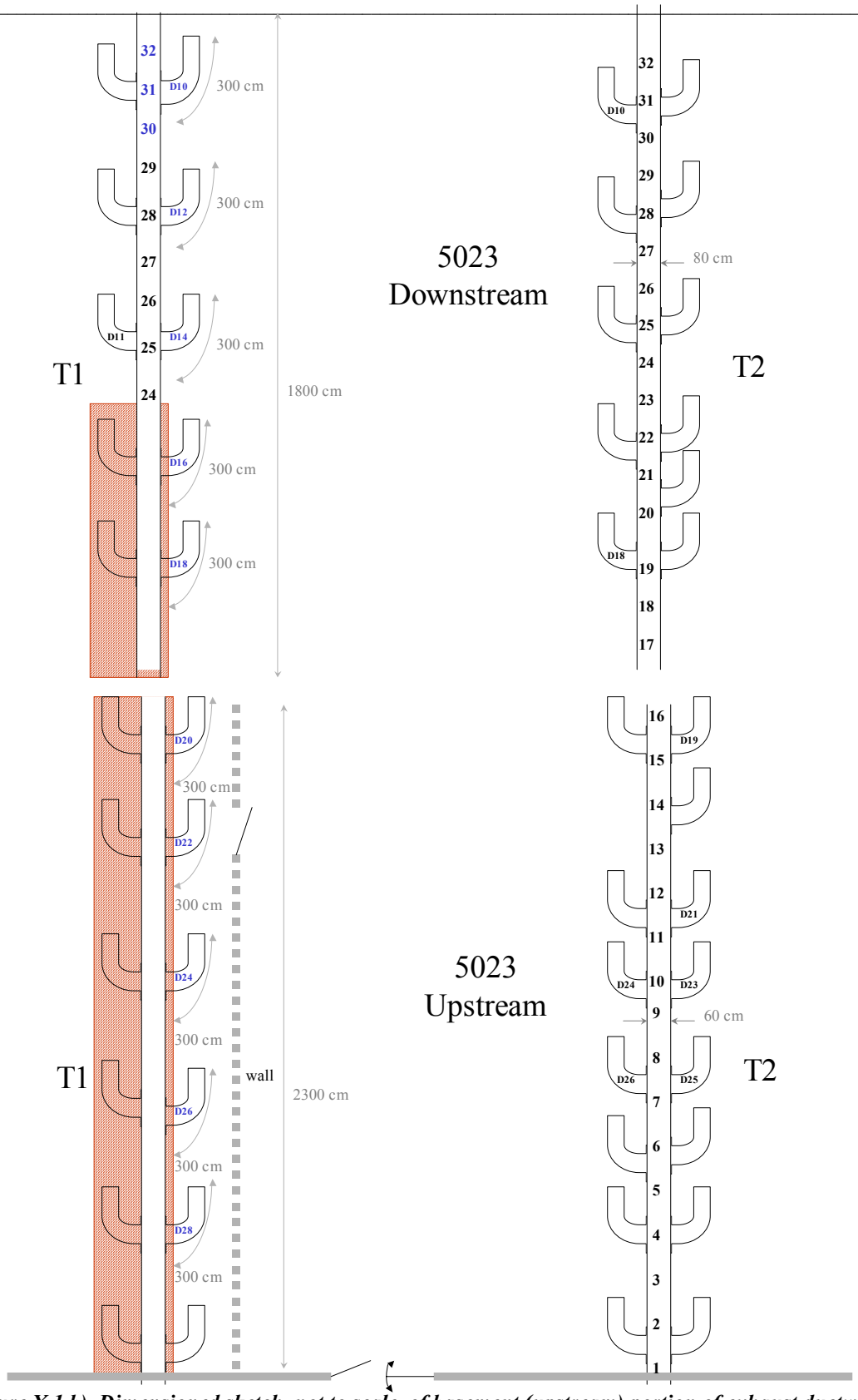

Figure X.1.b). Dimensioned sketch, not to scale, of basement (upstream) portion of exhaust ductwork from Figure X.1.a. Blue numerals/letters mark measurements performed by NaI at these positions, and black indicates that both NaI and Ge measurements were performed. The red-shaded areas were not accessible for measurement.

Engineering floor plans of the facility and equipment drawings can assist in creating the dimensioned sketches such as those in Figure X.1 or providing dimension details for such figures. Sometimes the engineering drawings can be scanned and labeled to create the required, electronic dimensioned sketch. However, engineering drawings may be outdated, especially for older facilities. Engineering drawings also lack indications of access status, such as the restricted areas indicated by the red diagonal shading in Figure X.1.b. Therefore, a walk-down and empirical assessment of the relevant equipment and process areas should precede completion of dimensioned sketches.

X.2. Equipment Walk-down, Radiation Survey, Determining Deposit Width *w*

The equipment walk-down is performed in advance of holdup measurements. Walk-downs provide knowledge that leads to a more efficient, effective and safe measurement campaign. Because holdup measurements may be scheduled during operations, knowledge determined during the walk-down can also minimize impacts of measurements on operations, and *vice versa*.

Personnel essential for the walk-down include the scheduled measurements personnel and the NDA specialist who plans the holdup measurements and possibly analyzes the results. A process engineer, operations specialist and health physicist round out the essential personnel. A representative of each immediate customer interest (this would include accountability, safety and waste management for a facility under D&D) might complement this group in that customer presence helps to align customer requests with process realities, but a subsequent planning meeting that includes customers is an alternative.

The equipment walk-down makes measurement personnel aware of operations and any protocols associated with the use of portable gamma spectroscopy equipment to measure holdup deposits. It reveals postings of radiation dose, which might be hand-noted on sketches during the walk-down as these may suggest areas in which either holdup deposits or room backgrounds are large. Measurement personnel should attempt to understand the source of high postings as part of the planning process and for the sake of ALARA. Understanding of the chemical process that might be gained during a walk-down can also be useful. An example is that chemical extractions that concentrate certain elements can also concentrate radionuclides: those of interest as well as potential interferences.

A walk-down of the process equipment reveals how to mechanically and directionally approach the equipment in order to perform measurements. The equipment walk-down supports the completion of dimensioned sketch that is used to plan and perform holdup measurements. Information obtained during the walk-down is used to update the preliminary sketches developed from engineering drawings. Modifications to the actual process equipment are common changes to the sketches that are indicated during the walk-down. Additional installations not directly associated with operation of the process of interest can impact the measurements in other ways. Examples of such impacts are unexpected backgrounds (from interim storage location established near the process of interest), attenuation (in the case of personnel shielding bolted onto glove box surfaces that severely reduces the gamma radiation signal), mechanical barriers (caused by the presence of large test equipment modules that limit personnel access for measurements), or contamination barriers (when no personnel access is permitted in the case of a spill). Illustrating the impacts of additional installations, contamination, and radiation as well as

actual changes in the process equipment in the sketches is recommended to assist in planning and performing measurements.

The walk-down may be used to verify equipment dimensions specified in the engineering drawings and to determine those dimensions not noted in the drawings. The specific dimensions required for each measurement are the thickness and material of the equipment and the width of the internal process cavity. The use of an ultrasonic thickness gauge is recommended to verify equipment thickness. Laser distance meters or tape measures serve to determine the overall equipment dimensions such as the linear dimension of a vacuum line, or the length, width, and depth of a glove box. They also serve to determine the distance to the nearby equipment in which additional radiological sources may be contained.

Determining or verifying equipment dimensions during the walk-down prior to the measurement campaign saves measurement time. Accumulating this information for the process equipment in advance of the measurement campaign has the additional advantage that the measurement geometry – position on the duct (for example), spacing between successive measurement positions, and distance between detector and duct – can be provided to the measurements personnel before the campaign begins. Sections X.3-X.5 discuss how to determine the parameters of the measurement geometry and to specify count time.

The walk-down is an opportunity to photograph the process equipment prior to performing measurements. Photographic documentation provides valuable planning assistance in helping customers to formulate realistic requirements, guiding measurement personnel to selected measurement locations, and assisting with interpretations in the analysis phase.

The walk-down is also an opportunity to use radiation survey meters to assess distributions of deposit materials and locate sources of room background. It is essential to always estimate $\boldsymbol{w}$, as described in Sections VIII.1-VIII.3.3, VIII.4.1-VIII.4.3, and especially VIII.6.1-VIII.6.4. The best empirical estimate of the deposit width $\boldsymbol{w}$ is important to the unbiased analysis of holdup measurements of point or line deposits. Some general guidance for estimating $\boldsymbol{w}$ follows.

- The upper limit on $\boldsymbol{w}$ is always the inner dimension (width) of process equipment that is measured as a point or line.
- Assume that $\boldsymbol{w}$ is the equipment inner dimension for vertical ducts or pipes/tanks that are measured as lines.
- Assume that $\boldsymbol{w}$ may be smaller than the equipment inner dimension for horizontal ducts or horizontal pipes/tanks in particular that are measured as lines.

Health physics survey meters can help determine $\boldsymbol{w}$ for large equipment. Radiation survey meters can be useful in obtaining such an estimate. The use of radiation survey meters during the measurements of holdup slows the measurement process. Performing radiation survey measurements during the walk-down also affords the advantage of the presence of an engineer and an operations specialist who may supplement observations from the survey measurements with insights on the process and materials.

The relatively large number of personnel and variety of activities involved in the walk-down attest to the importance of performing this activity prior to finalizing the measurement plan. A planning meeting following the walk-down can be a forum in which relevant information, including that obtained in the walk-down, is presented to all interests (those of operations, measurements personnel, and customers) by NDA specialists who establish the measurement plan. Specific customer requests can be made and discussed at this time. The NDA specialist

updates the dimensioned sketch with current dimensions of the process equipment determined during the walk-down and modifies the measurement positions based on the updated sketch, customer input and information on access restrictions, also obtained during the walk-down. The additional data gathered during the walk-down (deposit width w, deposit distributions, and sources of room background) can contribute to the determination of the measurement distance r and spacing l. (Refer to X.3 and X.4.)

X.3. Use Width/Spacing of Equipment to Bound Measurement Distance *r*

The distance r is the distance between the detector/crystal and the process deposit, analogous to the dimension r_0 used in the calibration expressions (employed throughout Section VIII). The deposit location varies according to equipment type and purpose. It is reasonable to assume that deposits are at the bottom of horizontal ducts/piping and at the center of vertical ducts/piping.

The components r (and r_0) are described in Section IX.1 and Tables IX.1 and IX.2. Note that r is the sum of the standoff distance established by the positioning device – such as the meter stick mounted on the detector collimator (Figure VII.8) – and several additional distance components specific to the process equipment design, detector design, crystal type and gamma-ray energy. Furthermore, if holdup measurements apply to equipment/surfaces other than that in contact with the mechanical positioning device (measurements of deposits within equipment inside a glove box or holdup in a large horizontal duct from the top looking down), a significant additional displacement distance of the deposit must be included in the sum that determines r. Because the practical measurement distance r can be no less than that determined by the closest proximity of the detector to the deposit permitted by the containment equipment, optimizing r as described below will not be possible when this distance is already larger than the prescription.

Because a goal of holdup measurements is to measure as much as possible of the holdup deposits, the practical holdup measurement distance r_P is chosen to give the widest field of view for measurements. This requires defining the largest practical measurement distance, which is constrained in most cases by two conditions:

- The proximity of sources in neighboring equipment.
- The ratio of signal to background.

Unless sources in the neighboring equipment or the equipment itself can be relocated, the distance d between sources in the neighboring equipment and the holdup measurement location is a well-defined parameter at each measurement location. We define d for convenience as the projected distance onto the axis or plane of the (line or area, respectively) holdup deposit. Figure VIII.3 represents the radial response measured for a collimated detector at the calibration distance r_0 of 40 cm. This empirical form is a straightforward guide to the determination of r_P. The guidance is that the deposits in neighboring equipment must be outside the field of view of the detector. The field of view measured at the time of calibration (when $r = r_0$) is the full width FW_0, which corresponds to 80 cm in Figure VIII.3. The user must scale the measurement distance so that one half of the correspondingly scaled full width does not exceed the projected distance d of the neighboring source. The resulting scaling formula for the largest practical measurement distance is

$$r_P \leq (r_0 \bullet d) / (\tfrac{1}{2} FW_0) . \qquad (68)$$

The largest practical measurement distance determined using the detector represented by the data in Figure VIII.3 is one meter based on this formula if a neighboring source is located at a projected distance ***d*** of one meter from the deposit. Note that the equipment surface defines the axis or plane for a line or area deposit. The user is constrained to align the detector axis perpendicular to this axis or plane to avoid bias from noncompliance with the geometric model. Rotating the detector axis about the line to avoid viewing a source in neighboring equipment is often possible with a line source. Moving to the opposite side of an area deposit is less often practical.

Background from the room may force the use of smaller measurement distances than that defined by Equation (68). Measurements of ^{235}U in HEU deposits are most immune to this problem because so little shielding is needed to eliminate 186-keV gammas from room background. (Refer to VII.1.) The average measurement distance used in campaigns to determine ^{239}Pu holdup tends to be significantly smaller that that for a comparable ^{235}U campaign because the 414-keV gamma ray is so much more penetrating of the same shielding. Measurements of LEU in which the deposit thickness determines whether the analysis is based on 1001 or 186 keV are constrained to comply with shorter distances to allow sufficient precision at 1001 keV should the deposit thickness force analysis at the higher energy.

Because room background tends to enforce reducing measurement distance, it is important to realize that there is also a limit for the smallest practical measurement distance. The limit is determined by the potential for the model governing the finite-source correction to fail as the finite deposit width becomes very large compared to the full width ***FW*** of the field of view. Figure VIII.9 illustrates this with a comparison between the Gaussian model of the radial response suggested for cylindrically collimated detectors and the actual response measured with 414-keV gammas for such detectors, particularly at larger displacements from the detector axis. The relative effect at large displacements is more pronounced for lower gamma-ray energies. A rule of thumb is to limit the measurement distance such that the ***FW.5M*** always exceeds the deposit width. The conservative statement of this rule is that the ***FW.5M*** always exceeds the width of the equipment cavity (duct inner diameter, *etc.*), ***D***. Scaling the measurement distance according to this rule of thumb leads to the following formula for the smallest practical measurement distance:

$$r_P \geq (r_0 \bullet D) / (FW.5M_0) . \qquad (69)$$

where $\boldsymbol{FW.5M_0}$ is the ***FW.5M*** determined at the time of calibration (22 cm in Figure VIII.3, when $\boldsymbol{r} = \boldsymbol{r_0}$ = 40 cm). The smallest practical measurement distance using the detector represented by the data in Figure VIII.3 is 55 cm based on this formula if the inner diameter ***D*** of the measured duct is 30 cm.

X.4. Determine Measurement Spacing *l* and Count Time *t*

Another goal of holdup measurements is for the measurements to achieve uniform sampling of the equipment that contains the holdup. Uniform sampling refers to measurements performed at successive intervals ***l*** spaced so that all positions on the equipment surface have been counted with the same total efficiency and time. Uniform sampling avoids bias that results when large deposits fall at the center (high bias) or edge (low bias) of the field of view of the randomly positioned detector. Uniform sampling is an ideal that requires more measurements than time

permits for most holdup measurement campaigns, even if the count time ***t*** is minimized. Figure X.2 shows that the spacing between adjacent measurements performed with a detector whose radial response is Gaussian-shaped must be 70% of the detector's ***FW.5M*** for the selected measurement distance in order to achieve uniform sampling. Approaching the ideal of uniform sampling requires many short counts rather than few long counts. However, similar to choosing the measurement distance ***r***, practical considerations limit the choice of the shortest practical count time, t_P.

The first practical constraint is the total time ***T*** that is available for measurements. A second practical constraint is the commitment to a duty factor (ratio of time spent counting to total time spent on measurements) of no less than 50%. The dead time (time between measurements when no counting is in progress) t_d can be specified for any measurement campaign performed with specified equipment. An example is equipment measured as a line with a total equipment dimension L_{TOT}. The shortest practical count time defined by the minimum duty factor is

$$t_P = t_d \tag{70}$$

and the corresponding measurement spacing is

$$l = L_{TOT} \bullet 2t_P / T \,. \tag{71}$$

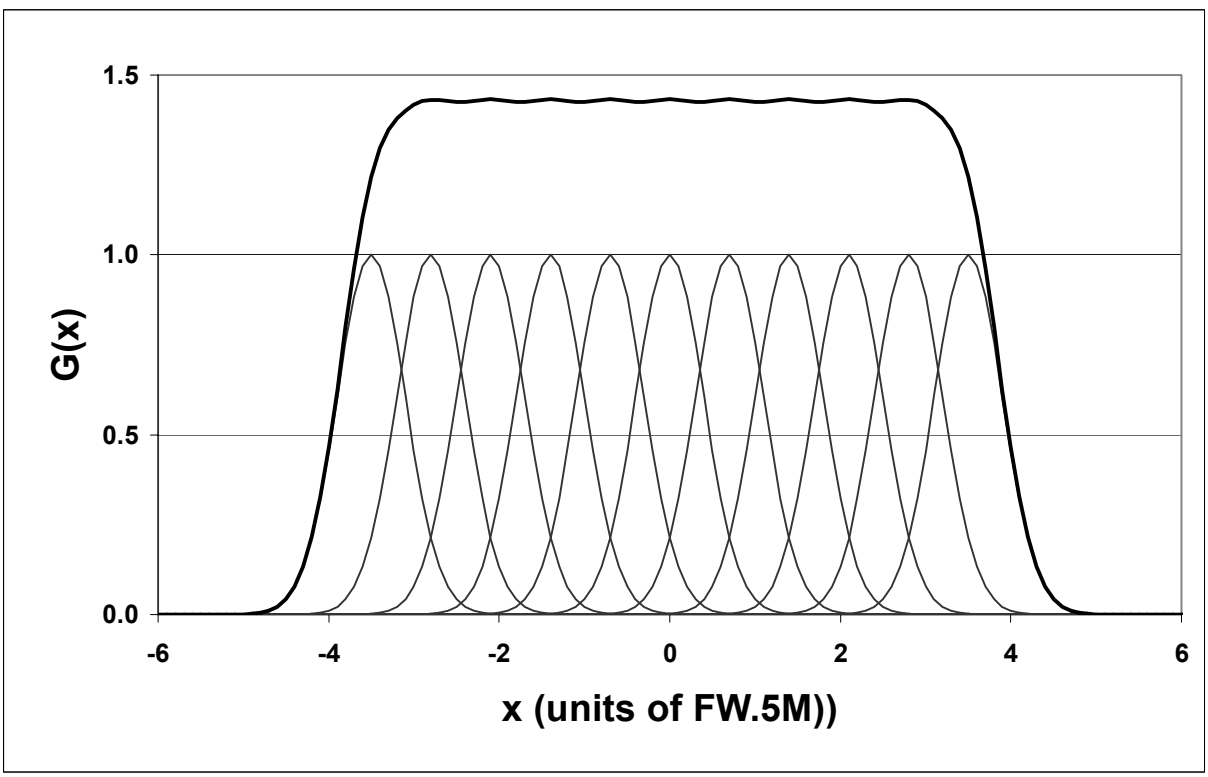

Figure X.2. Eleven normalized Gaussians displaced successively by 70% of one FW.5M sum to a uniform distribution (dark curve) between the first and last Gaussian.

Note that each and every measurement position may require two measurements, one of the deposit and one of room background. This is normally the case when higher energy gammas are used (refer to Section IX.3). If the two counts are performed in rapid succession, as usual, the quantity t_P can be considered the combined time for the pair of counts.

Measurement experience in the laboratory and in the plant shows that successive spacing such as that described in Figure X.2 achieves good results with distributed deposits of known total holdup mass.[45] However, still more experience with measurements performed at practical, constant intervals but much more widely than the ideal spacing shown in Figure X.2 gives good results overall. The reason is that constant spacing randomly samples deposits so that both high and low biases in holdup mass may be incurred for the relatively short intervals of equipment dimension between individual measurement positions, but the overall result from the numerous measurements of the extended equipment tends to be unbiased.[3, 9, 14, 19-21, 48] Positive biases will appear, in fact, if users seek out the hot spots, always include these in the array of measurement positions that may otherwise be assigned at random (with uniform spacing), and obtain the total deposit mass based on an average of results for such an array of measurements. The good results of measurement experience with constant spacing but rarely uniform sampling, and the practical constraint of limited time combine to argue strongly for choosing the shortest practical count time t_P and constant measurement spacing l as described above.

X.5. Mark/Tag Measurement Locations, Define Coordinates

Routine measurements of holdup demand cost-effective approaches. It is essential for cost-effectiveness that the time-consuming setup and planning activities for the first holdup measurement campaign, as described in X.1 and X.2, be an investment for all successive measurement campaigns, particularly for a facility with expectations of a long operating lifetime. Successive measurement campaigns can proceed with minimum overhead costs for planning and setup if the measurement parameters are those used in the original campaign and the positions are also the same or else a subset of the complete set defined in the original campaign. Furthermore, monitoring holdup deposits in time provides data to support the validation of models of accumulation of deposits for defined operational periods, process throughput, *etc*. The success of such models can reduce future measurement needs and further reduce costs. Monitoring holdup requires systematic remeasurement of holdup at the same locations measured previously. Therefore, very careful and detailed planning invested in the original campaign can pave the way for a economically sustainable program of holdup measurements.

The recommended approach for the first campaign is to define constraints such as total allotted measurement time T liberally to allow for a larger number of measurement positions spaced more closely. Similarly, estimating the minimum time between measurements t_d based on the assumption that the acquisition of future holdup measurement data will be automated gives a corresponding minimum in spacing between measurements. Marking measurement positions accordingly is an assurance that measurements performed in the future represent the equivalent or a subset of the original plan, so that the costs to plan and set up apply to the future.

Criteria that apply to the marking of measurement locations include readability, logical sequencing, robustness of tag media, and verifiability. Tags interpreted by radio frequency as opposed to optically scanned labels are more readable, robust, and verifiable technology options that will save measurement time, last longer, and adapt to safeguards verification.

Implementation of such technology is under consideration.[49] Activities under D&D, and sometimes even routine maintenance activities, add complexity to maintaining labels and markings as equipment – such as glove box shielding – is removed, replaced, or cleaned.

The coordinates of the holdup measurement locations must be dimensioned in order to quantify deposit mass for a defined portion of process equipment using the measured results for specific mass. The following recommendations apply to a system of coordinates that supports quantifying holdup mass and mapping deposits spatially in a manner that allows the map to be interpreted quantitatively by visual inspection or electronically. The recommendations also allow users of the holdup data to interpret accumulation sequences because successive coordinates are contiguous. Such interpretation supports the design of the measurement plan for future campaigns, in which it may not be necessary to perform measurements at every identified deposit location. (Refer to Section XI.)

- Assign coordinates according to displacement along the equipment, despite curves and bends in ducts and pipes, for example. The notation below uses ***l*** for the line-deposit coordinate and ***x***, ***y*** for the area deposit coordinates.
- Assign coordinates in linear dimensions. Use, for example, cm for ***l*** (line deposits) and cm_1,cm_2 for ***x,y*** (area deposits).
- Choose the most upstream location on the main trunk as the coordinate origin of equipment measured along a process flow axis.
- Increase coordinate values, both on the main trunk as well as on arms that feed it, in the downstream direction of the process flow.
- Choose as coordinate origin the lower-left position/corner (which may not be a measurement point) of equipment, such as a glove box surface, that is measured as a two-dimensional area.
- Where branched equipment intersects at a juncture, use common coordinates at the position of intersection.
- Default to the main trunk of branched equipment in assigning the origin and common coordinates.

XI. IMPLEMENTING HOLDUP MEASUREMENTS

XI.1. Three "M"s of Implementation: Measurement, Mapping, Monitoring

Section IV describes demands by production, safeguards, safety, and waste-management interests for holdup data. Implementation of holdup measurements must respond to the combined interests with cost-effective approaches. Three "M"s – measurement, mapping, and monitoring – are the functional deliverables of a practical implementation scheme that satisfies combined interests in the mass and distribution of holdup.

Measurements of holdup deposits directly determine specific mass (mass per unit length or area for line or area deposits), as described in VIII. Empirical knowledge of specific mass is only possible for deposits less than the maximum thickness for the gamma rays used to measure holdup. Therefore, the specific mass results are of immediate interest to criticality safety, as discussed in VIII. Reporting to safety customers is discussed briefly in XI.5. However, customer interest in holdup measurements at the time of the measurements usually includes the mass of holdup in a particular portion of the equipment – such as an MBA during inventory, a specific leg of ventilation ductwork designated for cleanout, a specific piece of equipment scheduled for removal and placement in a waste crate, *etc*. The recommended approach for obtaining the mass is to average the multiple measurements of specific mass for a defined portion of the equipment and multiply the average by the equipment dimension (length or area, respectively).

Electronic archival of specific mass data and automation of analysis applied to this data allows prompt reanalysis to give the holdup mass in any portion of the process equipment that has been measured. The archiving of specific holdup mass data is also required for the spatial mapping of holdup deposits.

A map is a (graphic) description of the spatial distribution of holdup in the process equipment. A presentation format for the spatial distribution is most effective if unambiguous to interpretation by operations, safeguards, safety and waste-management interests. Mapping holdup mass involves a unique decision for each process area regarding the equipment dimension associated with each mapped mass. This obscures the information needed from the spatial map to determine such important information as average and maximum thickness of localized deposits, and eliminates detailed distribution information that resides in the direct measurement results. Therefore, the mapping of specific mass – rather than holdup mass – *vs*. linear position (one- or two-dimensional-coordinates, as described in Section IX.5) for each measurement location is recommended. Such information is essential for safety assessments, scheduling cleanouts, planning future measurements, and coordinating D&D.

Figure XI.1 is a map of the measured specific mass of uranium in a portion of the ventilation system of a low-enriched uranium facility.[49] The map is a plot *vs*. linear position along the ventilation ductwork. The figure shows the main line of this ventilation system fed by two arms with the exhaust from various locations in the process. Holdup measured in the arms and the main line is represented in separate plots organized vertically with a common position axis. The linear position on each arm at its juncture with the main line is the position on the main line at this juncture. Because the width of ventilation ductwork varies with location, the thickness of measured deposits with the same specific mass can differ. Therefore, the inferred deposit width $\boldsymbol{w}$ is also plotted *vs*. linear position on each map so that an assessment of deposit thickness (areal

density or mass per unit area) can be made visually. Mapping the spatial distribution of holdup can be aided by a database of equipment parameters (the linear measurement position and equipment dimension for each measurement location) linked to the archive of holdup measurement data.

First-time creation of a map of specific mass such as that shown in Figure XI.1 requires an initial investment in time to create the electronic tables of measurement locations for the main trunk and arms of this equipment. By including all measurement locations (even those identified but not measured) in the table when the file is created, the original map of specific mass also serves as the template for future measurement campaigns on this equipment. Only specific-mass data from subsequent measurement campaigns need be entered into this template.

Information useful to the planning of future measurement campaigns comes from maps of specific mass. The maps can reveal a distribution template that allows future measurements to be performed at fewer measurement locations. Deposits at these selected locations can also be monitored (measured over time).

The graphic result of monitoring is a plot of the specific mass at a selected position (determined from the spatial mapping) *vs*. time. Monitoring is a vehicle for predicting holdup. Similar to the mapping the spatial distribution of holdup, plotting the specific holdup mass for a selected position *vs*. time can also be aided by a database of equipment parameters linked to the archive of holdup measurement data.

XI.2. Archiving Data to Support Future Measurements

Each measurement of holdup at a specific location produces three categories of holdup measurement data:

- raw data, consisting of a gamma-ray spectrum.
- reduced data, including the ROI integrals and spectrum-quality parameters (peak widths, and centroids, and dead time).
- analyzed data, corresponding to the measured specific mass and uncertainty. The analyzed data can be interpreted to give holdup mass for a specified portion of the process.

Electronic storage permits unlimited archiving of holdup measurement data. This includes spectra – usually acquired in rapid succession with short count times – which place the greatest demands on memory. Saving spectra offers the option of reanalysis in the event of unexpected interferences or any changes in spectrum quality that occur undetected by routine measurement control. Avoidance of repeat measurements reduces costs, minimizes operator radiation dose, and supports the full dedication of available time to the scheduled measurements. Nonetheless, the manual saving of spectra is prohibitively costly in time. Therefore the benefits of saving spectra are not realized without automating the acquisition of holdup measurement data.

Archiving of reduced spectral data (ROI integrals, spectrum-quality parameters) is not essential if spectra are saved. However, the additional memory needed to save such information is too little to be a significant issue. Reanalysis involving modified parameters (for attenuation, calibration, equipment, deposits, *etc.*), alternative attenuation forms, alternative background treatment, or numerical estimation of uncertainty requires no change in the reduced spectral data.

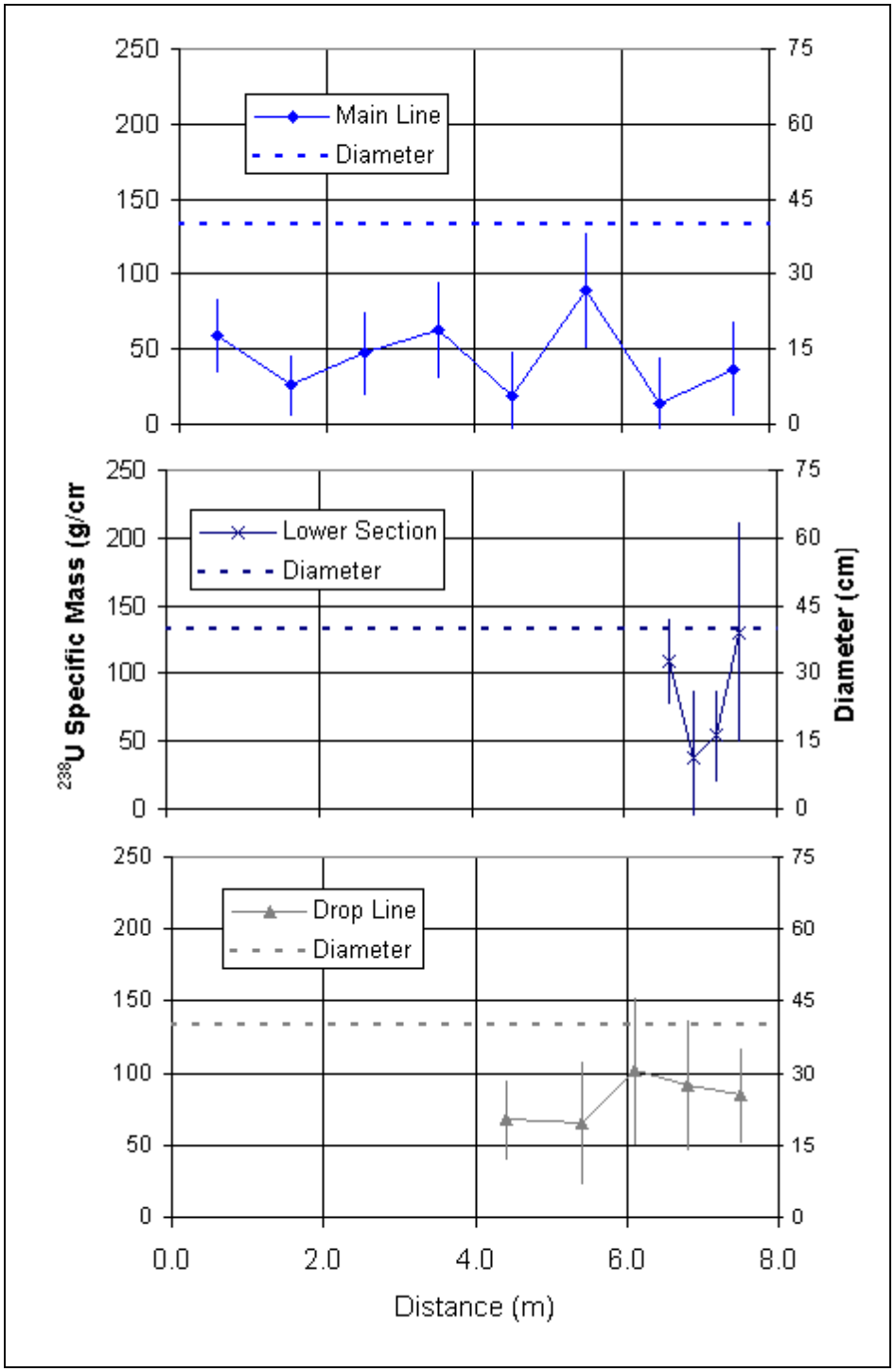

Figure X1.1. Measured specific mass of uranium is plotted vs. .linear position along part of the ventilation system of an LEU facility. Two arms (Lower Section and Drop Line) with exhaust from various process locations feed the Main Line of the system. Holdup measured in the arms and the Main Line is shown in separate plots with a common position axis. The linear position on each arm at its juncture with the Main Line is the position on the Main Line at this juncture. Because the width of ventilation ductwork varies with location, the thickness of measured deposits with the same specific mass can differ. Therefore, the width (diameter, in this case) of the equipment cavity is also plotted vs. linear position on each map for visual assessment of deposit thickness (areal density or mass per unit area). Distance increases in the direction of process flow.

Retrieving saved spectra to regenerate reduced spectral data for each reanalysis is costly in time, punctuating the benefits of archiving reduced spectral data. Automation – of the data-reduction and data-analysis functions in this case – allows these benefits to be realized.

Archiving of holdup measurement results for specific mass is also not essential if spectra are saved. Nonetheless, the frequent need to access holdup measurement results for mapping and monitoring, as described in XI.1, argues strongly in favor of automated archiving and retrieval of the holdup measurement results for specific mass.

The archiving of reports of holdup measurement results is important because a report typically provides the link between the holdup measurement data and the methods used to obtain it by referencing the methods in the reports.

The quantity of electronic archival data in all fields has exploded in recent decades because of the ability to digitize most types of media combined with an exponential increase in low-cost electronic storage capacity in the time period. Cataloging archives is an essential component to the useful retrieval of archival data. The electronic cataloging system for holdup data must support implementation needs (such as the three "M"s, section XI.1), respond to reporting needs described below (XI.3 and XI.4), and remain a robust resource through the inevitable transition – in both activities and oversight – from full operational status into extended shutdown periods and throughout D&D.

XI.3. Reporting for Communication within the Measurements Program

Holdup measurement results may be made available to the very personnel who schedule and perform holdup measurements. The first group, those who schedule the measurements, is covered in the following section. The second group, measurements personnel, requires a less formal report in that information is conveyed for the purpose of understanding the measurement issues for particular process equipment or types of process equipment.

Holdup measurements staff benefit most from maps of specific holdup mass in generic categories of process equipment. The following list of examples indicates the relevance of existing maps to measurements that may be scheduled in analogous process equipment.

- The spatial map of specific holdup mass in ventilation ductwork may indicate a highly uniform distribution in some sections and nonuniform distributions in others. The associated process activity may determine the degree of uniformity. Maps of specific deposit mass *vs*. position in such ducts can develop intuition among measurement personnel on when to measure conservatively (at short intervals) and when coarser sampling may suffice.
- Emptied solution tanks may indicate a monotonic decrease specific deposit mass *vs*. height. Such systematics may serve to reduce the number of measurement locations for similar tanks.
- Maps of the specific mass of holdup in wet vacuum lines may indicate dense deposits, suggesting measurements with longer count times (to minimize statistical ambiguity on the possibility that thickness exceeds the maximum correctable) for similar equipment.
- The two-dimensional map off specific mass on glove box surfaces can suggest tiered approaches to such measurements that concentrate the available measurement time on locations in which deposits are unpredictable.

XI.4. Reporting for Accountability, Safeguards Closeout, Waste Compliance

Many organizations call for reports of current and archived holdup measurement data organized according to the needs of each customer, as described below. The reports require, in common, references to documentation of the method, appropriate controls, relevant verification of the technique that determines mass, and sources and propagation of error terms for holdup.

The most detailed holdup reporting is that of the distribution of holdup mass in an operating facility. It includes the maps of specific holdup mass (Figure XI.1) and/or the graphs that monitor deposits over time. Errors in individual measurement results are also reported. Such detailed reports benefit the operating groups that plan and execute holdup measurements and cleanouts. Such reports are also of interest to the safety/health/environment organizations that place demands on the schedules for measurements and cleanouts. Reports utilizing detailed maps typically call for the most recent measurement results while those that use monitoring data call upon results from the archives. Most other interests in holdup measurements require reports of holdup mass quantities.

Reporting for accountability of nuclear materials and closeout of safeguards in nuclear facilities gives results for holdup mass. Accountability needs may be limited to the mass of holdup and its uncertainty for each process or material-balance area (MBA). Needs for safeguards closeout may be similar or even more general in requiring the reporting mass by building rather than MBA, for example. The reports, however, must be backed up by references to documentation on the method, appropriate controls, relevant verification of the technique that determines mass, and the sources and propagation of error terms.

Reporting holdup mass for compliance with requirements for packaging, shipment and storage of waste from D&D can be a bigger effort than responding to the needs of operations, safety and accountability. A number of factors contribute to the greater complexity of reporting for waste.

- Detailed reporting of mass in the specific sections of the process that are scheduled for removal and placement in waste containers involves the redetermination of holdup mass for each of the numerous specified sections of equipment.
- Access of archival data is essential in obtaining the required results for holdup mass in the uniquely specified sections of process equipment.
- Access of archival reports may be required to identify the methods and technologies (presumably documented) used to obtain older archival data.
- Safeguards closeout can precede disassembling sections of process equipment for packaging as waste. Therefore, the relevant holdup measurements could be relatively recent or very old if the facility has remained dormant for extended periods after an initial cleanout.
- Older archival data may be incomplete or difficult to interpret, and older measurement techniques or methodologies – including those implemented under former regulatory protocols – may provide insufficient confidence in the mass results.

Many requirements for the packaging, shipment and storage of waste have evolved recently. Facilities placed under environmental-management oversight before these requirements came into place may be challenged to demonstrate that the considerable data acquired previously to close out safeguards oversight remains sufficient to establish compliance with recent

requirements for waste. Planning the complete life cycle of a nuclear facility through the D&D phase and the relatively immediate execution of each sequential phase in time is the idealized solution to avoiding the difficulties of changes in procedure and oversight between "generations". A well-organized and complete archive of measurement data and reports along with well-documented measurement techniques and methodologies will typically support quantitative reassessments of measurement results obtained by approaches that have subsequently been replaced with better methods and technologies.

XI.5. Reporting for Criticality Safety Screening

Criticality safety screening applies to process equipment in which accumulations can reach unsafe limits. Process equipment is usually designed within safe limits for the intended material. Safety reviews of operational changes are necessary to prevent the use of a process for materials for which the equipment does not meet the associated safety criteria. Nonetheless, certain types of process equipment can remain vulnerable to safety concerns. Some examples are equipment designed for

- bulk solution processing if the possibility of solids buildup is considered.
- the bulk processing or transport of wet solids.
- process exhaust, which typically serves all processes in a facility.
- enrichment of uranium in an operating plant. Once shut down, potential safety issues arise with in-leakage of moisture (moist air).

Contact gamma-ray measurements are often performed to screen such equipment for criticality safety. The gamma count rate measured with an effectively shielded and collimated detector positioned at contact measures the areal density at the contact location if corrections are performed for equipment attenuation and the deposit does not exceed the maximum thickness. Maximum thickness indicates that the deposit thickness is undetermined, indicating a possible safety issue as discussed in Section VIII.4.3. A detector calibrated to measure the generalized area holdup deposit is a candidate in this application. However, it is usually in the best interests of measuring the mass of holdup that the measurements be performed not at contact but at the largest practical measurement distance, as described in Section X.3 and elsewhere. Furthermore, the screening measurements at contact are sensitive only to the contact location and are potentially vulnerable to missing locations including those that contain large deposits.

An alternative approach to screening for criticality safety is to survey – perhaps at contact – 100% of the piping and ducts to identify locations of large deposits and subsequently screen these particular locations at contact for maximum correctable deposit thickness. Automation should be implemented to simplify the survey process.[71] While such contact surveys can employ spectroscopy under automation, they are not candidates for quantitative measurements of mass unless deposit uniformity is likely. However, deposit uniformity can be assumed in particular situations. Examples are gaseous processes such as UF_6 diffusion where piping surfaces tend to be uniformly coated with holdup deposits.

Because the generalized approach to self-attenuation corrections determines the areal density of any deposit – point, line or area – directly from the measured specific mass, the method tests all deposits for maximum thickness. Therefore, all measurements screen deposits for safety. Figure XI.1 plots both the measured specific mass of uranium (g U/cm) in the line deposit and the inferred deposit width $\boldsymbol{w}$ (cm) *vs*. measurement position on a duct. The holdup data relevant to

criticality safety screening is areal density. The report of holdup measurements for criticality safety screening of a duct such as that represented in Figure XI.1, for example, would graph the ratio of specific mass to inferred deposit width ***w*** *vs*. measurement position on the duct along with the horizontal line representing the specific mass for maximum thickness. (Refer to Section IX.6.) Error bars on the measured areal density give a visual indication of the safety margin.

Holdup measurements performed frequently have a potential role in safety screening. The follow-up to exceeding alarm limits applied conservatively to the map of areal density could be a detailed measurement series with the collimated detector positioned at contact along the duct in the alarming region. Formalized use of holdup measurements in a dual safety role will require considerable testing in the plant.

XII. DOCUMENTING HOLDUP METHODS AND METHODOLOGIES

Multiple needs for documentation of methods reinforce the importance of complete and detailed documentation. Managing revisions adds complexity to multipurpose documentation because some interests require knowledge of the specific methodology applied in a given historical period of operation or shutdown, while many interests need the assurance that the documentation contains all current updates to the methodology. Reports of holdup measurements reference the applicable documentation, as discussed in Section XII.2. Other interests discussed in XII.1 make practical use of the documentation. An example of the comprehensive documentation of holdup methodology for a particular facility is published.[72, 73]

XII.1. Documentation for Training, Assessment, and New Operations

An aspect holdup measurement technology not discussed explicitly in this report is its evolutionary character. Three causes can explain this character. i) Changing operations, increasing regulation, and broader customer interests and needs compel portable measurements to provide better information and more of it faster, driving the responsible scientists to improve methods and methodologies. ii) Technologies for portable spectroscopy advance rapidly so that previous generations of hardware and software reach commercial obsolescence early because of the rapid improvements, driving hardware/software upgrades. iii) Because of the unique environment (including personnel, processes, protocols, *etc*.) of each facility, performing portable measurements precedes optimizing portable measurements, which precedes optimizing portable measurements, *etc*., defining an intrinsic evolutionary character of holdup measurement technology. All three contribute to the certainty of frequent changes to the methods and methodology and the need for frequent revisions in the documentation.

Users of documentation for ongoing measurements will require current documentation. The challenge to meeting the documentation needs of users for training/instruction purposes is keeping the documentation current in the face of rapid change. Access is less of a problem because the current documentation is what tends to be available.

Assessments of the results of previous holdup measurement campaigns underscore the importance of an electronic archive and cataloging system for documentation of methodology, like that for holdup data, which remains accessible through a facility's full operational status into extended shutdown periods and throughout D&D (Section XI.2). The need to retrieve archived reports of holdup measurements arises when the results of former measurement campaigns must be applied to current needs. The relevant current needs are most often meeting regulatory requirements for accountability, safety, security, packaging, shipment and storage of nuclear materials in a process or facility scheduled for dismantlement. It is common that such a process or facility has been inactive for a long period prior to the dismantlement, and that extensive measurements performed prior to the period of inactivity were required to declare a status on accountability, safety and security for the dormant status. Evolution of requirements for accountability, safety and security in the dormant period and the addition of new requirements for packaging, shipment and storage forces the need to assess the validity of the measurements performed at the start of the dormant period for the current needs. If these measurements were costly to perform before the dormant period, they will be more costly to perform currently.

The specific methodologies referenced in each measurement report, as well as the scope and quality of the reported results, must be assessed for validity in support of current needs. The relevant documentation of methodology, which may include multiple revisions, and does not generally include current documentation, must be accessible for this purpose. Therefore, all revisions of the documentation must be archived and catalogued, and the consequence of not doing so could be a very costly campaign to repeat the measurements. Likely consequences for old measurement results with well-documented methodologies include some reanalysis of archived data followed by global revisions to the previous measurement results. The latter consequence is only possible with complete documentation of the methodology for the archived data.

XII.2. Documentation for Reporting Results

Reports of holdup measurement results must reference the documented methodology that includes a complete treatment of the sources and magnitudes of random and systematic uncertainties.[72, 73] Current methodology, for which documentation would be readily available, will apply to the current reports in most cases. Archived reports will reference older revisions of the methodology documentation. Reporting holdup results requires referencing but not using documentation. Nonetheless, the report of holdup measurements must correctly reference the relevant revision of the methodology documents. This will support possible future assessments in which access to archived reports will typically also require access to the referenced documentation of methodology, as discussed in Section XII.1.

XIII. ACRONYMS AND ABBREVIATIONS

ALARA	As Low As Reasonably Achievable
BGO	Bismuth Germanate Detector
CPG	Coplanar Grid
CZT	Cadmium Zinc Telluride Detector
CdTe	Cadmium Telluride Detector
DA	Destructive Analysis
D&D	Decontamination and Decommissioning
DOE	(US) Department of Energy
DOT	(US) Department of Transportation
DQO	Data Quality Objective
DSP	Digital Signal Processing
DU	Depleted Uranium
FW.5M	Full Width at Half Maximum
Ge	Germanium Detector
GGH	Generalized-Geometry Holdup
HEU	High-Enriched Uranium
ID	Inventory Difference
$LaCl_3$	(Cerium-Doped) Lanthanum Chloride Detector
LEID	Limit of Error in Inventory Difference
LEU	Low-Enriched Uranium
MBA	Material Balance Area
MCA	Multichannel Analyzer
MC&A	Material Control and Accountability
MOX	Mixed (U-Pu) Oxide
NaI	(Thallium-Doped) Sodium Iodide Detector
NDA	Nondestructive Analysis
NIST	National Institute of Standards and Technology
NMC&A	Nuclear Material Control and Accountability
NTS	Nevada Test Site
PC	Personal Computer
PMT	Photomultiplier Tube

R&D	Research and Development
ROI	Region of Interest
SNM	Special (Accountable) Nuclear Materials
WIPP	Waste Isolation Pilot Plant

XIV. ACKNOWLEDGEMENTS

Funding from the US Department of Energy, Office of Security Policy, Policy Integration and Technical Support and its predecessor organizations has made possible the cumulative field experience of 25 years that has resulted in this application guide for portable plant-wide measurements of holdup using gamma techniques. Support from colleagues at Los Alamos and at other DOE sites is gratefully acknowledged. Particular thanks go to Anthony Belian, Jack Malcom, Doug Reilly, and Tracy Wenz of Los Alamos; Frank Lamb of Rocky Flats; Brian Keele of Hanford; Chris Pickett and Steve Smith of Oak Ridge National Laboratory; Cynthia Gunn, Rick Oberer, and Ken Thompson of Y-12; and Dick Mayer of USEC/Portsmouth for valuable contributions to and comments on the manuscript. This guide would not have been produced without the urging, encouragement, and technical advice of Norbert Ensslin.

XV. REFERENCES

1. M. C. Miller, H. O. Menlove, M. Seya, S. Takahashi, and R. Abedin-Zadeh, "Holdup Counters for the Plutonium Fuel Production Facility – PFPF," *Nucl. Mater. Manage.* ***XIX***, Proc. Issue, Northbrook IL: INMM (1990), pp. 323-327.
2. T. Asano, H. Kobayashi, S. Takahashi, H. Maruyama, J. Ninagawa, H. Menlove and T. Wenz, "Development of Improved Holdup Measurement System at Plutonium Fuel Production Facility," *Nucl. Mater. Manage.* ***XXVI*** CD ROM Proc. Issue, Northbrook IL: INMM (1997).
3. T. R. Wenz, P. A. Russo, M. C. Miller, H. O. Menlove, T. Takahashi, Y. Yamamoto and I. Aioki, "Portable Gamma-Ray Holdup and Attributes Measurements of High- and Variable-Burnup Plutonium," Los Alamos National Laboratory report LA-UR-91-3323 (September, 1991). *Proceedings of the Fifth International Conference on Facility Operation – Safeguards Interface*. LaGrange Park, IL: American Nuclear Society (1991), pp. 226-236.
4. D. H. Beddingfield and H. O. Menlove, "Distributed Source Term Analysis, a New Approach to Nuclear Material Inventory Verification," *Nucl. Instr. Meth.* A 485 (2002), pp. 797-804.
5. D. H. Beddingfield and H. O. Menlove, "A New Approach to Holdup Measurement in Uranium Enrichment Facilities," Los Alamos National Laboratory report LA-UR-00-2534 (July 2000). *Proceedings of the 41st Annual Meeting of the INMM*, CD ROM, Northbrook IL: INMM (2000).
6. NRC, "*In-Situ* Assay of Enriched Uranium Residual Holdup," NRC Regulatory Guide 5.37, Rev. 1, Washington D.C.: United States Nuclear Regulatory Commission (October 1983).
7. NRC, "*In-Situ* Assay of Plutonium Residual Holdup," NRC Regulatory Guide 5.37, Rev. 1, Washington D.C.: United States Nuclear Regulatory Commission (February 1984).
8. "Nondestructive Assay of Special Nuclear Materials Holdup," Los Alamos, NM: Los Alamos National Laboratory training manual LAUR-99-2597 August 1999 (or earlier versions, beginning in February 1991).
9. P. A. Russo, H. A. Smith, J. K. Sprinkle, Jr., C. W. Bjork, G. A. Sheppard and S. E. Smith, "Evaluation of an Integrated Holdup Measurement System Using the GGH Formalism with the M^3CA," Los Alamos National Laboratory report LA-UR-95-3321. *Proceedings of the Fifth International Conference on Facility Operation – Safeguards Interface*. LaGrange Park, IL: American Nuclear Society (1996), pp. 239-248.
10. J. K. Sprinkle, Jr., R. Cole, M. L. Collins, S.-T. Hsue, P. A. Russo, R. Siebelist, H. A. Smith, Jr., R. N. Ceo, and S. E. Smith, "Low-Resolution Gamma-Ray Measurements of Process Holdup," Los Alamos National Laboratory report LA-UR-96-3482 (October 1996).
11. S. E. Smith, K. A. Thompson, and R. N. Ceo, "Holdup measurement System 3 (HMS3) User's Guide and Software Documentation", Lockheed-Martin Energy Systems report Y/DK-1104 (1997).

12. S. E. Smith, J. S. Gibson, J. K. Halbig, S. F. Klosterbuer, P. A. Russo, and J. K. Sprinkle, "The Holdup Measurement System II (HMSII)," *Nucl. Mater. Manage.* ***XXII***, Proc. Issue, Northbrook IL: INMM (1993), pp. 508-512.

13. S. E. Smith, K. A. Thompson, J. Malcom, and P. A. Russo, "Holdup Measurement System 4 (HMS4) - Automation & Improved Accuracy," Y-12 report Y/DK-2190 (June 2004). *Proceedings of 45th Annual Meeting of the INMM*, CD ROM, Northbrook IL: INMM (2004).

14. P. A. Russo, J. K. Sprinkle, Jr., C. W. Bjork, T. O. McKown, G. A. Sheppard, S. E. Smith, and J. F. Harris, "Evaluation of the Integrated Holdup Measurement System with the M^3CA for Assay of Uranium and Plutonium Holdup", Los Alamos National Laboratory report LA-13387-MS (August 1999).

15. R. Hoyt, "Plutonium Finishing Plant Operations Overview (1949-2004): Contamination Events and Plutonium Isotope Distributions of Legacy Holdup Material in Process Systems," Fluor Hanford report HNF22064 (August 2004).

16. "Design Considerations for Minimizing Residual Holdup of Special Nuclear Material in Equipment for Wet Process Operations," NRC Regulatory Guide 5.25 (June 1974).

17. "Design Considerations for Minimizing Residual Holdup of Special Nuclear Material in Equipment for Dry Process Operations," NRC Regulatory Guide 5.42 (January 1975).

18. "Design Considerations for Minimizing Residual Holdup of Special Nuclear Material in Drying and Fluidized Bed Operations," NRC Regulatory Guide 5.8 (May 1974).

19. P. A. Russo, R. B. Strittmatter, E. L. Sanford, M. M. Stephens, T. L. Brumfeld, S. E. Smith, E. E. McCullough, I. W. Jeter, and G. L. Bowers, "Automated Instruments for In-Line Accounting of Highly Enriched Uranium at the Oak Ridge Y-12 Plant," Los Alamos National Laboratory report LA-10243-MS (February 1985).

20. P. A. Russo, T. R. Wenz, and K. D. Veal, *In-Situ* Measurement of Process Solution Inventory of ^{235}U," Los Alamos National Laboratory report LA-UR-00-2470 (June 2000).

21. P. A. Russo, J. K. Sprinkle, Jr., and T. H. Elmont, "Holdup Measurements of the Rocky Flats 371 Precipitator Canyons," Los Alamos National Laboratory report LA-10967-MS (April 1987).

22. P. A. Russo, R. Siebelist, J. A. Painter, and J. E. Gilmer, "Evaluation of High-Resolution Gamma-Ray Methods for Determination of Solid Plutonium Holdup in High-Throughput Bulk Processing Equipment," Los Alamos National Laboratory report LA-11729-MS (January 1990).

23. P. A. Russo, J. R. Sprinkle, Jr., M. M. Stephens, T. L. Brumfield, C. S. Gunn, and D. R. Watson, "Stationary and Portable Instruments for Assay of HEU Solids Holdup," Los Alamos National Laboratory report LA-UR-87-3739. *Proceedings of Third International Conference on Facility Operation – Safeguards Interface*. LaGrange Park, IL: American Nuclear Society (1988), pp. 101-115.

24. C. Bonner, D. C. Garcia, J. E. Malcom, J. M. Pecos, P. A. Russo, and R. Siebelist, "Fissile Material Holdup in the CMR Basement: I. Wing 3 and II. Wing 5," Los Alamos National Laboratory report LA-UR-01-2397 (May 2001).

25. C. Bonner, D. C. Garcia, J. E. Malcom, J. M. Pecos, P. A. Russo, and R. Siebelist, "Fissile Material Holdup in Wing 7 of the CMR Basement," Los Alamos National Laboratory report LA-UR-01-860 (February 2001).

26. G. A. Sheppard, P. A. Russo, M. C. Miller, T. R. Wenz, E. C. Piquette, F. X. Haas, J. B. Glick, and A. G. Garrett, "Models for Gamma-Ray Holdup Measurement at Duct Contact," Los Alamos National Laboratory report LA-UR-91-2507 (July 1991). *Nucl. Mater. Manage.* ***XXI***, Proc. Issue, Northbrook IL: INMM (1991), pp. 68-73.

27. J. B. Glick, F. X. Haas, A. G. Garrett, P. A. Russo, G. A. Sheppard, M. C. Miller, E. C. Piquette, and T. R. Wenz, "A New Approach to Performing Holdup Measurements on Glove Box Exhausts," *Nuclear Mater. Manage.* ***XX*****,** Proc. Issue, Northbrook IL: INMM (1991), pp. 64-67.

28. F. X. Haas, J. B. Glick, J. N. McKamy, A. G. Garrett, P. A. Russo, G. A. Sheppard, T. R. Wenz and M. C. Miller, "Holdup Measurements of Plutonium in Glove Box Exhausts." *Proceedings of Fifth International Conference on Facility Operation – Safeguards Interface*. LaGrange Park, IL: American Nuclear Society (1991), pp. 237-242.

29. R. S. Marshall, "SNM Holdup Assessment of Los Alamos Exhaust Ducts: Final Report," Los Alamos National Laboratory report LA-12700 (February 1994).

30. "Control and Accountability of Nuclear Materials," US Department of Energy order DOE O 474.1A (November 2000).

31. "Manual for Control and Accountability of Nuclear Materials," US Department of Energy manual DOE M 474.1-1A (November 2000).

32. B. R. Douglas, F. L. Lyons, C. A. Finleon, and S. A. Doty, "MC&A System Changes in Support of Site Closure," *Proceedings of 44th Annual Meeting of the INMM*, CD ROM, Northbrook IL: INMM (2003).

33. B. R. Douglas, F. L. Lyons, C. A. Finleon, D. K. Sullivan, and S. A. Doty, "An Approach to Campaign-Based Inventories," *Proceedings of 44th Annual Meeting of the INMM*, CD ROM, Northbrook IL: INMM (2003).

34. W. H. Aufderhyde, M. Castro, B. Douglas, F. W. Lamb, and F. L. Lyons, "Holdup Accountability at Rocky Flats," *Proceedings of 44th Annual Meeting of the INMM*, CD ROM, Northbrook IL: INMM (2003).

35. J. S. Hansen and T. D. Reilly, "Nondestructive Analysis (NDA) Tutorial for Nuclear Criticality Safety," Los Alamos National Laboratory report LA-UR-04-4049 (November 2004).

36. "Nevada Test Site Waste Acceptance Criteria – NTSWAC Revision 5". Nevada Site Office publication DOE/NV-325-Rev. 5 (October 2003).

37. US DOE and CFO, "Contact-Handled Transuranic Waste Acceptance Criteria for the Waste Isolation Pilot Plant – Revision 1." Carlsbad NM: Carlsbad Field Office publication DOE/WIPP-02-3122 (March 2004).

38. S. E. Smith and K. A. Thompson, "The Y-12 Uranium Holdup Standards, Y-12 document Y/DK-2110 (June 2004).

39. J. L. Parker, *Attenuation Correction Procedures*, in D. Reilly, N. Ensslin and H. Smith, Jr, Passive Nondestructive Assay of Nuclear Materials (NUREG/CR-5550, NRC FIN A7241), Chapter 6. Springfield, VA: National Technical Information Service, 1991.

40. S.-T. Hsue, J. E. Stewart, and M. S. Krick, "Preparation of Pure Plutonium Metal Standards for Nondestructive Assay," Los Alamos National Laboratory report LA-13760-MS (November 2000).

41. B. A. Guillen, S. T. Hsue, J. Y. Huang, P. A. Hypes, S. M. Long, C. R. Rudy, P. A. Russo, J. Stewart, and D. J. Temer, "Preparation of Small, Well Characterized Plutonium Oxide Reference Materials and Demonstration of the Usefulness of Such Materials for Nondestructive Analysis," Los Alamos National Laboratory report LA-13991-MS (December 2002).

42. R. L. Mayer II, "Peak Analysis Users Guide," Portsmouth Gaseous Diffusion Plant Report POEF- 344-05-071 (February 2005).

43. D. S. Bracken, personal communication: "Standard Guide for Passive Gamma Measurements Using Modeling," ASTM International, Subcommittee C26.10, Working Document WK909 (2005).

44. P. A. Russo, M. S. Krick, J. K. Sprinkle, Jr., and J. E. Swansen, "Measurement of In-Process Plutonium in the 771 Rotary Calciner," *Safeguards and Security Progress Report, 1985*, Los Alamos National Laboratory report LA-10787-PR (March 1986), pp. 9-14.

45. J. Bailey, R. C. Hagenauer, R. L. Mayer II, B. R. McGinnis and R. R. Royce, "A Comparative Study of Nondestructive Assay Estimates to Chemical Recovery and Operator-Declared Inventory for Large-Scale Gaseous Diffusion Process Equipment," Portsmouth Gaseous Diffusion Plant Report POEF-TO-21 (July 1994).

46. R. L. Mayer II, B. R. McGinnis, J. N. Cooley, J. M. Whitaker, and T. D. Reilly, "Nondestructive Assay Measurements in Support of the Cooperative Effort Between the United States and Argentina," Portsmouth Gaseous Diffusion Plant Report POEF-TS-03 (May 1995).

47. H. Preston and W. Symons, "The Determination of Residual Plutonium Masses in Gloveboxes by Remote Measurements Using Solid Thermoluminescent Dosimeters," AEA report AEEW-R1359, Winfrith UK (1980).

48. F. W. Lamb, "A Frank Look at Lessons Learned During Holdup Measurements at RFETS: Part 2 – Measurements," Rocky Flats Environmental Technology Site report RFP#5560 (April 2005), to be published in the *Journal of Nuclear Materials Management*.

49. A. P. Belian, T. D. Reilly, P. A. Russo, S. J. Tobin, N. N. Nikolaenko, G. Sokolov, Y. V. Yasko, A. Ustimovich, G. Strygin, Y. Tchyrnuha, A. Chahid, A. LeBrun, and L. Bourva, "Holdup Measurements at the Ulba Metallurgical Plant," Los Alamos National Laboratory report LA-UR-05-2020 (March 2005).

50. J. B. Glick, F. W. Lamb, D. Weier, R. Boan, G. A. Sheppard, and A. Goldman, "Characterization And Propagation Of Uncertainties Associated With Holdup Measurements at Rocky Flats," *Nucl. Mater. Manage.* ***XXI***, Proc. Issue, Northbrook IL: INMM (July 1992) 282-286.

51. H. A. Smith and M. Lucas, *Gamma-Ray Detectors*, in D. Reilly, N. Ensslin and H. Smith, Jr, Passive Nondestructive Assay of Nuclear Materials (NUREG/CR-5550, NRC FIN A7241), Chapter 3. Springfield, VA: National Technical Information Service (1991).

52. G. F. Knoll, Radiation Detection and Measurements, Hoboken NJ: Wiley (2000) 234-237.

53. K. D. Ianakiev, S. T. Hsue, M. C. Browne, and J. M. Audia, "Apparatus and Method for Temperature and Expanded Count Rate of Inorganic Scintillation Detectors," Los Alamos National Laboratory Patent Application S-102, 304, Serial No.10/858,620 (June 2004).

54. P. A. Russo, T. R. Wenz, and J. A. Painter, "Experimental Evaluation of Software-Driven Digital Gain-Drift Compensation in Scintillator Gamma-Ray Spectroscopy," Los Alamos National Laboratory report LA-12390-MS (1992).

55. D. T. Vo and P. A. Russo, "PC/FRAM Plutonium Isotopic Analysis of CdTe Gamma-Ray Spectra," *Nucl. Instr. Meth.* A 486 (2002) 813-824.

56. D. T. Vo and P. A. Russo, "Testing the Plutonium Isotopic Analysis Code FRAM with Various CdTe Detectors," Los Alamos National Laboratory report LA-UR-02-543 (February 2002).

57. D. T. Vo and P. A. Russo, "Plutonium and Uranium Isotopic Analysis in the X-ray Region with the CdTe Detector," Los Alamos National Laboratory report LA-UR-03-4730 (August 2003). SPIE 5198 (2004), pp. 182-190.

58. P. A. Russo, T. H. Prettyman, S. E. Smith, J. F. Harris, J. S. Massengill, and E. Stair, Jr., "Comparison of Detectors for Portable Gamma-Ray Spectroscopy at Y-12," Los Alamos National Laboratory report LA-UR-99-199 (January 1999).

59. K. Chung, A. P. Belian, E. A. McKigney, and P. A. Russo, "Application of Lanthanum Halide Scintillators and Low-Resolution Dense Plastics for Modern MC&A Needs," Los Alamos National Laboratory report LA-UR-04-4472 (June 2004).

60. R. Redus, A. Huber, J. Pantazis, T. Pantazis, T. Takahashi, and S. Woolf, "Multielement CdTe Stack Detectors for Gamma-Ray Spectroscopy," *IEEE Trans. Nucl. Sci*., **51**, No. 5, 1 (October, 2004) 2386-2394.

61. D. T. Vo and P. A. Russo, "Comparisons of the Portable Digital Spectrometer Systems," Los Alamos National Laboratory report LA-UR-03-4730 (August 2003).

62. P. A. Russo, A. P. Meier, M. Rawool-Sullivan, T. H. Prettyman, H. Y. Huang, D. A. Close, M. C. Sumner, R. A. Cole, P. N. Luke, and S. A. Soldner, "A New Room-Temperature Gamma-Ray Detector for Improved Assay of Plutonium", Los Alamos National Laboratory report LA-UR-97-2782 (July 1997). *Nucl. Mater. Manage.* **XXVI** (Proc. Issue) CD-ROM (1997).

63. P. N. Luke. "Single-Polarity Charge Sensing in Ionization Detectors Using Coplanar Electrodes," *Applied Physics Letters*, **65**, No. 22 (November 28, 1994), pp. 2284-2286.

64. P. N. Luke and E. E. Eissler, "Performance of the CdZnTe Coplanar-Grid Detectors," *IEEE Trans. Nucl. Sci.,* **43**, No. 4 (August 1995), pp. 207-213.

65. K. Parnham, "Recent Progress in Cd1-XznXTe Radiation Detectors," *Nucl. Instr. Meth.* **A377** (1996), pp. 487-491.

66. P. A. Russo, T. R. Wenz, S. E. Smith, and J. F. Harris, "Achieving Higher Accuracy in the Gamma-Ray Spectroscopic Assay of Holdup," Los Alamos NM: Los Alamos National Laboratory report LA-13699-MS (September 2000).

67. P. A. Russo, T. R. Wenz, S. E. Smith, and J. F. Harris, "Achieving Higher Accuracy in the Gamma-Ray Spectroscopic Assay of Holdup," Los Alamos National Laboratory report LA-UR-00-3047 (July 2000). *Proceedings of 41st Annual Meeting of the INMM*, CD ROM, Northbrook IL: INMM (2000).

68. P. A. Russo, M. C. Sumner, T. K. Li, H. O. Menlove and T. R. Wenz, "Quantitative Verification of In-Process Inventory of High-Burnup Plutonium Using Room-Temperature Gamma-Ray Detectors and the GGH Formalism," Los Alamos National Laboratory report LA-12953-PR (March 1997), pp. 68-73.

69. R. B. Oberer, C. A. Gunn, and L. G. Chiang, "Improved Background Corrections for Uranium Holdup Measurements," Y-12 National Security Complex report Y-DK-2107 (June 2004).

70. C. A. Gunn, R. B. Oberer, L. G. Chiang, and R. N. Ceo, "Generalized Finite Source Calibration Factor: A Natural Improvement to the Finite Source Correction Factor for Uranium Holdup Measurements," Y-12 National Security Complex report Y-DX-2525 (January 2003).

71. A. P. Belian, P. A. Russo, and D. R. Weier. "Independent Review of Non-Destructive Assay for the K-25/K-27 D&D Project," Los Alamos National Laboratory report LA-UR-05-0148 (January 2005).

72. B. D. Keele. "PFP Generalized Geometry Holdup Calculations and Total Measurement Uncertainty," Fluor Hanford report HNF-23383 Rev. 1 (December 2004).

73. Brian Keele, Kevin Chase, Thurman Cooper, Sam Hurlbut, Jeremy James, Vernon Jennings, John Pestovich, and Joseph Pestovich. "Status of Portable Non-Destructive Assay at the Plutonium Finishing Plant," Hanford abstract HNF-23383 Rev. 1 (February 2005). Paper to be presented at the 46th Annual Meeting of the INMM, Orlando FL (July 2005).

This report has been reproduced directly from the best available copy. It is available electronically on the Web (http://www.doe.gov/bridge).

Copies are available for sale to U.S. Department of Energy employees and contractors from:
Office of Scientific and Technical Information
P.O. Box 62
Oak Ridge, TN 37831
(865) 576-8401

Copies are available for sale to the public from:
National Technical Information Service
U.S. Department of Commerce
5285 Port Royal Road
Springfield, VA 22161
(800) 553-6847

Los Alamos
NATIONAL LABORATORY
EST. 1943